accuracy lie in the range 7 arcmin, with more or less accurate versions available from some vendors.[9]

Resolvers are basically rotating transformers. The construction of a typical device and the output waveforms for a 360° rotation are shown in Fig. 3.7. An alternating voltage connected to the reference input provides primary excitation. The range of frequencies used can be 400 to 20 kHz depending on the construction of the resolver; most resolvers are optimized for the 2 to 5 kHz frequency range. The reference signal is coupled to the rotor via a transformer mounted at one end of the rotor shaft. A second rotor winding couples to two orthogonally oriented stator windings. The stator coils are wound so that as the rotor shaft rotates, the amplitudes of the outputs of the stator windings vary as sine and cosine of the shaft angle relative to some zero.

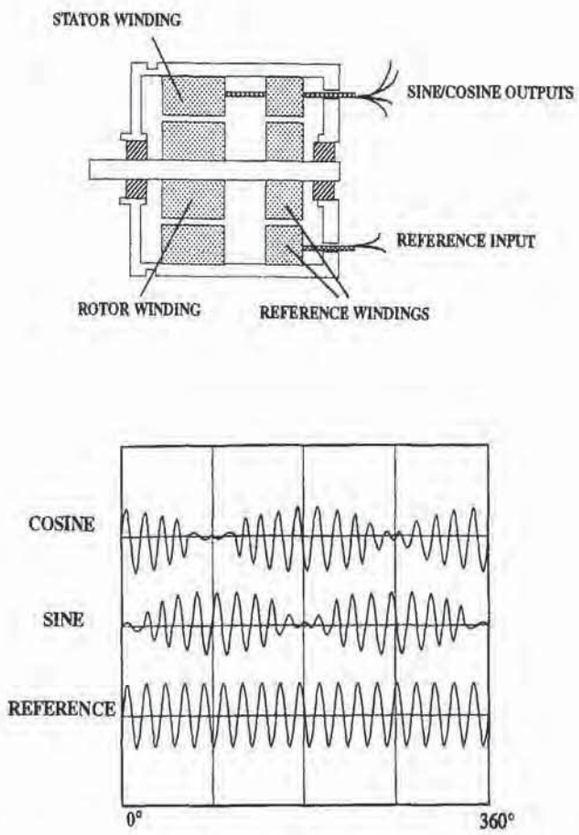


FIGURE 3.7 Resolver construction and output format.

By far, the most economical way of decoding the output of a resolver is to use an IC resolver-to-digital converter (R to D). A functional block diagram of a typical converter is shown in Fig. 3.8. The sine and cosine amplitude-modulated input signals from the resolver representing a shaft angle θ are multiplied by the cosine and sine, respectively, of the current value ϕ of the up/down counter. The resulting signals are subtracted giving:

$$VE = A \sin(\omega t) \sin(\theta - \phi) \tag{3.4}$$

where $A \sin(\omega t)$ represents the reference carrier.

This signal is synchronously demodulated and an integrator and voltage-controlled oscillator form a closed loop with the counter/multiplier, which seeks to null $\sin(\theta - \phi)$. When the

PETITIONER'S EXHIBIT 1002
US PATENT NO. 6,557,540

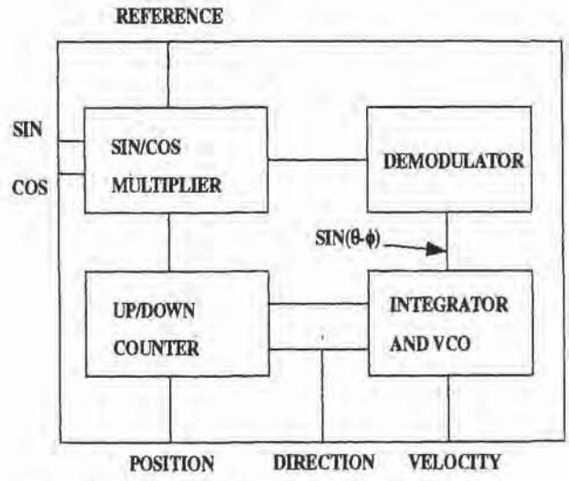


FIGURE 3.8 Tracking resolver-to-digital converter.

null is achieved, the counter value represents the resolver shaft angle within the rated accuracy of the converter. IC R-to-D converters are available that provide parallel or serial digital outputs with resolutions of from 10 to 16 bits and accuracies from 2 to 30 arcmin. Versions are available[10] that emulate standard optical encoder outputs for applications where absolute position measurement is not required but the environment is too harsh for an optical encoder. The system described is a type 2 servo loop which is characterized by zero position and velocity error (not including the limitations of the amplifiers in the IC). R-to-D converters of this type also provide a signal proportional to the angular speed of the resolver from zero to some upper limit, typically 1000 s of rpm, depending on the converter characteristics.

Inductive potential dividers are another class of transducers that are available in many variants.[11,12] A good example is the *rotary variable transformer* or ROVAT.[12] This device comprises a single coil wound on a circular ferromagnetic stator with a number of teeth wound as alternate polarity poles. The stator is excited with an AC signal of around 20 kHz. A rotor with a semicircular conductive screen on its inside surface encircles the stator. The screen reduces the flux linkage between the rotor and stator and the inductance of the screened portion of the stator is reduced, reducing the voltage drop across this portion of the stator. The voltage measured at a central tap on the stator is linearly proportional to the angle of the rotor. Further taps at 90° and 270° from the nominal zero allow a waveform to be measured with amplitude in quadrature with the signal measured at the center point. This allows a 360° absolute angle transducer to be realized, using decoding techniques similar to those which will be described later for the LVDT.

Inductive Linear Displacement Sensors. Shading ring or short-circuit ring sensors are absolute displacement sensors consisting of an E-shaped core with a winding on the central leg of the E. The winding is excited with high-frequency alternating current. An electrically conductive ring of Al or Cu is allowed to slide, maintaining an air gap along the central leg. The ring is attached to the mechanical component, whose position is to be measured. The ring is equivalent to a short-circuited secondary turn in a transformer. The ring has a shading effect, preventing any flux coupling between the legs of the core from its position along the central leg of the core to the open ends of the core (Fig. 3.9).[13] An inductance change can be measured at the terminals of the excitation coil. These sensors are usually used in a potential divider configuration with a reference inductance of similar construction to the main sensor connected in series with the main sensor. A reference alternating voltage is applied across the series-connected reference and sensor inductances, forming an inductive potential divider. The output is then proportional to the ratio of the inductances. This renders the sensor insensitive to tem-

PETITIONER'S EXHIBIT 1002
US PATENT NO. 6,557,540

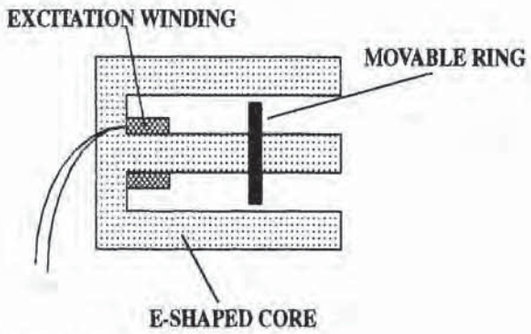


FIGURE 3.9 SCR sensor construction.

perature variations and allows easy adjustment of offsets. Signal-processing electronics can be used to rectify and filter the output and transmit the result to a remote control unit. An alternative construction is to replace the movable ring with an angled channel which can move, relative to the E-shaped core, in a plane perpendicular to the core. Again, the inductance of the sensor is proportional to the linear movement of the angled channel.

Another form of absolute linear displacement sensor is the linear variable differential transformer or LVDT.[14] LVDTs are rugged and reliable and capable of working in harsh environments. Suitable automotive applications include mounting inside hydraulic cylinders in suspension control systems.

LVDTs are constructed from a primary excitation coil positioned centrally on a cylindrical hollow former. Two identical secondary coils are positioned on either side of the primary. The coils have a common core which is free to move within the cylindrical former (Fig. 3.10). The secondaries are normally connected in series, with opposing phases such that with the core centrally positioned and coupling equally to each secondary, the voltage at the node common to both coils will be zero. With this connection, as the core is moved from one extreme of travel through the center to the other extreme, the output signal will vary from a maximum value in phase with the excitation through zero to a maximum value in antiphase with the excitation.

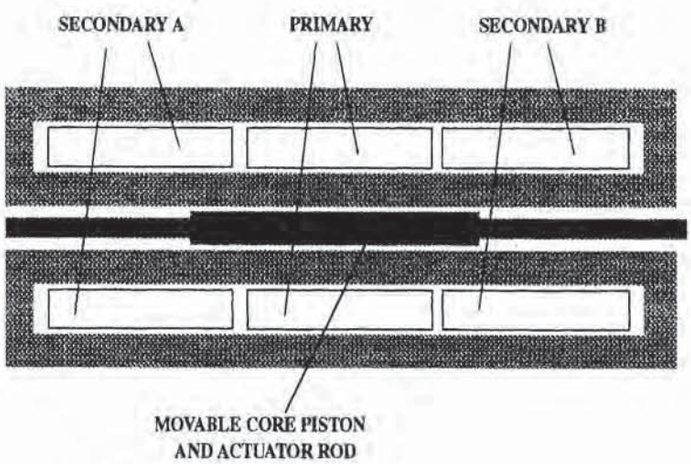


FIGURE 3.10 LVDT construction.

PETITIONER'S EXHIBIT 1002
US PATENT NO. 6,557,540

LVDTs are designed to give a linear output within some tolerance, typically ±0.25 percent, over a specified proportion of the available stroke length. The distribution of turns on the secondary coils is carefully arranged to maximize linearity over the widest possible range. LVDTs are available that maintain good linearity with stroke lengths from ±0.05 to ±10 in.

LVDTs operate with effective transformer ratios of between 10:1 to 2:1. The range of primary excitation frequencies can be from 20 Hz to 20 kHz, depending on the construction of the device. Most LVDTs are optimized for the 2- to 5-kHz frequency range. The output signal from an LVDT can be decoded in several different ways and a number of analog and digital integrated circuit solutions exist for this purpose.[15] An example of a typical connection scheme using an LVDT-to-digital converter is shown in Fig. 3.11. In this example, it is assumed that the sum of the voltages across the series-connected secondaries $V_A + V_B$ is a constant over the range of displacements of interest. The majority of LVDTs in production meet this criterion; for those that do not, an additional nonlinearity will result. The IC decodes the function $(V_A - V_B)/(V_A + V_B)$ over the range $[(V_A - V_B)] \leq (V_A + V_B)/2$ into a 13-bit digital word that can be accessed via a three-wire serial interface. Additional bits indicate null and over or under range for signals outside the linear range. The ratiometric decoding scheme described here is insensitive to primary-to-secondary phase shifts, temperature, and any residual null voltage that the transducer may have due to stray capacitive coupling.

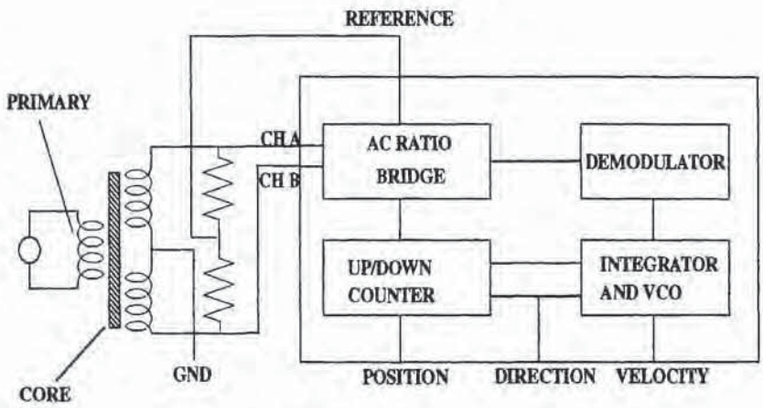


FIGURE 3.11 Tracking LVDT-to-digital converter.

Analog methods of decoding utilize the same basic algorithm as the converter already described. An analog decoder senses the secondary output voltages and evaluates the ratiometric function introduced earlier. The decoder output is filtered and amplified to produce an output voltage proportional to the position of the movable core.

Magnetoresistive. An interesting group of sensors utilize the property of some FeNi alloys such that their resistivity is strongly affected by the presence of a magnetic field. The magnetoresistive effects of one of the useful alloys, Permalloy, which is 81 percent nickel and 19 percent iron, enables sensitive magnetic field sensors with full-scale fields of 5 mT to be built. The variation in resistance is around 2.5 percent for a field of this magnitude. The resistance decreases with increasing field strength; the relationship between field strength and resistance is very nonlinear, approximating a cosine-squared function. Using thin films of Permalloy deposited on a silicon substrate allows signal-conditioning electronics to be integrated with the sensor. Despite the nonlinearity of the phenomenon, accurate linear sensors can be constructed by using the sensor in a bridge arrangement together with flux nulling means, such as a servo-driven coil surrounding the sensor, to effectively operate the sensor at constant resistance. An alternative construction uses opposing "barber pole" thin-film elements.[16] An element is composed of a rectangular thin film of Permalloy overlaid with a series of shorting

PETITIONER'S EXHIBIT 1002
US PATENT NO. 6,557,540

stripes of aluminum at 45° to the long axis. Two series-connected elements, which are mirror images of each other (reflected about the long axis), form a potential divider. Magnetoresistive sensors generally exhibit high sensitivity, but this leaves them prone to interference from unwanted fields and, therefore, they are unsuitable for some applications.

Magnetostrictive. Magnetostriction is a property of materials that respond to a change of magnetic flux by developing an elastic deformation of their crystal structure. Magnetostrictive linear displacement sensors utilize this phenomenon by launching a compression wave down a cylindrical waveguide using electromagnetic means, usually a current pulse. The waveguide passes through a movable permanent magnet ring at some distance from a receiver site. The compression wave generated at the magnet position travels to the receiver site at approximately 2800 m/s where it causes a change of flux and generates a voltage pulse in a sense coil. The time of flight of the pulse can be measured to determine the distance of the movable ring magnet down the wire. Transducers with stroke lengths in excess of 7.5 m are available that use this technique.

3.3.5 Other Technologies

A number of other technologies can be applied to position-sensing problems, limited only by engineering ingenuity. Some, like capacitive-sensing techniques, are not tolerant of the automotive environment due to sensitivity to humidity, vibration, or temperature or pressure extremes. Others, like resolvers of traditional construction, are sufficiently rugged but prohibitively expensive unless low-cost manufacturing techniques can be found. Occasionally, a nonobvious method finds a niche. An example is a fuel-level sensor disclosed by workers at Bosch,[17] which, in principle, could be applied as a position sensor. The device operates by exciting a metal rod with acoustic waves such that it resonates. One end of the rod is immersed in the fuel. The resonant frequency is a function of the depth of immersion and the fuel level can be determined by suitable electronics.

A significant influence in the selection of technologies for automotive use is the mandatory inclusion of safety systems. Microwave or laser-ranging techniques can be applied to anticollision systems to anticipate obstacles at nighttime or in poor-visibility driving conditions. These will be a ubiquitous component of automobiles in years to come.

3.4 INTERFACING SENSORS TO CONTROL SYSTEMS

All sensors, whether they have digital or analog outputs, provide measurement of real-world phenomena that are then interpreted by another system to either indicate a value, a warning, or close a control loop. It is vitally important that the integrity of the data is maintained by the proper choice of interface.

Cost and reliability in automotive systems are primary drivers in the choice of interface. For a given performance, the sensor that requires the fewer connections will always be selected. In some cases, such as LVDTs where the basic sensor requires 5 or 6 wires, it may be advantageous to locate the signal-conditioning electronics with the sensor and communicate the processed data to a remote controller via a simple serial interface. Interfacing incremental or serial binary data to a microcontroller is straightforward. In the case of incremental data, typically the mechanical system being monitored is moved until some limit or index is detected. Knowledge of the absolute position of the mechanical component is then known. A counter or register can be set to an initial nonzero value or reset to zero. As the motion is detected, pulses from the incremental sensor can be counted and stored as a measure of position. The indexing cycle must be performed each time power is applied. Binary serial data can be read into a register and used directly with no further processing.

PETITIONER'S EXHIBIT 1002
US PATENT NO. 6,557,540

Analog-to-digital converters (ADCs) require some special considerations to optimize performance. Not least of these is grounding. In most applications, chassis ground returns cannot be used. Modern automobiles may have voltage drops of 1 V or more between the chassis at the ECU and the sensor site, due to return currents from electric equipment. This voltage is likely to be noisy with many transients and will certainly upset all but the crudest sensors.

Previous sections have discussed the advantages of ratiometric sensors that can use the same reference as the converter. The advantage is that a least-significant bit of the ADC is always a fixed percentage of the sensor span. This eliminates gain, offset, and temperature errors that may occur if separate references are used. Resolution and gain accuracy of a system can be further optimized by making certain that the span of the sensor output uses all of the available input span of the converter. Many ADCs include on board a microcontroller and use switch capacitor techniques to acquire the analog input values. These present a transient load to the sensor once or twice per conversion cycle. Some sensor outputs, particularly sensors with buffer amplifiers, require isolation from this transient to achieve rated accuracy. A simple technique is to use a simple RC filter on the output of the sensor. This limits the transient current that the sensor output sees and shunts the ADC input with a capacitor.

GLOSSARY

Absolute output sensor The sensor output is an unambiguous measure of position and is valid when power is applied.

Arcminute An angular measure. There are 60 arcminutes in 1 degree of arc.

Incremental sensor The sensor indicates changes in position. An additional position reference, such as a limit switch, is often used with this type of sensor.

Linearity error The amount by which the sensor output differs from an ideal characteristic. Usually expressed in percent.

Ratiometric output sensor An input stimulus causes the output to be a fraction of a reference voltage.

REFERENCES

1. Hewlett-Packard, *Optoelectronics Designers Guide,* San Jose, Calif., 1991–1992.
2. Novatechnik Position Sensor Data, Ostfildern, Germany, 1992.
3. P. Hammond, *Electromagnetism for Engineers,* Pergamon Press Ltd., Oxford, England, 1965.
4. Roland K. Kolter, European Patent Application EP 0 019 530 A1, Applicant Bendix, 1980.
5. Henry P. Baltes, and Popovic, Radivoje S., "Integrated magnetic field sensors," *Proceedings of the IEEE* vol. 74, no. 8, Aug. 1986, pp. 1107–1132.
6. Hartmut Jasberg, "Differential Hall IC for gear-tooth sensing," *Sensors and Actuators,* A21–A23, 1990, pp. 737–742.
7. AD22150 Data Sheet, Analog Devices, Norwood, Mass.
8. Charles S. Smith, U.S. Patent 4 962 331, Assigned to Servo-Tek Products Co. Inc., Hawthorne, N.J., 1990.
9. Clifton Precision, Analog Components Data, Clifton Heights, Pa.
10. AD2S90 Data Sheet, Analog Devices, Norwood, Mass.
11. Novatechnik Angle Sensor Data, Ostfildern, Germany, 1993.

PETITIONER'S EXHIBIT 1002
US PATENT NO. 6,557,540

12. Donald L. Hore, and Flowerdew, Peter M., "Developments in inductive analog transducers for 360° rotation or tilt and for linear displacement," *IEE International Conference,* No. 285, 1988.
13. E. Zabler, and Heintz, F., "Shading-ring sensors as versatile position and angle sensors in motor vehicles," *Sensors and Actuators* **3**, 1982/3, pp. 315–326.
14. *Schaevitz Linear and Angular Displacement Transducers Catalog,* Pennsauken, N.J.
15. AD2S93 and AD598 Data Sheets, Analog Devices, Norwood, Mass.
16. F. Heintz and Zabler, E., "Application possibilities and future chances of 'smart' sensors in the motor vehicle," *SAE Technical Paper Series* #890304.
17. E. Zabler, "Universal low-cost fuel-level sensor," Robert Bosch GmbH, Ettingen, Germany.

ABOUT THE AUTHOR

Paul Nickson is product line manager for Analog Devices' Sensor and Automotive Group in Wilmington, Mass. He has BSc Honours in Electronic and Electrical Engineering from the University of Birmingham, England and 16 years' experience in integrated circuit design. For the past five years, he has focused on silicon sensors and sensor signal conditioning.

PETITIONER'S EXHIBIT 1002
US PATENT NO. 6,557,540

CHAPTER 4
FLOW SENSORS

Robert E. Bicking
Senior Engineering Fellow
Honeywell, Micro Switch Division

4.1 INTRODUCTION

Measurement of flow rate is important to optimize the performance of several key engine control subsystems. Mass air flow sensors are replacing the indirect calculation of intake mass air flow for improved performance, driveability, and economy. New requirements for on-board diagnostics are opening new applications for flow sensing in the automobile.

If the parameter to be measured is a gaseous mass flow as opposed to a volume flow, this further focuses the sensing technology selection since only a few technologies inherently measure mass flow. For liquid flow, either a mass flow or volumetric flow approach may be used since the density of a liquid changes only a small amount with atmospheric pressure and temperature.

This chapter is intended to give the reader an understanding of where and why flow sensors are being specified for use in engine control systems and an understanding of the trade-offs among alternative technologies in particular applications.

4.2 AUTOMOTIVE APPLICATIONS OF FLOW SENSORS

4.2.1 Intake Air Mass Flow

Electronic fuel injection has almost universally replaced the carburetor in the auto engine. This is because it provides better performance and is the only way to meet government mandated emissions standards. To do fuel injection, the mass flow rate of air going into the engine must be determined. There are two competing approaches to determining the mass air flow rate. The first, *speed density*, calculates the mass flow rate by measuring engine speed (RPM), intake air temperature (T_a) and intake manifold pressure (P). The per-cylinder nominal displacement (V) is known, as is the gas constant of air (R_a). The engine's volumetric efficiency (η) may be modeled as a function of speed. Then, the mass flow rate ($\dot{m}_a$) is calculated as follows:

$$\dot{m}_a = \frac{(\mathrm{RPM}\, V \eta\, P)}{(R_a T_a)} \tag{4.1}$$

PETITIONER'S EXHIBIT 1002
US PATENT NO. 6,557,540

By using a mass flow sensor, this calculation is eliminated and $\dot{m}_a$ is measured directly. The advantages of using a direct measurement include better accuracy under dynamic conditions because the manifold pressure changes more slowly than the mass flow rate. Also, no assumptions are made about engine displacement or volumetric efficiency, both of which affect the speed density calculation. Volumetric efficiency can change as the intake system becomes contaminated. Mass air flow sensors are presently being used on roughly 20 percent of the cars sold in the United States. They are not more widely used because they cost more than the pressure sensor needed to do the speed-density calculation. The largest drawback to using a mass flow sensor is that a wide dynamic range sensor is needed since the mass flow rate can change over a 100-to-1 range from idle to full throttle, whereas the manifold pressure only changes over a 5-to-1 range. Other important factors in sensor selection include resistance to contamination and particulate damage, accuracy, ability to measure reverse flow, and sensitivity to upstream and downstream ducting.

Fuel is injected to each cylinder on a sequential basis for optimum performance. This requires using the crankshaft sensor and camshaft sensor outputs to time the injection of fuel into the intake manifold at the proper point on the intake stroke. The fuel injector is fed with a constant pressure and is pulse-width modulated to control the amount of fuel injected. The calculation of the mass rate ($\dot{m}_f$) of fuel injected follows:

$$\dot{m}_f = \dot{m}_a \lambda \tag{4.2}$$

where $\dot{m}_a$ = mass air flow rate
λ = stoichiometric air/fuel ratio

4.2.2 Potential or Future Applications of Flow Sensors

Fuel Flow for Gas Mileage Measurement. Driver information systems that predict range and gas mileage need to know the amount of fuel flow. As seen from the preceding discussion of mass air flow measurement, the fuel flow is calculated from the air flow so that this data is already in the engine control computer. By simply summing the injector "on" time over a revolution or multiple revolutions, the fuel flow is known.

Alternatively, the fuel flow can be measured by taking the difference between the fuel coming into the fuel rail and that being returned. This approach could be subject to substantial error, however, due to the fact that these flows are purposely much larger than the net flow into the engine so that the fuel rail will be maintained at a constant pressure. Future fuel-handling systems may simplify the measurement by eliminating the return line and simply modulating the fuel pressure pump to maintain constant pressure. Then, the measured flow would be simply that flow going into the engine.

Exhaust Gas Recirculation Flow. Exhaust gas recirculation (EGR) is performed to reduce the emission of nitrous oxides (NO_x) by cooling the combustion process. If the EGR valve begins to clog or only partially opens, its flow will be reduced and emissions will increase. In the near future, OBDII legislation will require cars to have on-board diagnostics capable of determining when an emissions-related failure (such as that just described) occurs. Measurement of the flow is one way to diagnose a faulty EGR valve. Another way would be the use of an NO_x sensor to measure the emissions. However, no low-cost NO_x sensors have yet been developed.

Secondary Air Pump Flow. The secondary air pump is used to reduce the emissions of carbon monoxide (CO) and hydrocarbons (HC). Measurement of its flow rate is an approach to verifying that it is operating properly and doing its part to reduce emissions. Another way, of course, would be to directly measure the emissions of HC and CO in the exhaust. To date, however, there is no low-cost real-time means to do that. A way to verify air pump operation

PETITIONER'S EXHIBIT 1002
US PATENT NO. 6,557,540

without using any additional sensors is to command the air pump full-on when the fuel injection is slightly rich of stoichiometry. The oxygen sensor output should switch from rich to lean if the air pump is operating properly.

Fuel Flow for Fuel-Air Ratio Feedback Control. Present engine control systems treat the fuel flow as a dependent variable, measuring the intake air flow and then operating the fuel injectors to meter the proper amount of fuel into the engine. This tacitly assumes that each of the injectors is precisely calibrated so that a given "on" time provides a given amount of fuel. Fuel injectors typically use a needle valve in an orifice to meter the fuel. The orifice area is proportional to the square of the diameter so that the fuel flow error will be proportional to two times the diameter tolerance. By measuring the fuel flow, the accuracy of fuel injection could be improved. Table 4.1 summarizes the performance requirements by application.

TABLE 4.1

Application	Measurement type	Range, kg/h	Accuracy, %
Intake air	Mass	10–1000	±4
Fuel flow	Mass/vol.	1–66	±10
EGR flow	Mass	30–100	±10
Air pump flow	Vol.	50	±20
Fuel flow	Mass/vol.	1–66	±4

4.3 BASIC CLASSIFICATION OF FLOW SENSORS

4.3.1 Energy Additive or Energy Extractive

Flowing fluid possesses energy, both potential and kinetic. One approach to flow measurement extracts energy from the flow. Alternately, energy may be added to the flow and its effect observed. The energy-additive approach typically is nonintrusive, so the act of measuring doesn't affect the flow. As might be expected, flowmeter selection involves a number of factors, as will be discussed later.

4.3.2 Measurement of Mass Flow or Volume Flow

Intake air measurement requires that the mass of air flowing into the engine be measured. This favors a mass-flow approach, since, otherwise, pressure and air temperature must be measured to calculate the mass flow from the volume flow. The mass flow rate ($\dot{m}_a$) is calculated as follows:

$$\dot{m}_a = \dot{V}_a \rho \tag{4.3}$$

where ρ = air density
$\dot{V}_a$ = volumetric flow rate

The density, in turn, is calculated as follows:

$$\rho = \frac{P}{ZR_aT_a} \tag{4.4}$$

where P = air pressure
Z = compressibility factor
R_a = gas constant for air
T_a = air temperature

PETITIONER'S EXHIBIT 1002
US PATENT NO. 6,557,540

4.4 APPLICABLE FLOW MEASUREMENT TECHNOLOGIES

4.4.1 Gaseous Flow

Vane. The vane simply consists of a vane or paddle which is located in the flow duct and is restrained by a spring so that it blocks the duct with no flow. The deflection of the vane is thus proportional to flow. This deflection is read out by a potentiometer. The largest drawback of a vane sensor is that it increases the pressure drop in the intake tract, reducing the volumetric efficiency of the engine. This approach was used in the earliest engine control systems and is being replaced by technologies such as hot-wire air flow sensors which offer much lower pressure drop.

Thermal. This is the favored approach and is used in all engines currently being manufactured that employ direct measurement of the intake air mass. Depending on design details, it provides a nearly direct measurement of the mass flow and thus simplifies the engine control strategy. A variety of designs exists, from the straightforward hot-wire air flow sensor to more complex schemes. The basic idea is to heat a fine wire, and then as the gas flows past the wire, convection removes heat. The amount of heat removed can be measured with an electronic circuit and is proportional to mass air flow rate as the following equation shows:

$$\Delta P \cong \Delta T\,[C_t + (2\pi d C_v \dot{m}_a)^{1/2}]^* \tag{4.5}$$

where ΔP = change in electric power due to a given flow rate
ΔT = temperature difference between air and sensor
C_t = thermal conductivity of air
d = diameter of hot wire
C_v = thermal capacity of air
$\dot{m}_a$ = mass flow rate of air

Note that the first term of the equation isn't proportional to flow rate. Either this needs to be modeled and removed or the change in ambient air temperature needs to be minimized to accurately measure mass flow rate. A hot-wire air flow sensor and its control circuit is shown in Fig. 4.1. Control circuits typically either supply constant power to the heated element or

* From Joseph P. DeCarlo, *Fundamentals of Flow Measurement*, Instrument Society of America, 1984, pp. 173 and 176.

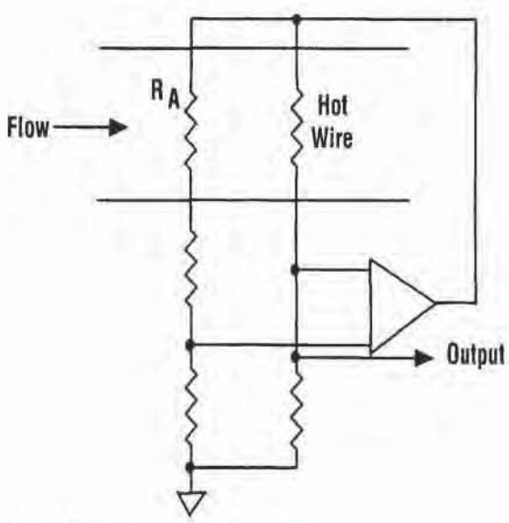


FIGURE 4.1 Hot-wire air flow sensor.

PETITIONER'S EXHIBIT 1002
US PATENT NO. 6,557,540

operate it at a constant temperature delta above the ambient temperature. The latter is shown in Fig. 4.2 and is preferred because it simplifies temperature compensation.

One of the problems with the hot-wire sensor is that fine dust particles may pass through the air filter and, under full-throttle conditions, can impact the hot wire with sufficient force to break it. Particulate build-up is also a source of error and has been alleviated by placing the heated element in a bypass channel or by incorporating a burn-off cycle at power-on. Most of the development in hot-wire sensors has been to ruggedize them to withstand the automotive environment and to desensitize them to upstream and downstream flow anomalies. Figure 4.2 is an example of a bypass design for a hot-element mass air flow sensor. It uses a platinum wire wound on a ceramic mandrel and coated with glass as the sensing element. It is located in a bypass channel away from the main flow to reduce the likelihood of particulate contamination. The bypass exits into the main channel through slots which are intended to desensitize it to backflows and backfires.

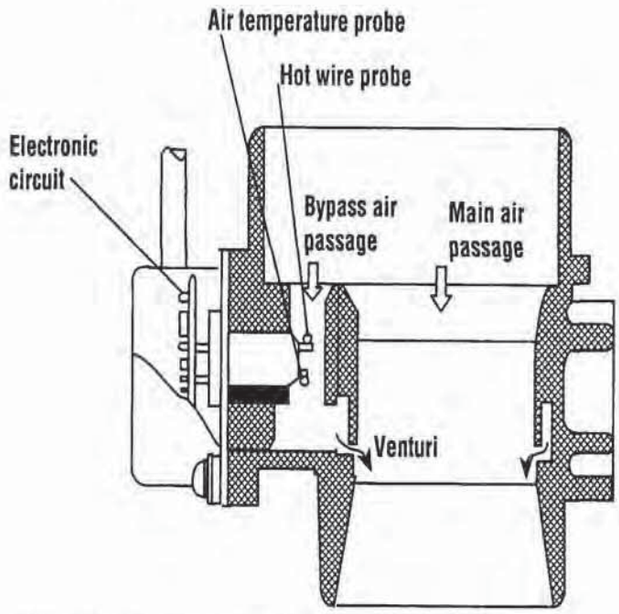


FIGURE 4.2 Bypass hot-wire air flow sensor. *(U.S. Patent 4,264,961)*

Backflow can occur in engines with four or fewer cylinders at low speed. It is most desirable for the sensor to measure the backflow, but most either don't measure it at all or rectify it, which makes the measured flow appear larger than it really is. This error is compensated by measuring the backflow on an engine and then using software to remove the nominal error. One of the issues with bypass designs is that upstream ducting of the air may affect measurement accuracy. A bend just ahead of the sensor will cause the air to move toward the outside of the bend and, depending on where the bypass is located, it may read either too low or too high. This effect is minimized by placing a screen or honeycomb in the sensor to straighten the flow.

Micromachined air flow sensors have been available commercially for several years and efforts are underway to adapt them to automotive applications. Their primary advantages include the low cost of the sensing element due to batch fabrication; excellent performance over temperature due to the close proximity of the heated and reference elements; the ability to measure reverse flows; low operating power due to the small size of the heated element; and fast response, again due to the small size of the heated element. Because of the use of integrated circuit manufacturing techniques, it is no more difficult to include additional resistors on the sensor chip than to simply replicate a hot wire. A calorimetric flow sensor may be constructed by separating the heater and sensor functions as shown in Fig. 4.3. The advantage

PETITIONER'S EXHIBIT 1002
US PATENT NO. 6,557,540

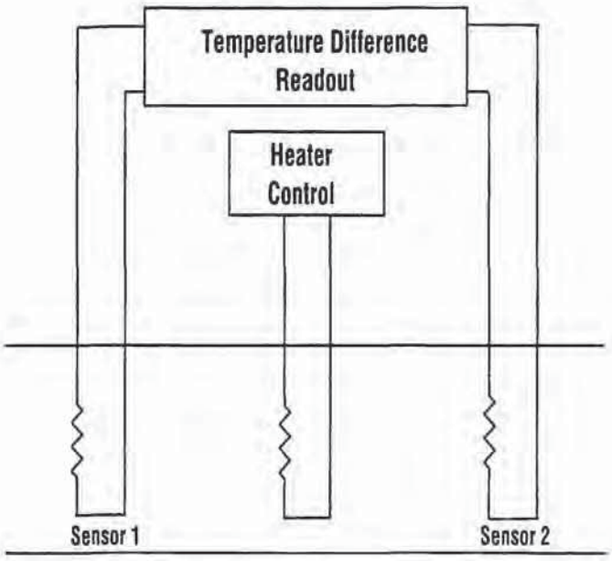


FIGURE 4.3 Calorimetric flow sensor.

of a calorimetric flow sensor is that it does measure the mass flow rate as the following equation shows:

$$\Delta P = \dot{m}_a C_p \Delta T^* \tag{4.6}$$

where ΔP = change in power due to a given mass flow rate
$\dot{m}_a$ = mass air flow rate
C_p = thermal capacity of air
ΔT = temperature difference between air and sensor

One of the issues with microstructure sensors is protection from damage due to particle impact and preventing build-up of contamination. This requires clever packaging.

Table 4.2 compares the main types of thermal mass air flow sensors.

Differential Pressure. A simple way to measure volumetric flow is to place an obstruction in a flow channel and measure the differential pressure drop across it. The flow is proportional to the square root of the differential pressure. This only works well for narrow flow ranges because to operate over a given flow range, the pressure sensor must operate over the square of that range. For the automotive intake flow range of 100 to 1, a pressure sensor with a range of 10,000 to 1 is required, which is not achievable except at high cost. An important advantage of this approach is that it is resistant to contamination, since the pressure sensor merely needs

* From "Fundamentals of Flow Measurement," Joseph P. Decarlo, Instrument Society of America, 1984, pp. 173 and 176.

TABLE 4.2

Type	Effect of contamination	Meas. rev. flow	Affected by ducting	Power used
Hot Wire	High*	Rectifies	Low	Medium
Hot RTD Bypass	Low	Ignores	High	High
Micro RTD	Low	Yes	Low	Low

* Burn-off cycle used to alleviate.

PETITIONER'S EXHIBIT 1002
US PATENT NO. 6,557,540

to sense the pressure difference across the flow restriction (in the case of an orifice plate or venturi). The differential pressure approach could be suitable for some low-accuracy or low dynamic range applications such as EGR valve flow. Venturis (Fig. 4.4), flow restrictions (Fig. 4.5), and pitot tubes (Fig. 4.6) all operate on the same principle.

4.4.2 Liquid Flow

Differential Pressure. The preceding discussion on differential pressure sensing applies equally to liquid flows.

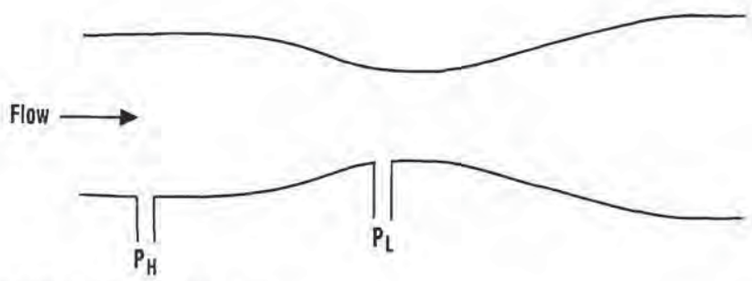


FIGURE 4.4 Venturi flow sensor.

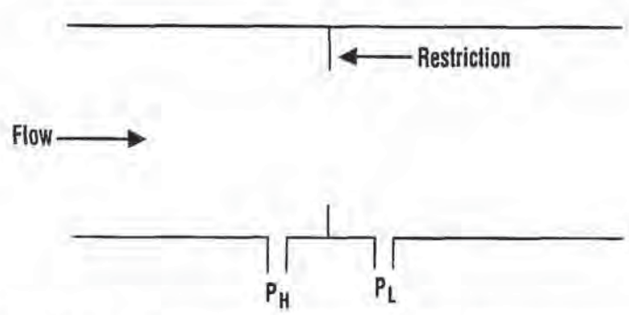


FIGURE 4.5 Flow sensor using a restriction to develop a differential pressure.

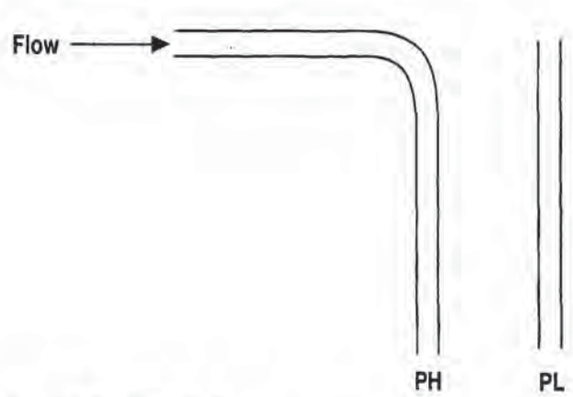


FIGURE 4.6 Pitot tube flow sensor.

PETITIONER'S EXHIBIT 1002
US PATENT NO. 6,557,540

Turbine. A turbine blade placed in a flow channel can offer low restriction to flow, and by counting the speed of rotation it can also measure flow. It is analogous to the vane described previously except that it is more subject to wear since it is revolving, not merely deflecting. Use of a noncontacting means of counting revolutions (such as a Hall effect sensor) is recommended. This approach is well-suited to measurement of fuel flow.

Vortex Shedding. Oscillations may be induced in a fluid by placing an obstruction in the flow stream. The oscillations may be measured thermally, by pressure changes or using ultrasonics. This approach doesn't work well at low flow rates due to instability in the vortex shedding mechanism, so it is not suited to wide dynamic range applications such as intake air measurement. An example of a vortex shedding flow sensor is shown in Fig. 4.7.

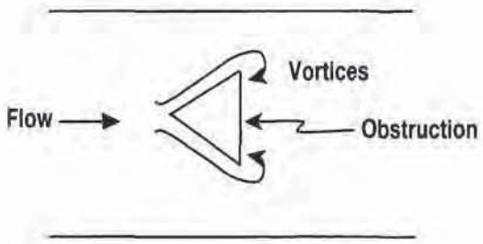


FIGURE 4.7 Vortex shedding flow sensor.

Other Technologies. There are a number of other technologies which are not well-suited to automotive applications, primarily due to cost considerations. A variety of flow sensors has been developed for industrial applications where performance is paramount and cost is secondary. These include the use of ultrasonics, gyroscopic effects, ionization of gases, and so on. These will not be discussed herein. Information on these technologies is given in the books by DeCarlo and Norton. See the list of suggestions for further reading.

GLOSSARY

Backflow The flow of air out of the intake system of an engine. This occurs at low speeds in engines containing only a few cylinders when all intake valves are closed at once.

Exhaust gas recirculation A process in which exhaust gases (containing primarily nitrogen) are returned to the intake system to reduce emissions by lowering the combustion temperature.

Micromachining Formation of very small three-dimensional structures in a semiconductor material.

Speed density A method of calculating the intake mass air flow rate by measuring engine speed and air density.

Stoichiometry The air-to-fuel ratio at which all the oxygen is consumed during combustion.

Volumetric efficiency The volume flow rate of air into the intake system divided by the volume rate of piston displacement.

PETITIONER'S EXHIBIT 1002
US PATENT NO. 6,557,540

BIBLIOGRAPHY

Adler, Ulrich, *Automobile Electric/Electronic Systems,* Robert Bosch, Stuttgart, 1988.

DeCarlo, Joseph P., *Fundamentals of Flow Measurement,* Instrument Society of America, Research Triangle Park, 1984.

Heywood, John B., *Internal Combustion Engine Fundamentals,* McGraw-Hill, New York, 1988.

Norton, Harry N., *Handbook of Transducers,* Prentice Hall, Englewood Cliffs, N.J., 1989.

ABOUT THE AUTHOR

Robert E. Bicking received the B.E.E. and M.S.E.E. degrees from the University of Minnesota and has been involved with sensors nearly all of his 32 years in engineering. He is currently involved with the development of new automotive sensors at the Micro Switch division of Honeywell. He has been awarded three U.S. patents and is the author of over 24 technical papers. He is a member of the I.S.A., I.E.E.E., and S.A.E.

PETITIONER'S EXHIBIT 1002
US PATENT NO. 6,557,540

PETITIONER'S EXHIBIT 1002
US PATENT NO. 6,557,540

CHAPTER 5

TEMPERATURE, HEAT, AND HUMIDITY SENSORS

Randy Frank
Motorola Semiconductor Products

5.1 TEMPERATURE, HEAT, AND HUMIDITY

Temperature sensing and taking into account the effect of temperature on the performance and reliability of automotive components, and therefore the systems that contain these components, is one of the more important aspects of vehicle design. The heat sources that are present on modern automobiles range from the engine itself to catalytic converters, losses in power conversion (e.g. the alternator), and specific heat-generating devices such as heated windshields, seats, and mirrors. Humidity adds to the effect that temperature has on the reliability of components and also impacts vehicle performance and passenger comfort.

5.1.1 Temperature—the Effect of Heat

The temperature of a body or substance is (1) its potential of heat flow, (2) a measure of the mean kinetic energy of its molecules, and (3) its thermal state with reference to its ability to transfer heat to other bodies or substances.

Temperature affects every aspect of automobiles, from the performance of the engine and various vehicle systems to the comfort of the driver and passengers. The wide range of worldwide vehicle operating temperatures (from –60° to +57 °C) and the subsequent localized electronic module temperature ambients underhood (from –40 to +125 °C) and in the passenger compartments (from –40 to +85 °C) affect both the performance and reliability of electronic components. The viscosity of lubricating and cooling fluids is also affected by the wide temperature variations that must be tolerated. Even paint, fabric, plastics, rubber, and other organic and inorganic materials must be designed to survive the environmental extremes of temperature and humidity. Sensing the temperature of these components is essential during vehicle development.

5.1.2 Conduction, Convection, and Radiation

Heat energy is transferred with corresponding temperature changes by conduction, convection, and/or radiation. Conduction occurs by diffusion through solid material or in stationary liquids or gases; convection involves the movement of a liquid or gas between two points, and radiation occurs through electromagnetic waves.

PETITIONER'S EXHIBIT 1002
US PATENT NO. 6,557,540

5.1.3 Heat Sources in Vehicles

In addition to the temperature rise that can be generated by sunlight on the metal and glass that form the body of the vehicle, there are several heat-generating devices in a vehicle as shown in Table 5.1. The foremost heat source is the engine in internal combustion engine equipped vehicles. This causes the engine compartment to generally be classified as a +125 °C ambient for electronic components, although considerably higher temperatures are reached within the combustion chamber (≥1000 °C) or on the engine block.

The catalytic converter used to reduce unburnt hydrocarbons and carbon monoxide emissions has a peak catalyst efficiency around 450 °C, minimum operating temperature around 350 °C, and high temperature operation in the area of 1000 °C.

Tire flexure and friction generated between the tires and the road surface are major sources of heat. Moreover, heat is generated by friction between any moving components of a vehicle. Gears and bearings in transmissions, rear axle, and pumps are most notable for generating a significant temperature rise. Brake surfaces also create high temperatures when the brakes are applied.

Even though they do not generate heat, in the process of reducing the temperature of other components, heat exchangers—such as coolant or transmission radiators for the passenger compartment heater and their associated plumbing and electronic heat sinks—have considerably higher than ambient temperatures.

Electric heating elements, including heated back light, windshield, windshield wiper, mirrors, and seats, increase the temperature to improve visibility and driver comfort. Heated windshield wipers can be maintained at 15 °C even when outside temperatures are around −40 °C. In some cases, temperatures in the area of 350 °C are produced by supplemental heating elements for components such as the catalytic converter, the oxygen sensor, and some advanced electric vehicle batteries.

The windings of electric components such as the starter motor, heater motor, alternator, and solenoids are a source of heat and high temperatures, especially in continuously moving, heavily loaded units like the alternator. The resistance in the windings as well as resistance in semiconductor components like alternator rectifiers and power transistors creates a power loss proportional to the square of the current being conducted ($P = I^2R$). In semiconductors, the change in temperature is related to the power dissipated through the thermal resistance.

$$\Delta T = R_\theta P \tag{5.1}$$

where R_θ = thermal resistance in °C/W
ΔT = temperature difference in °C (frequently $T_{junction} - T_{case}$)
P = power in watts

TABLE 5.1 Heat Sources in Vehicles

General category	Example	Max. temperature °C
Engine	Combustion/ignition process	>1000
Catalytic converter	Chemical reaction	>1000
Road/tire friction	Tires	<100
Brakes	Disk/drum	250
Mechanical motion (gears, bearings)	Transmission/rear axle/air pump/power steering pump	200
Heat exchangers	Radiator (coolant, transmission), heater, heatsink	>175
Electric heaters	Windshield, backlight, seats, mirrors	Ta + 25
Electric windings	Motors, alternator, solenoids	<155 (Class F)
Resistors	Ballast resistor	150
Lamps	Headlamps, tail lamps, dash lamps	125
Power transistors	Ignition driver, voltage regulator	Up to 200
Electric vehicle battery	Sodium sulfur	300

PETITIONER'S EXHIBIT 1002
US PATENT NO. 6,557,540

Lamps have a significant inrush current (10 · steady state) and a high steady state value which generate high temperatures as well.

Temperature at various locations in the vehicle are shown in Table 5.2.

TABLE 5.2 Temperature at Various Vehicle Locations

Location	Temperature, °C		Slew Rate	Humidity		Frost
	Low	High		High	Low	
Underhood—Engine						
Exhaust manifold	–40	+649	–7 °C/min	95% at 38 °C	0	Yes
Intake manifold	–40	+121	–7 °C/min	95% at 38 °C	0	Yes
Underhood—Dash Panel						
Normal	–40	+121	Open	95% at 38 °C		
Extreme	–40	+141	Open	80% at 66 °C		
Chassis						
Isolated	–40	+85	NA	98% at 38 °C	0	Yes
Near heat source	–40	+121	NA	80% at 66 °C	0	Yes
At drive train temperature	–40	+177	NA	80% at 66 °C	0	Yes

5.1.4 Effect of Humidity

Humidity affects the comfort of the drivers and the passengers as well as the performance of the engine and impacts the reliability of vehicle components. The primary measurement for humidity is relative humidity RH, the ratio of water partial pressure to saturation pressure. Other measurements include dew point (temperature); specific humidity (mixing ratio); the mass of water per unit mass of dry gas; and volume ratio, the parts of water vapor per million parts of air. The dew point is a direct measure of vapor pressure and absolute humidity. Humidity is the water vapor in gas. Water in a solid or liquid is called moisture. High humidity and low dew point can lead to increased moisture content which can affect the operation of vehicle fluids such as fuel and brake fluid and impact solid surfaces like the windshield or brake linings.

5.1.5 Reliability Implications to Electronic Components

The effect of temperature on electronic components was recognized as "one of the most severe environments generally encountered on the automobile." Warm-up time of engine liquids and local ambient temperatures are as high as several tens of minutes, especially in cold weather. A recommended practice, SAE J1211, was published in November 1978 that still serves as a guideline to developing environmental design goals for electronic equipment, especially in the area of temperature variations within various vehicle locations.

Temperature affects the performance and expected life of electronic components. Mechanical stress created by different coefficients of thermal expansion can cause failures in thermal cycling test (air-to-air) or thermal shock (water-to-water) transitions.

The failure of electronic components also occurs because the mechanical durability, solder strength, or glass transition of plastic mold compound is exceeded. Electrical properties including thermal runaway in bipolar transistors and loss of gate control in MOS-gated (Sec. 5.4.6) devices also directly cause failure due to temperature extremes.

The typical failure rate for a semiconductor component can be expressed by the Arhennius equation:

$$\lambda = A \cdot \exp \frac{\theta}{kT} \tag{5.2}$$

PETITIONER'S EXHIBIT 1002
US PATENT NO. 6,557,540

where λ = failure rate
A = constant
exp = 2.72
θ = activation energy
k = Boltzmann's constant
$8.62 \cdot 10^{-5}$ eV/°K
T = temperature in °K

The failure rate of semiconductor components typically doubles for every 10 to 15 °C increase in operating temperature. However, increased testing and design improvements have minimized the failures due to specific failure mechanisms. Semiconductor components manufactured in the 90s are orders of magnitude more reliable than those first used in vehicles in the 60s. However, their response time is considerably faster than vehicle liquids and local ambients. For example, the transient thermal response, $r(t)$ $R\theta_{JC}$, which is a reduced level of the thermal resistance (Sec. 5.1.4) based on the transistor operating in a switching mode and being off for a period of time, approaches the dc level within a second. Excessive temperatures can be generated quickly and must be detected within milliseconds to prevent failure.

Accelerated life testing is performed at elevated temperatures to determine the reliability of electronic components and obtain the maximum amount of information in the minimum amount of time. The actual failure mechanisms are a result of the component design and environment in which they operate. Life testing seeks to identify areas that are vulnerable in a particular design and provides minimum acceptable criteria for qualification.

The activation energy is directly proportional to the degree of influence that temperature has on the chemical reaction rate. Temperature acceleration factors for a particular failure mechanism can be expressed as the ratio of the failure rates at two different levels of stress:

$$F_a = \exp\left(\frac{\theta}{k}\right) \cdot \frac{1}{T_r - 1/T_t} \tag{5.3}$$

where F_a = acceleration factor
θ = activation energy
k = Boltzmann's constant, $8.62 \cdot 10^{-5}$ eV/°K
T_r = junction temperature in °K at the rated ambient temperature
T_l = junction temperature in °K at the life test ambient temperature

To determine a component's ability to withstand the adverse effects of temperature and humidity extremes to which the vehicle is exposed, a number of reliability stress tests are included in the qualification procedure. These tests include:

- *High-temperature Storage Life* is performed to accelerate failure mechanisms which are thermally activated through extreme temperatures.

  Typical test conditions: T_a = 70 to 200 °C, no bias, time = 24 to 5000 h
- *Temperature Cycling* (air-to-air) evaluates the ability of a device to withstand both exposure to temperature extremes and transition between temperature extremes. This test also exposes excessive thermal mismatch between materials.

  Typical test conditions: T_a = –65 to 200 °C, cycle = 10 to 4000 (1000 most common)
- *Thermal Shock* (liquid-to-liquid) testing evaluates the ability of the device to withstand both exposure to extreme temperature and sudden transitions between temperature extremes. This testing also exposes extreme thermal mismatch between materials.

  Typical test conditions: T_a = 0 to 100 °C, cycle = 20 to 300 (100 most common)
- *H^3TRB* (high-humidity, high-temperature reverse bias) is an environmental test designed to measure the moisture resistance of plastic encapsulated devices. A bias is applied to accelerate corrosive effects on internal components of semiconductors.

  Typical test conditions: T_a = 85 to 95 °C, RH = 85 to 95%, bias = 80 to 100% of max rating, time = 96 to 1750 h

PETITIONER'S EXHIBIT 1002
US PATENT NO. 6,557,540

- *Autoclave* (or pressure cooker) testing is performed to measure device resistance to moisture penetration and resulting galvanic corrosion. This is a highly accelerated and destructive test.
  Typical test conditions: T_a = 121 °C, RH = 100%, p = 1 atmosphere, time = 24 to 96 h
- *Moisture Resistance* testing evaluates the moisture resistance of components under tropical environments.
  Typical test conditions: T_a = −10 to 65 °C, RH = 80 to 98%, time = 24 h/cycle, cycle = 10

In addition, a number of high-temperature tests under different biasing conditions are also performed for semiconductor devices, including high-temperature forward bias, high-temperature reverse bias, and high-temperature gate bias.

5.2 AUTOMOTIVE TEMPERATURE MEASUREMENTS

Numerous temperature measurements are made during the development of the vehicle to ensure the proper operation of systems and components. Some measurements are included in the control system strategy or as diagnostics for production vehicles. A list of the potential temperature and humidity measurements that can be made and may be incorporated in future systems is shown in Table 5.3. The technique used to measure temperature may vary from development to production mode, from one vehicle manufacturer to another and even from system to system within a given vehicle manufacturer. The choice in technology for production sensors depends upon performance, reliability, and cost. For development vehicles, cost is not a major concern, but availability of test probes, compatibility with readout equipment, and ease of use are additional factors that should be taken into consideration.

Common vehicle temperature measurements will be explained in the remainder of this section.

5.2.1 Measuring Liquid Temperatures

A number of liquid temperatures are measured during vehicle development, especially under high vehicle ambient temperatures and severe driving conditions, such as trailer towing up steep grades and stop-and-go Phoenix traffic during summer months. These include coolant, engine oil, transmission oil, fuel, power steering, brake, and battery electrolyte. Monitoring coolant temperature is common in engine control systems in production vehicles. Engine and transmission oil temperature are being evaluated for future monitoring. Racing vehicles frequently monitor oil and fuel temperature in addition to coolant temperature to achieve peak performance. Sensing fuel temperature may be required to meet future emissions standards. A latent heat cooling system has been developed that uses a temperature sensor to control the engine under various operating conditions. The system employs control valves that control the flow of vaporized coolant based on temperature in a manifold connected to the top of the combustion chamber.

Mounting location, fluid contacting the sensor, and packaging are critical concerns for liquid temperature sensors. Upper temperature limits are typically around 150 to 200 °C and operation down to −40 °C is usually required.

Battery temperature measurements in vehicle development use glass thermometers or glass-shielded thermocouple probes to protect the sensor from the corrosive electrolyte.

5.2.2 Battery Temperature

Maintaining the proper state of charge in the vehicle's battery is essential for obtaining adequate cranking rpm during starting and for ensuring optimum battery life. The charge accep-

PETITIONER'S EXHIBIT 1002
US PATENT NO. 6,557,540

TABLE 5.3 Sensing Requirements versus Vehicle Systems

System	Parameter
Engine control	Air charge (intake air) temperature Engine coolant temperature Intake air humidity Ambient temperature Fuel temperature
HVAC (climate control)	Humidity in passenger compartment (PC) Temperature (PC) Outside air temperature
Electronic transmission (continuously variable transmission)	Transmission oil temperature
Driver information (body computer inputs)	Coolant temperature Ambient air temperature Temperature (PC) Tire surface temperature Rain sensor Windshield moisture Sun sensor Battery temperature
Multiplex/diagnostics Cruise control Idle speed control Memory seat Navigation	Multiple usage of sensors
Antiskid brakes	Brake fluid temperature
Traction control/ABS	Brake moisture sensor
Air bags	
Suspension	
Electronic power steering	Power steering fluid temperature (also electric assisted)
Four-wheel steering Security and keyless entry	

tance curves of lead-acid batteries require that the charging voltage be modified for temperature. A higher voltage is required at lower temperatures. Cold temperatures also place the most difficult requirements on the battery because the viscosity of engine oil is low and the load on the cranking system is very high.

Compensation circuitry in the voltage regulator in the charging system is designed to provide a voltage that is within an acceptable range over the entire vehicle operating temperature range as shown in Fig. 5.1. Semiconductor sensing techniques (Sec. 5.4.6) are used in this approach. The most desirable location for the voltage regulator is close to the battery. However, some systems integrate the regulator inside the alternator and provide a temperature environment that can be considerably different from the battery. The temperature of the battery can also vary by several degrees from cells closest to the engine to those further away from the engine. The overall mass of the battery prevents these temperatures from changing very quickly. However, a failed voltage regulator that applies full voltage to the alternator can easily cause excessive battery temperatures to be generated.

PETITIONER'S EXHIBIT 1002
US PATENT NO. 6,557,540

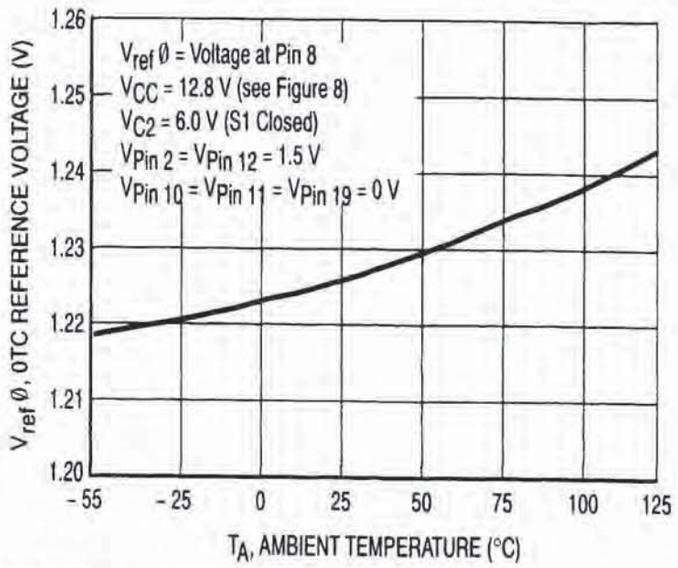


FIGURE 5.1 Temperature compensation in voltage regulator.

Batteries for electric vehicles (EVs) may require maintaining a specified high-temperature operating range. Sodium sulfur cells can store four times the energy of lead acid cells, but the battery's operating temperature must be kept within 300 to 350 °C. Solid oxide fuel cells operate at 1000 °C. If higher-temperature batteries are adopted for use in EV systems, sensing the battery temperature could be part of the diagnostic and fault detection.

5.2.3 Air Temperature Measurements

Air is measured for ambient temperature, passenger compartment temperature, and inlet air on production vehicles. For development purposes, a number of location ambients are always evaluated as potential mounting locations for electronic components. Upper temperature ranges are lower than liquid measurements, with 85 or 125 °C being common upper limits.

5.2.4 Catalyst Temperature

Measuring catalyst temperature during vehicle development has been performed since the earliest implementation of these devices. Concern for excessive temperatures in nearby vehicle locations meant that a number of measurements were made. However, the converter must be at a minimum temperature, usually above 350 °C, to be effective. Tougher exhaust emission standards are spurring manufacturers to utilize the converter sooner after the vehicle is started. Techniques are being pursued that would decrease the warm-up time for the catalyst to increase its effectiveness in controlling emissions. One technique involves heating the catalyst briefly by igniting a measured mixture of fuel and air in an afterburner ahead of the catalyst. Another technique utilizes electric heating to reduce the warm-up time. The power required for this approach would require an excessive power drain from the vehicle's power system. A linear temperature sensor has been developed to measure the temperature across the catalyst. A thermistor (see Sec. 5.4.1) is inserted diagonally inside the converter. A range of resistance has been evaluated and a time constant of about 2 s has been achieved. For fault condition monitoring, the sensor is able to detect a localized hot spot inside the catalyst and may prove to be able to detect misfire as part of future on-board diagnostic equipment required by the California Air Resources Board or the federal Environmental Protection Agency.

PETITIONER'S EXHIBIT 1002
US PATENT NO. 6,557,540

The temperature of exhaust gases increases rapidly under severe operating conditions such as continuous high speed or insufficient octane rating. One company has monitored their efforts at controlling the engine's operating temperature by locating a temperature sensor in the exhaust manifold. If the sensor detects an exhaust gas temperature rise above an established limit, a computer sends a command to inject extra fuel into the combustion chamber to cool the engine. Since exhaust gas temperatures can reach 1000 °C, a specially designed magnesium oxide thermocouple in a metal tube is used to sense the temperature (see Sec. 5.4.2). This approach may also be used in the future to reduce catalyst warm-up time.

5.2.5 Oxygen Sensor

The oxygen sensor used as the feedback element in closed-loop engine control systems generates a signal based on the difference in the oxygen concentration from inside the exhaust gas and ambient. As shown in the Nernst equation:

$$V_S = RT/4F \ln (P_a/P_g) \tag{5.4}$$

where V_S = the generated output voltage
P_a = oxygen partial pressure of the air
P_g = oxygen equilibrium pressure
R = gas constant
F = Faraday's constant
T = absolute temperature of the sensor

In addition to being affected by temperature, the oxygen sensor requires a minimum temperature to operate properly and provide a closed-loop control system. Typically, this minimum temperature is ≥450 °C. To reduce the oxygen sensor's warm-up time, heaters are added. A heated oxygen sensor achieves operating temperature much sooner than an unheated unit and allows closed-loop operation to be initiated. Monitoring temperature during engine and vehicle development is part of control strategy and component development.

5.2.6 Tire Temperature Sensing

Sensing the temperature within the tire is part of the pressure measurement and fault detection provided by tire pressure measuring and automatic adjustment systems. In a system like the one developed by Michelin (Fig. 5.2) that is used on Peugot's experimental sports car, the Proxima, both a pressure and temperature sensor are located on each wheel. A circular antenna and a transceiver allow these signals to be sent to an electronic processing module. An air compressor attempts to maintain desired tire pressure under normal conditions. If the pressure-temperature indications go above 85 °C, the system recommends speeds be held below 240 km/h (148 m/h). For temperatures above 90 °C, the limit is 160 km/h and for 95 °C, the limit is 80 km/h. For temperatures in excess of 100 °C, the system recommends stopping the vehicle.

5.2.7 Fault Detection for Electronic Components

As indicated in Sec. 5.1.6, temperature can cause reliability failures from several mechanisms in electronic systems. Therefore, detecting excessive temperature and designing system strategies to account for excessive temperatures can minimize improper operation and catastrophic failures.

Sensing for fault conditions, like a short circuit, is an integral part of power ICs or smart power transistors. The ability to obtain temperature sensors in mixed Bipolar-CMOS-DMOS semiconductor processes provides protection and diagnostics as part of the features of smart power ICs, like Motorola's SMARTMOS™ products. The primary function of the power IC is to provide a microcontroller-to-load interface for solenoids, lamps, and motors. It is a definite

PETITIONER'S EXHIBIT 1002
US PATENT NO. 6,557,540

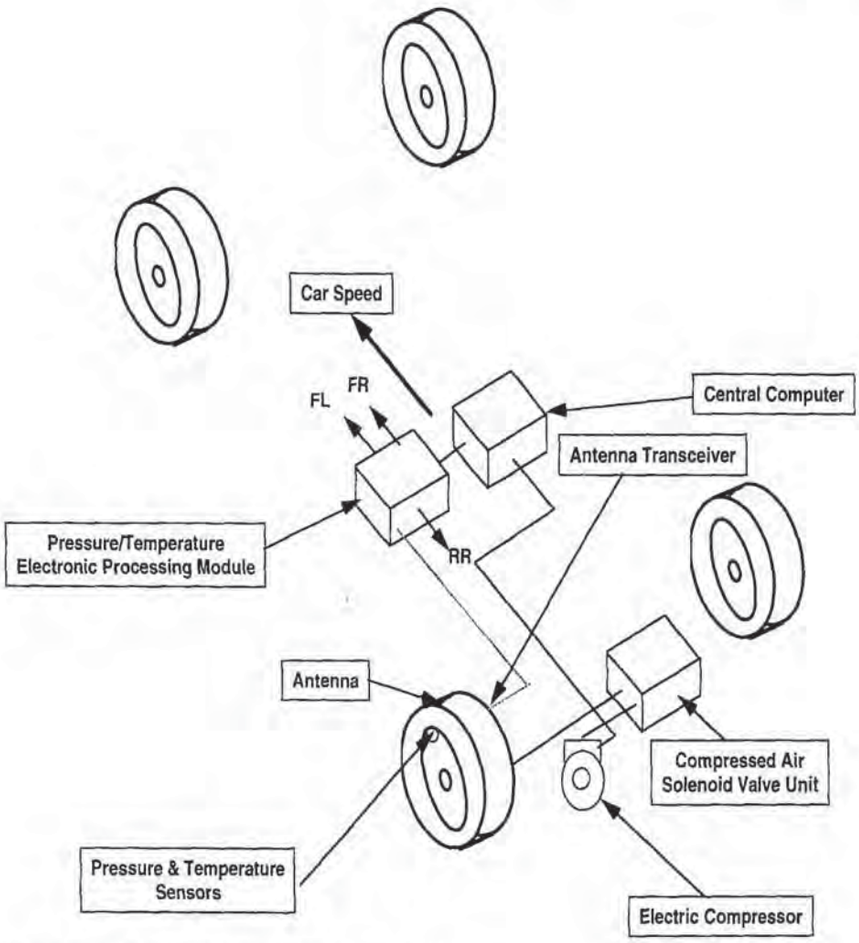


FIGURE 5.2 Temperature sensing in tire pressure control.

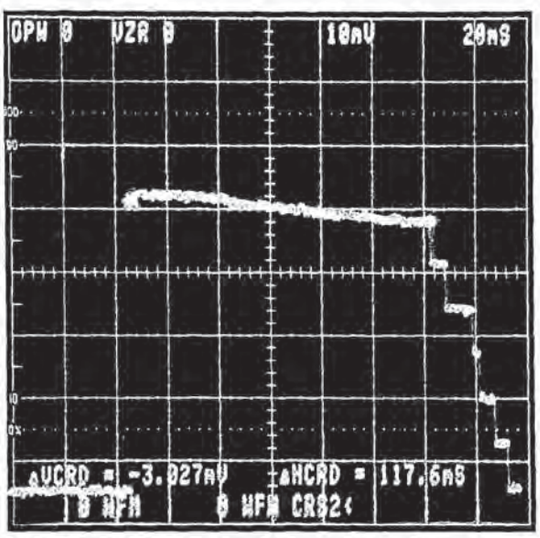


FIGURE 5.3 Thermal shutdown of six outputs of smart power IC.

PETITIONER'S EXHIBIT 1002
US PATENT NO. 6,557,540

advantage in multiple-output devices, to sense the junction temperature of each device, provide status input to the microcontroller and, if necessary, shut down a particular unit that has a fault condition. The sequential independent shutdown of six output drivers with a short applied across each unit's load is shown in Fig. 5.3. The action that is taken based on sensing a fault condition can vary depending on the control system. Sensing excessive temperature in a power device may mean that the device can turn itself off to prevent failure in one case and in another situation, a fault signal provides a warning but no action is taken. The remaining portion of the system is allowed to function normally. With the fault conditions supplied to the MCU, an orderly system shutdown can be implemented.

5.2.8 Mass Air Flow Sensor

The generalized model of a transducer is shown in Fig. 5.4. In addition to the desired input, undesired environment effects, like temperature and, to a lesser extent, humidity, are factors that affect the performance and accuracy of the transducer and must be taken into account during the design of the transducer.

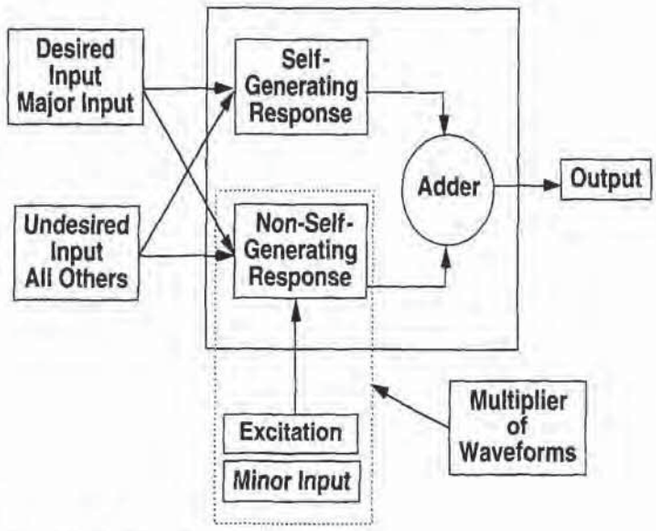


FIGURE 5.4 Generalized model of a transducer.

In the case of mass air flow sensing, temperature effects are used as part of the measurement process. A typical approach for mass air flow involves a hot-wire anemometer with a platinum wire as the sense elements, as shown in Fig. 5.5. The air temperature probe detects the temperature of the air flowing into the combustion process. The hot-wire probe is heated by current supplied from a power transistor. The difference in temperature between the probes is detected as a difference in electrical resistance. The electronic circuitry regulates the heating current to the hot-wire probe to keep the temperature difference constant at any flow rate (Fig. 5.6). The current required is proportional to the air flow rate. One of the main issues in this type of sensor is the response time. Improvements which reduce the response time from 50 to 30 ms have been made in recently developed units.

A microbridge silicon mass air flow sensor has been developed that utilizes temperature-resistive films laminated within a thick film of dielectric material and micromachined cavity as shown in Fig. 5.7. The resistors are suspended over the etched cavity, which also provides thermal isolation for the heater and sensing resistor. Heat is transferred from one resistor to the other as the result of flow. The imbalance in the resistance caused by the heat transfer

PETITIONER'S EXHIBIT 1002
US PATENT NO. 6,557,540

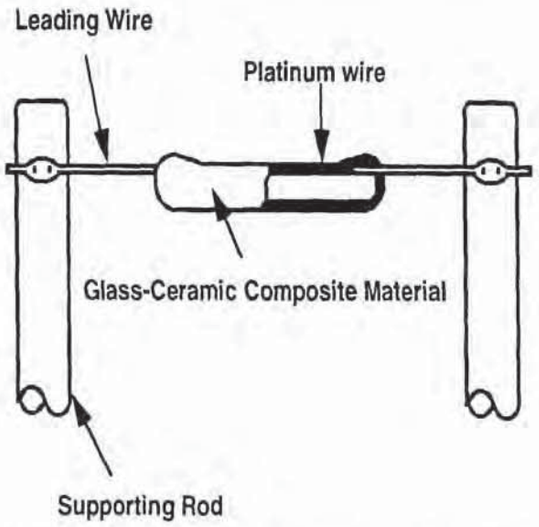


FIGURE 5.5 Probe for hot-wire anemometer mass air flow sensor.

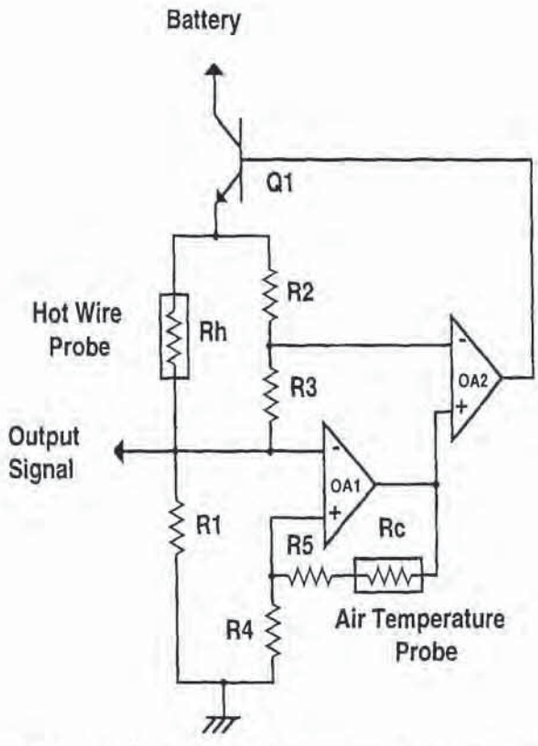


FIGURE 5.6 Circuit for hot-wire anemometer mass air flow sensor.

PETITIONER'S EXHIBIT 1002
US PATENT NO. 6,557,540

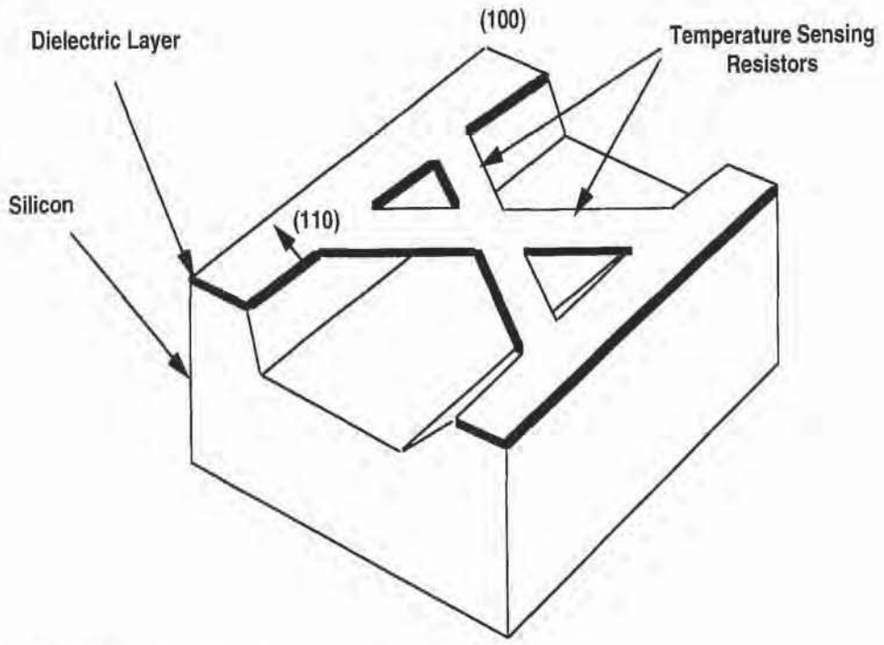


FIGURE 5.7 Temperature sensor in microbridge mass air flow sensor.

is directly proportional to the flow. The small size of the resistors allows fast response time (≤3 ms) and high sensitivity to flow. The device has also been found to be useful as a differential or absolute temperature sensor.

5.2.9 Temperature Measurements in New Systems

As new vehicle systems are developed or existing systems are modified to provide improved performance, or meet legislated or customer demands, new applications for temperature sensors will occur. An example of two systems, air bags and thermo accumulator, is provided.

In inflatable restraint systems, the air bag is inflated based on the ignition of a gas generant. In this system, an igniter receives an electric impulse, passes it through to a heating filament, and actuates a small pyrotechnic charge to ignite the gas generant, which produces nearly pure nitrogen gas to inflate the bag. The initial temperature is high but the nitrogen gas cools rapidly, so a fully deployed bag is only slightly above room temperature. Measuring the temperatures that occur during this event is part of the development activity.

A heat battery, or thermoaccumulator, can store the latent heat from a previously driven vehicle for up to three days at an ambient temperature of –29 °C. The accumulator is made of salt-based crystals which change from solid to liquid form above 78 °C. Heat provided by this device has proven to reduce the emissions which are generated during the first 20 s of the federal emissions test procedure. The unit also has potential application in passenger compartment heating.

5.3 HUMIDITY SENSING AND VEHICLE PERFORMANCE

Correlation of a number of vehicle tests requires that the humidity be monitored. Variations in humidity can explain variations that occur in test results.

PETITIONER'S EXHIBIT 1002
US PATENT NO. 6,557,540

Significant, repeatable, and controllable results may lead to humidity sensing being part of future engine control systems and passenger compartment comfort control systems.

Some sensors, such as rain (and/or windshield moisture) or sun sensors, are already being used on some vehicles to control wiper blade and fan controls.

5.3.1 Engine Performance

Injecting water to cool the intake charge and prevent premature detonation is a technique that has been used in high-compression (≥10:1) engines. The cooling effect from evaporation reduces the operating temperature.

An increase in inlet air humidity has been shown to reduce the nitric oxide emissions. Condensation in the gas tank can add a considerable amount of moisture to the fuel. Measuring the actual amount of humidity or moisture present during development tests is useful to identify all variables that can affect performance.

5.3.2 Passenger Compartment Comfort

A traditional passenger temperature control system shown in Fig. 5.8 uses only temperature as the indication for the system to open or close blend doors in the HVAC (heater, ventilating, and air conditioning) system. Laboratory evaluations monitor the HVAC systems' effectiveness under known and controlled humidity conditions. A fuzzy logic system combining temperature and humidity sensing has been investigated by researchers for home use. In this case, additional humidity is available to speed up the effect of adding heat. In a vehicle application, the blower speed could be adjusted based on the presence of humidity or an alternate strategy could be developed which uses less energy from the vehicle to make the driver and passengers comfortable.

The development of new test techniques frequently involves either the development of new sensors or novel use of existing sensors. A sweat impulse test developed at Volkswagen AG allows researchers to evaluate the ability of a seat to direct sweat away from its surface.

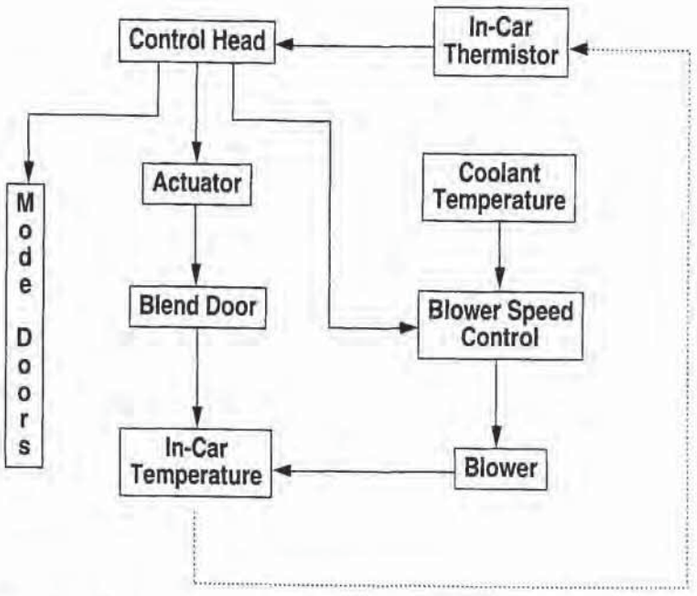


FIGURE 5.8 Automatic temperature control diagram.

PETITIONER'S EXHIBIT 1002
US PATENT NO. 6,557,540

As part of the measurement process, a platinum RTD (Sec. 5.4.5) and a capacitive humidity sensor provide data. In excessive sweating situations, the fabric is unable to absorb sufficient moisture, so it is passed to the surrounding environment as increased humidity.

5.3.3 Brake Moisture Sensing

Brake fluids are hygroscopic and, therefore, absorb moisture. Sufficient moisture lowers the boiling point of the brake fluid, and eventually vaporizes the fluid resulting in loss of stopping power. A meter has been developed that can be inserted into the master cylinder reservoir and measure the boiling point of the brake fluid. A heating element boils a sample of the brake fluid. A microcontroller calculates the actual boiling point by the initial temperature reading, temperature drop, and time between cooling and boiling. This approach may be applicable to other vehicle fluids that can be checked during maintenance procedures.

5.4 SENSORS FOR TEMPERATURE

Several different sensing techniques are used in production vehicles and during vehicle development to provide the temperature measurements. Table 5.4 shows a list of these techniques and the temperature range that is typical for this approach. Characteristics of temperature-sensing devices that allow a designer to determine if the approach will meet development or production requirements are explored in this section. In addition to the operating temperature range, linearity, response time, packaging, reliability, and cost are factors that must be considered. Temperature sensors can be as simple as thermal expansion devices, such as mercury or alcohol thermometers, or as complex as infrared sensors used in night vision systems. Common sensors and some recent additions to temperature sensing are covered in this section. Other sensor techniques, including the temperature-generating characteristics of quartz and temperature-sensing reed switches, are also possible but not covered.

5.4.1 Thermistors

Thermistors have found broad application acceptance in several vehicle systems that require temperature sensing from the coolant system to control the engine. The thermistor is a special

TABLE 5.4 Temperature Sensing Techniques versus Operating Range

Sensing technique	Temperature range, °C	Usage: Production (P) Development (D) Future (F)
Thermistor	0 to 500	P
Thermocouple	−200 to +3000	D
Bimetallic switch	−50 to +400 (650)	P
Potentiometer temperature sensor	−40 to +125	P
Platinum wire resistor (RTD)	−200 to +850 (−40 to +200)	D (P)
Semiconductor (junction)	−40 to +200	P
Thermostat (pressure spring)	−50 to +500	P
Fiber optic temperature sensor	+1800	D/F
Temperature indicator	+40 to +1350	D
Infrared	>Ta	F
Liquid thermometer	−200 to +1000	D

PETITIONER'S EXHIBIT 1002
US PATENT NO. 6,557,540

class of resistance temperature sensor (Sec. 5.4.5) based on semiconductor type materials that exhibit a wide range of temperature coefficients. The resistivity depends upon the material used to form the thermistor. Both negative (NTC) and positive temperature coefficient (PTC) devices can be produced. Commercially available thermistor forms are beads, probes, disks, and rods. The characteristics of thermistor output are shown in Fig. 5.9. The exact relationship between temperature and resistance depends on the material used for the sensor, but the general form of the output can be expressed by the equation

$$R = R_O \cdot e^{\beta(1/T - 1/T_O)} \tag{5.5}$$

where R = resistance at temperature T in ohms
R_O = resistance at temperature T_O in ohms
e = base of natural log
T, T_O = absolute temperature in K
β = indicator of shape of NTC curve

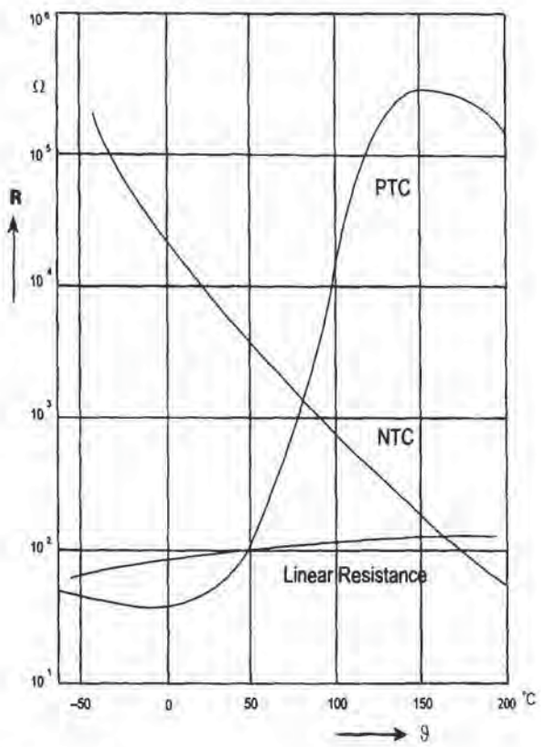


FIGURE 5.9 Thermistor output versus temperature.

This accounts for the high degree of nonlinearity in the output. However, the thermistor's nonlinearity can either be tolerated in many automotive applications, or corrected by an MCU or by circuit techniques. In the case of the water temperature indicator, for example, the thermistor's resistance is matched to a normal operating point on the gage; thus, the nonlinearity during conditions that generate higher temperature is not a problem.

Thermistors have a usable temperature range from –250 to +650 °C. Recent developments in automotive thermistors have focused on techniques to reduce cost and improve the manufacturability and reliability.

PETITIONER'S EXHIBIT 1002
US PATENT NO. 6,557,540

5.4.2 Thermocouples

Thermocouples are used frequently during the development phase of the vehicle because of their low cost, the broad range of temperature measurements that are possible from a single thermocouple such as iron-constantan, ease of extending the range through other materials, ease in obtaining a variety of form factors (especially small shapes), ease in forming the thermocouple, and ease in interfacing to temperature-recording equipment. The thermocouple type, wire size, and construction are factors that allow different units to be used from –250 to +1700 °C.

A thermocouple is formed by a pair of dissimilar conductors connected at one end. A voltage output E, proportional to the difference in temperature T_1 and T_2, is the basis of thermoelectric temperature measurements, also known as the Seebeck effect.

Thermocouple junctions can be formed by welding, soldering, or pressing materials together. Measurements can be made very easily; however, the highest accuracy is obtained by taking into account a number of factors, including reference junction considerations and a number (five) of laws that govern thermocouple behavior. Common types and their operating characteristics are shown in Table 5.5.

TABLE 5.5 Common Thermocouples and Application Factors

	Conductor		Temperature	Standard error	Seebeck
ISA code	Positive	Negative	Range, °C	Limit, °C	Coefficient, μV/°C
E*	Chromel	Constantan	0 to +316	±2	62
J*	Iron	Constantan	0 to +277	±2	51
T*	Copper	Constantan	–59 to +93	±1	40
K*	Chromel	Alumel	0 to +277	±2	40
N*	Nicrosil	Nisil	0 to +277	±2	38
S*	Platinum†	Platinum	0 to +538	±3	7
R*	Platinum‡	Platinum	0 to +538	±3	7

* Other temperature ranges and error limits are available.
† 10% Rhodium.
‡ 13% Rhodium.

5.4.3 Bimetallic Switch

A bimetallic temperature switch uses two metal strips with different coefficients of linear expansion that are welded together. Increasing temperature causes the strips to warp predictably. A switch point can be established by an initial calibration that indicates that a critical temperature has been reached and provides an input to an electronic control unit or a lamp indication. Switch types can be disk or cantilever construction. The use of switches does not require analog-to-digital conversion in control systems with microcontrollers, but provides limited information (only above or below a desired operating point) about the system. Early engine control systems used a disk switch in the air cleaner to indicate operation below 13 °C and a cantilever design in the engine coolant to indicate temperature above 71 °C.

5.4.4 Potentiometer Temperature Sensor

A bimetallic actuator can be combined with a high-resolution potentiometer to provide a temperature sensor for automotive applications. The linear movement of the bimetallic stack is transmitted by a stainless steel tube and measured as a distance by a conductive plastic film potentiometer providing a linear indication of temperatures up to 650 °C. The time constant for the sensor is approximately 70 s.

PETITIONER'S EXHIBIT 1002
US PATENT NO. 6,557,540

5.4.5 RTDs

A resistive temperature detector, or RTD, made of platinum is the highest inherent accuracy temperature sensor. The RTD has an output that varies with temperature based on the following equation:

$$\text{RTD} = R_O \cdot (1 + A \cdot T + B \cdot T^2) \tag{5.6}$$

where RTD = value of RTD at 0 °C in ohms and is 100 Ω for Pt100 and 200 Ω for Pt200
A = detector constant = $3.908 \cdot 10^{-3}$ ($°C^{-1}$) for Pt100
B = detector constant = $-5.802 \cdot 10^{-7}$ ($°C^{-2}$) for Pt100
T = temperature in °C

A constant current is applied to the RTD to obtain a voltage output over the range from −200 to +850 °C. Linearity can be within 3.6 percent for a range of 0 to 850 °C.

Other metals like nickel, nickel-iron alloy, copper, and aluminum can also be used for the RTDs. In addition to wire-wound RTDs, thin-film techniques also allow an RTD to be applied to a substrate, such as ceramic or silicon.

5.4.6 Semiconductor Techniques

Several semiconductor parameters vary linearly over the operating temperature range. As shown in Fig. 5.10, the gate threshold voltage of a power MOSFET changes from 1.17 to 0.69 times its 25 °C value when the temperature increases from −40 to 150 °C. Also, the breakdown voltage of the power MOSFET varies from 0.9 to 1.18 times its value at 25 °C over the same −40 to 150 °C temperature range (Fig. 5.10). These relationships are frequently used to determine the critical temperature (junction temperature) of semiconductor components in actual circuit operation. External package-level temperature measurements can be several degrees different than the junction temperature, especially during rapid, high-energy switching events. The actual junction temperature and the resulting effect on semiconductor parameters must be taken into account for the proper application of semiconductor devices. Semiconductors can be used for sensing temperature within their operating temperature range.

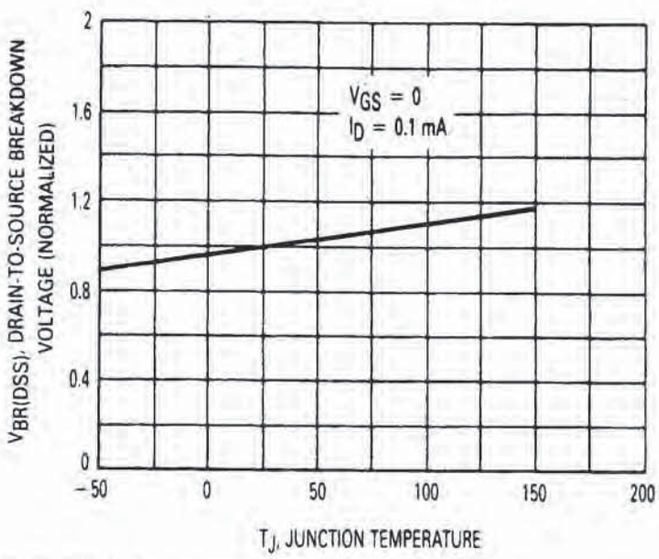


FIGURE 5.10 Breakdown voltage versus temperature.

PETITIONER'S EXHIBIT 1002
US PATENT NO. 6,557,540

The most commonly referenced transistor temperature measurement is the V_{BE} relationship to temperature. A silicon temperature sensor that utilizes this effect has a nominal output of 730 mV at –40 °C and an output of 300 mV at 150 °C. The linearity of this device is shown in Fig. 5.11. The total accuracy is within ±3.0 mV including nonlinearity which is typically within ±1 °C in the range of –40 to 150 °C. The readings are made with a constant (collector) current of 0.1 mA passing through the device to minimize the effect of self-heating of the junction.

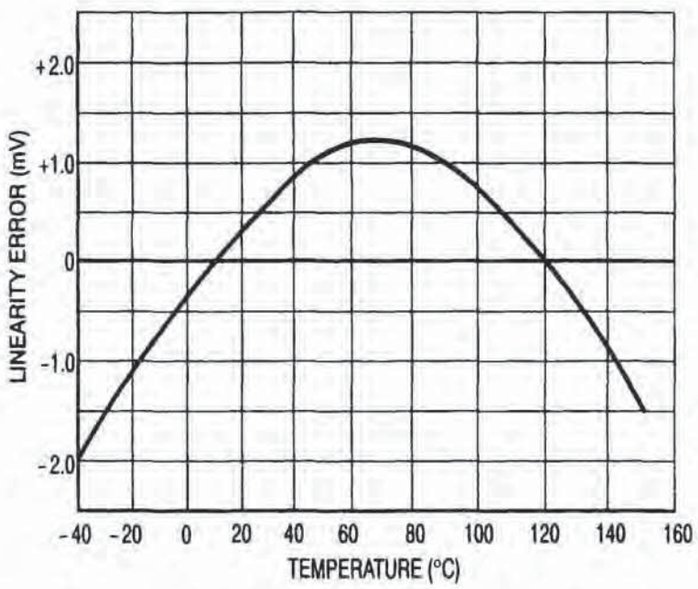


FIGURE 5.11 Linearity of silicon temperature sensor.

The linear relationship of the V_{BE} of a transistor to temperature provides a considerable improvement in accuracy over a thermistor. However, the limited operating range of semiconductor temperature sensors (–40 to 150 °C) has limited their application in vehicles. To be cost-effective in automotive applications, semiconductor sensing is usually incorporated with other sensing or interface devices.

An RTD (Sec. 5.4.5) with an aluminum metal film has been integrated with a semiconductor process to provide a temperature sensor that can directly drive the analog-to-digital input in a microcontroller unit (MCU). The sensor has better than ±2 percent accuracy over a –50 to 150 °C temperature range. On-chip linearization techniques avoid look-up table linearization by the MCU.

Another integrated semiconductor temperature sensor uses the fact that two identical transistors operating at a constant ratio of collector current densities r results in the difference in base-emitter voltages being $(kT) \cdot (\ln r)$. Both Boltzman's constant k and the charge of an electron q are constant, so the resulting voltage is directly proportional to absolute temperature. The voltage is then converted to a current by low-temperature coefficient thin-film resistors.

Polysilicon diodes and resistors can be produced as part of a power MOSFET semiconductor manufacturing process and used as temperature-sensing elements to determine the junction temperature of the device. The thermal sensing that is performed by the polysilicon elements is a significant improvement over power device temperature sensing that is performed by an external temperature-sensing element. An extreme thermal gradient exists between the maximum junction temperature at the top (active area) of the power device and the remote point which is able to be measured by a thermistor or thermocouple. Placing the thermal-sensing element inside the package improves the measurement process considerably.

PETITIONER'S EXHIBIT 1002
US PATENT NO. 6,557,540

By sensing with poly resistors or diodes, the sensor can be located close to the center of the power device near the source bond pads where the current density is the highest and, consequently, the highest die temperature occurs. The thermal conductivity of the oxide that separates the polysilicon diodes from the power device is two orders of magnitude less than that of silicon. However, because the layer is thin, the polysilicon element offers an accurate indication of the actual peak junction temperature.

A very low on-resistance power FET that incorporates a temperature sensing diode is shown in Fig. 5.12. The power device achieves an on-resistance of 5 milliohms (including packaging resistance) at 25 °C utilizing a production power FET process. The power FET process was chosen instead of a power IC process because a large die size was required to meet the power dissipation requirements of a very cost sensitive application. A minor modification (the addition of a single masking layer) to a production power FET process allows both sensing and protection features to be integrated. Devices that are produced using the SMARTDISCRETE technology, as this approach is called by Motorola, are one way to provide more cost-effective, smart power semiconductors, especially for high-current or low on-resistance power applications.

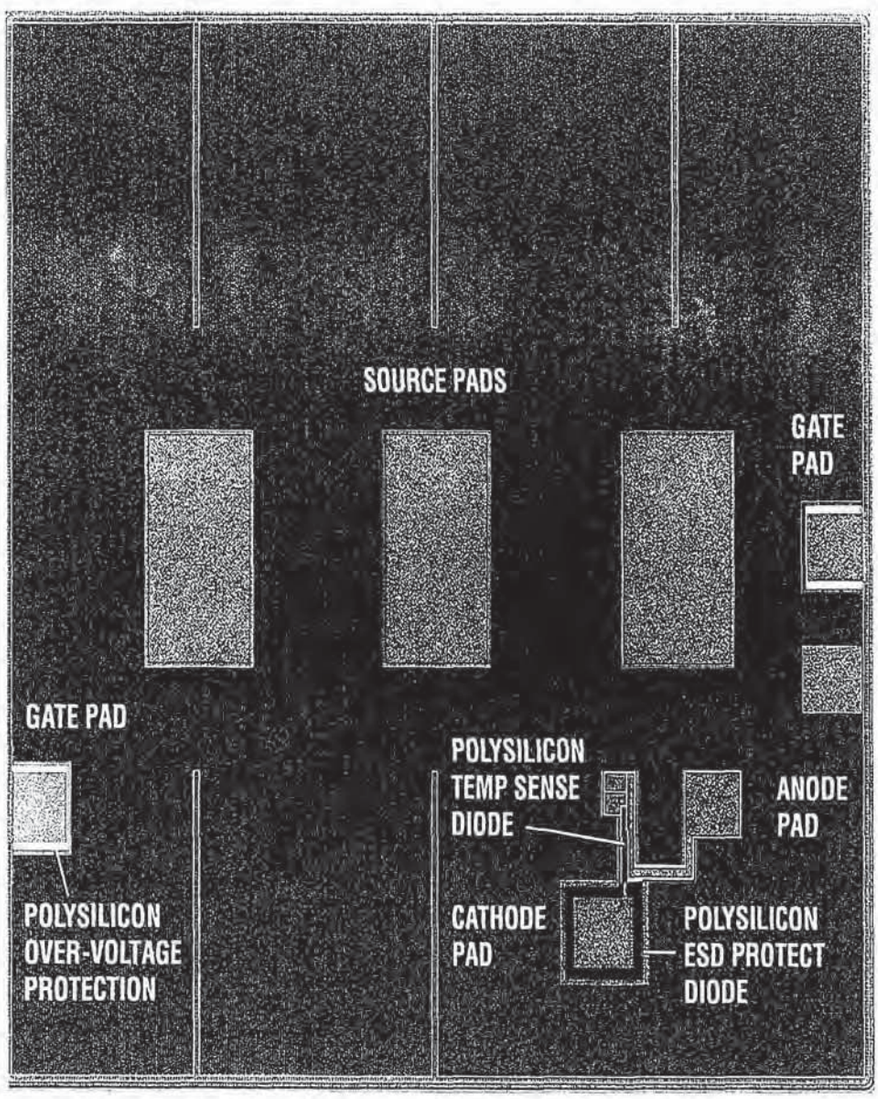


FIGURE 5.12 Temperature sensor integrated in power MOSFET. *(Die photomicrograph Courtesy Motorola Inc.)*

PETITIONER'S EXHIBIT 1002
US PATENT NO. 6,557,540

An accurate indication of the maximum die temperature is obtained by monitoring the output voltage when a constant current is passed through the integrated polysilicon diode(s). A number of diodes are actually provided in the design. A single diode has a temperature coefficient of 1.90 mV/°C. Two or more diodes can be placed in series if a larger output is desired. For greater accuracy, the diodes can be trimmed during wafer-level testing by blowing fusible links made from polysilicon. The response time of the diodes is less than 100 μs which has allowed the device to withstand a direct short across an automobile battery with external circuitry providing shutdown prior to device failure. The sensing capability also allows the output device to provide an indication (with additional external circuitry) if the heatsinking is not proper when the unit is installed in a module or if a change occurs in the application which would ultimately cause a failure.

A smart power IC, like Motorola's SMARTMOS™ process, can have multiple power drivers integrated on a single monolithic piece of silicon. Each of these drivers can have a temperature sensor integrated to determine the proper operating status and shut off only a specific driver if a fault occurs. The temperature sensor is basically a band gap reference. In this case, two diodes' junctions are biased with different current densities. Circuitry in the smart power IC process establishes a voltage reference and a trip point.

5.4.7 Thermostat (Mechanical Temperature Sensing)

The earliest method of temperature regulation used in vehicles is still in use today—the thermostat. The expansion element usually activates a valve which redirects the flow of coolant into a radiator bypass line when a specific temperature is reached.

5.4.8 Fiber Optic Temperature Sensors

High-temperature sensors capable of operating up to 1800 °C have been developed using optical fibers. The response time of the sensor is on the order of 500 ms and the accuracy is within ±0.5 percent. The noncontact sensor uses a single optical fiber that has an outside diameter of 0.5 to 1.0 mm. The probe structure is critical to the sensor's sensitivity and the distance coefficient that relates the detection surface area to the distance at which the probe will be placed for measurement.

A sapphire fiber optic sensor has been developed to measure high temperatures such as those found near the tip of a spark plug during combustion. The sensor can withstand temperatures up to 4000 °C and has an accuracy of 0.2 percent at 1000 °C. The sensor has been used to identify knock and to characterize flame front propagation.

5.4.9 Temperature Indicators

Temperature-indicating materials have been developed with melting points that can be calibrated to ±1 °C. When the temperature of the device is exceeded, a phase change occurs and the material changes color. The material is available in paint, patch, pellet, and applicator stick form. Temperature ranges from 38 to 1371 °C are available. This kind of indication is useful during the development phase of automotive components to verify that a critical design temperature has not been exceeded.

5.4.10 Infrared Temperature Sensing

Blackbody emittance is the basis for infrared (IR) thermometry. Objects at temperatures above –273 °C emit radiant energy in an amount proportional to the fourth power of their

PETITIONER'S EXHIBIT 1002
US PATENT NO. 6,557,540

temperature. An IR sensor consists of collecting optics, lenses, and/or fiber optics, spectral filtering, and a detector as the front end. The primary characteristic of the optics is the field of view (FOV) which allows a specific target to be measured at a prescribed distance.

Infrared sensors have been used extensively for noncontact temperature measurements in process control. In automobiles, infrared sensors use temperature variations to produce a monochrome image in night vision systems. Board-level temperature testing also utilizes IR-sensing techniques to identify hot spots and potential failure points.

5.4.11 Thermal Actuators/Thermal Cooling

Chemical sensors like the oxygen sensor described in Sec. 5.2.6 require a minimum operating temperature to be effective. Semiconductor technology allows platinum and silicon heaters and temperature sensors to be produced on a thin diaphragm, or window, etched into a silicon substrate. Temperatures can be produced in the window which exceed 1200 °C, while the supporting rim of silicon remains essentially at room temperature. This ability may allow fast-response sensors to be developed for vehicle applications.

Other silicon development activity using micromachining techniques may allow heat pipes and silicon-level heatsinks to remove heat more effectively from rapidly switching semiconductor devices.

5.5 HUMIDITY SENSORS

Humidity sensors are used extensively during vehicle and component development, especially in determining the ability to withstand humidity and temperature cycling tests. Engine performance can be affected by humidity. A sensor that can pass rigorous automotive qualification tests and meet the desired specifications and cost criteria would provide additional input for the engine control system. In a less rugged application, HVAC systems may benefit from the input from humidity sensors. Humidity sensors are not used on production vehicles at the present time. However, some potential techniques that are used in development and nonautomotive applications are described in this section.

Techniques to measure humidity are listed in Table 5.6. Most of these are actually laboratory instruments. The most well known approach to humidity measurements is the use of wet bulb and dry bulb thermomometer readings interpreted through the use of a psychrometric chart which relates all basic humidity readings. The effect of humidity on polymers and the use of semiconductor-processing techniques has created actual sensors that do not require the constant calibration, have less drift, improved reliability, and potentially can achieve automotive cost objectives. Three sensing techniques that have potential for future vehicle use are capacitive, resistive, and oxidized porous silicon.

5.5.1 Capacitive Humidity Sensors

A thin-film polymer capacitive-type relative humidity sensor can be produced by using semiconductor technology. The dielectric constant of the polymer thin film changes linearly with changes in atmospheric relative humidity. A desirable feature, in addition to long-term stability and operation to 180 °C, is fast wet-up/dry-down performance.

A temperature sensor can easily be added to the RH sensor, which increases the operating range and the functionality.

PETITIONER'S EXHIBIT 1002
US PATENT NO. 6,557,540

TABLE 5.6 Techniques for Measuring Humidity/Moisture

Principle	Type measurement
Gravimetric hygrometer	Instrument
Pressure-humidity generator	Instrument
Wet bulb/dry bulb (psychrometer)	Instrument
Hair element	Instrument
Electric conductivity	Instrument
Dew cell	Instrument
Chilled mirror	Instrument
Karl Fisher titration	Instrument
Electrolytic	Instrument
Lithium chloride	Instrument
Capacitance hygropolymer	Production sensor
Bulk polymer (resistance)	Production sensor
Thin-film polymer (capacitance)	Production sensor
Gold/aluminum oxide	Production sensor
Oxidized porous silicon (OPS)	Experimental sensor

5.5.2 Resistive Humidity Sensors

Both surface and bulk polymer resistance sensors have been developed for measuring relative humidity. In bulk polymer film units, mobile ions are released from the molecular structure with increased humidity levels resulting in orders-of-magitude change in resistance over the operating range. Diode temperature compensation is used to improve accuracy over the temperature range. With an ac excitation at 1 kHz, a change from 10 to 100 percent RH produces a corresponding resistance variation from $2 \cdot 10^7$ to $2 \cdot 10^3$ ohms.

5.5.3 Oxidized Porous Silicon

A capacitive-type sensor has been developed that uses oxidized porous silicon (OPS) as a moisture-absorbing dielectric between the electrodes of the capacitor. An electrolysis process is used to create a thin porous layer on the top of a silicon wafer. The silicon is converted to OPS by a high-temperature treatment in either oxygen or steam. Metal electrodes are deposited on the top and back of the OPS to complete the capacitive structure.

When water vapor contacts the sensor, it permeates through the porous structure between the electrodes. The response of a typical sensor increases 800 percent when exposed to an RH change from 1 to 40 percent. Since semiconductor techniques are used in the manufacturing process, the potential to integrate signal conditioning and other sensors may provide an attractive solution for future vehicle sensing requirements.

5.6 CONCLUSIONS

Several factors are influencing the temperature-sensing requirements for future vehicles. The ultra-efficient vehicle will operate at higher temperatures and utilize brake energy-recovery. Both of these aspects will increase the temperature environment for other vehicle components.

The requirements for sensors in future vehicle systems include improved performance (sensitivity) and reliability in spite of operating at higher temperatures, lower cost, space and weight reduction, greater functionality including diagnostics and self-test, and ease of inter-

PETITIONER'S EXHIBIT 1002
US PATENT NO. 6,557,540

facing with an MCU for adaptive control and interchangeability. The capability of semiconductor technology to provide sensing information for failure detection provides a means for increased reliability in several vehicle subsystems.

All trademarks are the property of their respective owners.

GLOSSARY

Accuracy A comparison of the actual output signal of a device to the true value of the input. The various errors (such as linearity, hysteresis, repeatability, and temperature shift) attributing to the accuracy of a device are usually expressed as a percent of full-scale output (FSO).

Maximum operating temperature The maximum body temperature at which the thermistor will operate for an extended period of time with acceptable stability of its characteristics. This temperature is the result of the internal or external heating, or both, and should not exceed the maximum value specified.

Negative temperature coefficient (NTC) An NTC thermistor is one in which the zero-power resistance decreases with an increase in temperature.

Operating temperature range The range of temperature between minimum and maximum temperature at which the output will meet the specified operating characteristics.

Self-generating Providing an output signal without applied excitation, such as a thermoelectric transducer.

Self-heating Internal heating resulting from electric energy dissipated within the unit.

Storage temperature range The range of temperature between minimum and maximum which can be applied without causing the sensor (unit) to fail to meet the specified operating characteristics.

Temperature coefficient of full-scale span The percent change in the full-scale span per unit change in temperature relative to the full-scale span at a specified temperature.

Temperature hysteresis The difference in output at any temperature in the operating temperature range when the temperature is approached from the minimum operating temperature and when approached from the maximum operating temperature with zero input applied.

Thermal time constant The thermal time constant is the time required for a thermistor to change to 63.2 percent of the total difference between its initial and final body temperature when subjected to a step function change in temperature under zero-power conditions.

Transfer function A mathematical, graphical, or tabular statement of the influence which a system or element has on the output compared at the input and output terminals.

BIBLIOGRAPHY

Automotive Electronics Reliability Handbook, SAE, Warrendale, Pa., 1987.
Automotive Handbook, Robert Bosch GmbH, 1986.

PETITIONER'S EXHIBIT 1002
US PATENT NO. 6,557,540

BR923/D Discrete and Special Technologies Group Reliability Audit Report 1Q90, Motorola Semiconductor Products Sector, Phoenix, Ariz.

Collings, N., W. Cai, T. Ma, and D. Ball, "A linear catalyst temperature sensor for exhaust gas ignition (EGI) and on board diagnostics of misfire and catalyst efficiency," SAE SP-957, *U.S. and European Automotive Technology Emissions Technology,* International Congress and Exposition, Detroit, March 1–5, 1993.

De Vera, D., T. Glennon, A. A. Kenny, M. A. H. Khan, and M. Mayer, "An automotive case study," *Quality Progress,* June 1988, pp. 35–38.

Dosher, J., "Smart and active sensors," *Proceedings of Sensors Expo West,* 1991, pp. 103C-1–6.

Hao, T., E. F. Malinowski, and C-C. Liu, "High temperature fiber optic sensor for industrial applications," *Proceedings of Sensors Expo West,* San Jose, Calif., March 2–4, 1993, pp. 227–228.

Norton, Harry N., "Section 10—Transducers and Sensors," in D. G. Fink and D. Christiansen (eds.), *Electronics Engineers' Handbook* (3d ed.), McGraw-Hill, New York, 1989.

Pressure Sensor Device Data, Motorola Semiconductor Products Sector, Phoenix, Ariz., 1993.

Recommended Environmental Practices for Electronic Equipment Design, SAE J1211, Warrendale, Pa., Nov. 1978.

Temming, J., "Measuring seat comfort," *Automotive Engineering,* July 1993, pp. 25–30.

PETITIONER'S EXHIBIT 1002
US PATENT NO. 6,557,540

CHAPTER 6
EXHAUST GAS SENSORS

**H.-M. Wiedenmann, G. Hötzel,
H. Neumann, J. Riegel, and H. Weyl**
Robert Bosch GmbH
Lambda Oxygen Sensor Development

6.1 BASIC CONCEPTS

6.1.1 Combustion

The sole products of complete fuel combustion are the nontoxic substances carbon dioxide and water:

$$C_mH_n + \left(m + \frac{n}{4}\right) 0_2 \rightarrow m\,CO_2 + \frac{n}{2}\,H_2O \tag{6.1}$$

The theoretical air requirement for this process is 14.7 kg air for each kilogram of fuel; this corresponds to approximately 10 m^3 air per liter of fuel. The air/fuel ratio is defined as stoichiometric when the engine is supplied with the exact quantity of air required for complete combustion.

6.1.2 Definition of Normalized air/fuel Ratio Lambda

The mixture ratio is defined by the normalized air/fuel ratio lambda (λ):

$$\lambda = \frac{\text{current air-fuel ratio}}{\text{stoichiometric air-fuel ratio}} \tag{6.2}$$

Because the conditions within the engine do not correspond to the absolute ideal required for perfect combustion, a number of products of incomplete combustion occur, even if a stoichiometric air/fuel ratio ($\lambda = 1$) is maintained. Thus, the CO_2 and H_2O are joined by CO, H_2, and HC (hydrocarbons C_xH_y) along with corresponding amounts of not reacted (free) oxygen. The water-gas equilibrium defines the ratio of CO to H_2. At high combustion temperatures, the N_2 and O_2 in the air supply form nitrous oxides such as NO, NO_2, N_2O (generic designation: NO_x).

6.1.3 Composition of Untreated Exhaust Gas

The composition of the exhaust gases entering the catalytic converter (untreated or raw emissions) varies according to the quality of combustion and, even more importantly, as a function

PETITIONER'S EXHIBIT 1002
US PATENT NO. 6,557,540

of the normalized air/fuel ratio lambda (λ) (Fig. 6.1). Rich mixtures (lambda < 1, excess fuel) produce high concentrations of CO, H_2, and HC, while lean mixtures (lambda > 1, excess oxygen) generate higher levels of NO_x and free oxygen. The lower combustion-chamber temperatures associated with mixture ratios of lambda > 1.2 result in reductions in NO_x concentrations accompanied by increased HC concentrations. Maximum emissions of CO_2 (greenhouse gas) occur at a slightly lean mixture (lambda ≈ 1.1).

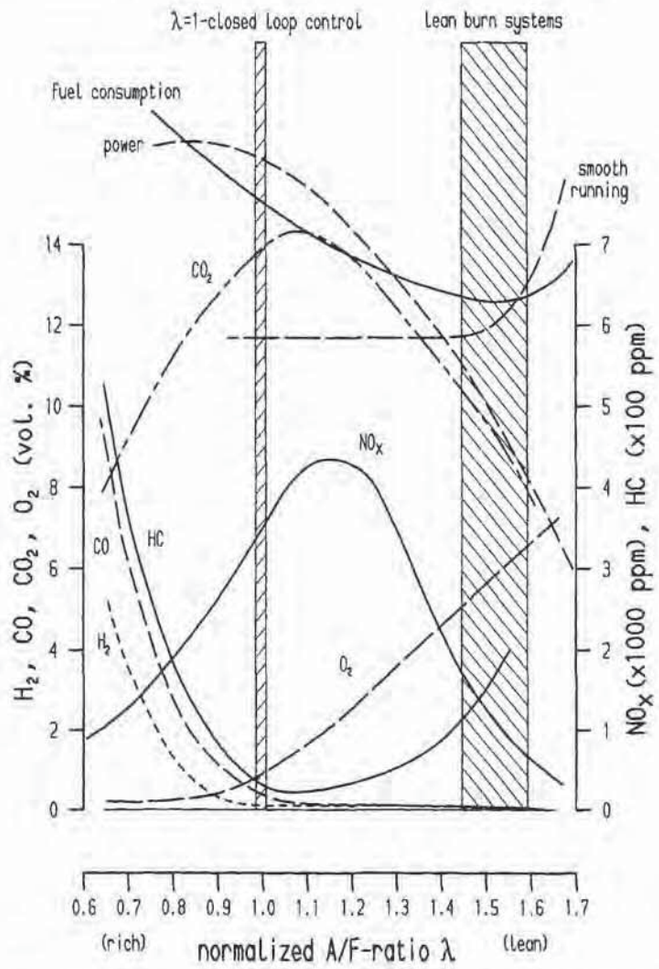


FIGURE 6.1 Typical curves for fuel consumption, power, smoothness, and composition of raw exhaust gases relative to lambda in a spark-ignition engine.

6.1.4 Lambda Closed-Loop Control: Design Concepts

Lambda Control Ranges. The main elements considered in defining the range of the lambda closed-loop control system (Table 6.1) are engine design, emission limits, fuel consumption, and the requirements for performance and smooth running.

Treatment of Exhaust Gases. Catalytic treatment of exhaust gases is essential for achieving compliance with the stringent current United States emission standards (Table 6.2). In the catalytic process, CO, H_2, and HC are oxidized to form CO_2 and H_2O, while the constituents of

PETITIONER'S EXHIBIT 1002
US PATENT NO. 6,557,540

TABLE 6.1 Lambda Control Ranges

	Lambda = 1—spark ignition engine	Lean-burn concept	Lean-mix concept	Diesel engine
Lambda-control range	Lambda = 1 ± < 0.005	1.4–1.7	1.4–1.7 and lambda = 1	1.1–7
Target	Opt. catalytic aftertreatment	Fuel economy low CO, HC, (NO_x)*	Improved fuel economy within allowable emission	Reduced emissions particles and NO_x
Lambda sensors	Lambda = 1 sensor	Lean A-F sensor	Wide-range A-F sensor	Lean A-F sensor
Exhaust gas aftertreatment	Three-way-catalyst (TWC)	Oxi-cat NO_x-cat*	TWC NO_x-cat*	Particle filter* NO_x-cat*
Control concepts	Conventional or continuous	Continuous	Lean: continuous lambda = 1: conventional	Full-load and EGR-control
Series production	Discont. control	—	Yes	—

* Not available yet.
TWC: three-way-catalyst; Oxi-cat: oxidation-catalyst; NO_x-cat: NO_x-reduction-catalyst.

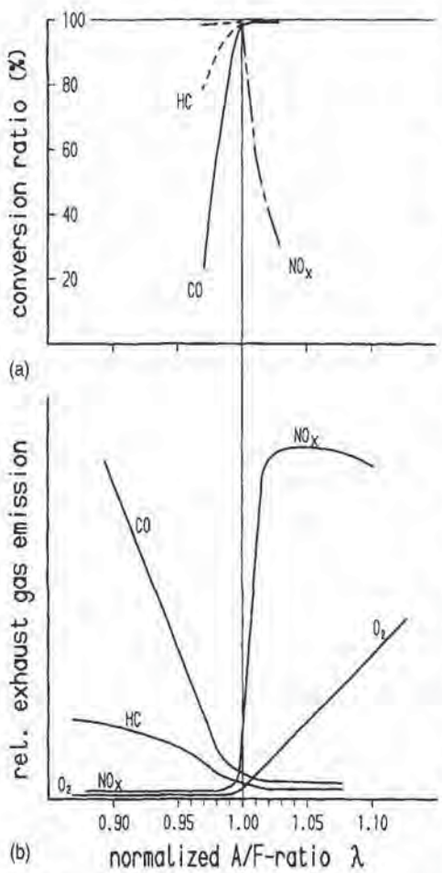


FIGURE 6.2 (*a*) Conversion rates for CO, NO_x, and HC in a new three-way catalytic converter; (*b*) typical curve for exhaust-gas composition downstream from a new three-way catalytic converter.

NO_x are reduced to N_2 and O_2. A three-way catalytic converter TWC (selective catalytic converter) and closed-loop control system featuring a lambda sensor are essential elements in achieving adequate reductions in all three pollutants (Fig. 6.2). The engine must be operated within a narrow range of $|\Delta\lambda| < 0.005$ at lambda = 1.

Oxidation catalysts are sometimes employed to reduce CO and HC emissions from lean-burn and diesel engines. Meanwhile, NO_x reduction catalysts and particle filters are being developed for future applications (Table 6.1).

Lambda Closed-Loop Control. Lambda closed-loop control is incorporated in the engine's electronic control system. The control system regulates lambda upstream from the catalytic converter with the aid of an oxygen sensor. System lag results in relatively long control-response delays, especially at low rpm. For this reason, the system must incorporate a pilot-control function capable of adjusting the mixture to the desired lambda with the highest possible degree of precision. This arrangement makes it possible to avoid excessive control deviations and harmful emission peaks of the kind that lead to high emission levels and reduced vehicle performance.

Conventional Closed-Loop Lambda Control. The closed-loop control concept pre-

PETITIONER'S EXHIBIT 1002
US PATENT NO. 6,557,540

TABLE 6.2 Summary of Emission Levels for Spark-Ignition Engines
(Status: July 1992)

		Exhaust emission limits						
	Start of sale	HC	CO	NO_x	HC + NO_x	Unit	Remarks	
California	MY 1993	0.25	3.4	0.4	—	g/mile		
	MY 1994	0.125	3.4	0.2	—	g/mile	TLEV 10 %	% of fleet,
	MY 1997	0.075	3.4	0.2	—	g/mile	LEV 25 %	stepwise
	MY 1997	0.04	1.7	0.2	—	g/mile	ULEV 2 %	increase
	MY 1998	0.0	0.0	0.0	—	g/mile	ZEV 2 %	
USA (Fed.)	MY 1983	0.41	3.4	1.0	—	g/mile		
	MY 1994	0.25	3.4	0.4	—	g/mile		
	MY 2003	0.125	1.7	0.2	—	g/mile	on need	
Japan	4/1981	0.25	2.1	0.25	—	g/km	10-mode	
EG	1992	—	2.72	—	0.97	g/km	MVEG I	
	10/1996	0.15	2.1	0.3	—	g/km	MVEG II	proposal parliament
		—	2.2	—	0.5	g/km		proposal commission
	1996	—	1.5	—	0.2	g/km	MVEG III	proposal Germany

TLEV: Transitional Low-Emission Vehicles
ULEV: Ultra Low-Emission Vehicles
LEV: Low-Emission Vehicles
ZEV: Zero-Emission Vehicles
MVEG: Motor Vehicle Emission Group

sently in use in spark-ignition engines is based on 2-point lambda = 1 control (Fig. 6.3) with the mixture composition oscillating around the optimum lambda. When the exhaust mixture shifts from rich to lean, the voltage from a lambda = 1 probe drops from approximately 800 mV (lambda < 1) to approximately 100 mV (lambda > 1), with a steep signal change (lambda jump) occurring at lambda = 1 (Sec. 6.2.1). Once the signal from the sensor crosses beyond the specified threshold value (e.g., 450 mV), the system responds by progressively leaning out the mixture until the probe signal drops below this border again. Once this process is completed, the system reverts to graduated mixture enrichment. Depending upon the system lag, the subsequent control-oscillation rate will lie in the 0.5 . . . 5 Hz range, with an amplitude of $\Delta\lambda = \pm 0.01 \ldots 0.05$ relative to the median lambda. During the lean-operation period, the catalytic converter stores oxygen for release during the rich-mixture phases. This arrangement ensures high conversion rates despite the control oscillations. Preferably an algorithm with proportional plus integral characteristics (PI controller) is used. Variations in system lag and integrator pitch affect the amplitude and the frequency of the oscillations. The proportional factors have to be adapted. Because load and rpm have a major effect on system lag, control parameters are defined and stored in a load/rpm control map.

Continuous Lambda = 1 Control. A continuous lambda = 1 control can be employed to achieve substantially smaller control deviations, providing attendant reductions in emissions, especially when used with aged catalytic converters. An oxygen sensor with a roughly linear or linearized lambda characteristic curve is required for this arrangement (Secs. 6.2.5 and 6.2.6).

6.1.5 On-Board Diagnosis (OBD II)

From the 1994 model year onward, on-board devices capable of monitoring the operation of all emission-relevant vehicle components will be required in the United States. Pollutant emission sensors (see Sec. 6.6) to measure levels of CO, NO_x, and HC emissions downstream from the catalytic converter represent an ideal means of monitoring the performance of both converter and oxygen sensor. Unfortunately, there are still no sensors of this type suitable for

PETITIONER'S EXHIBIT 1002
US PATENT NO. 6,557,540

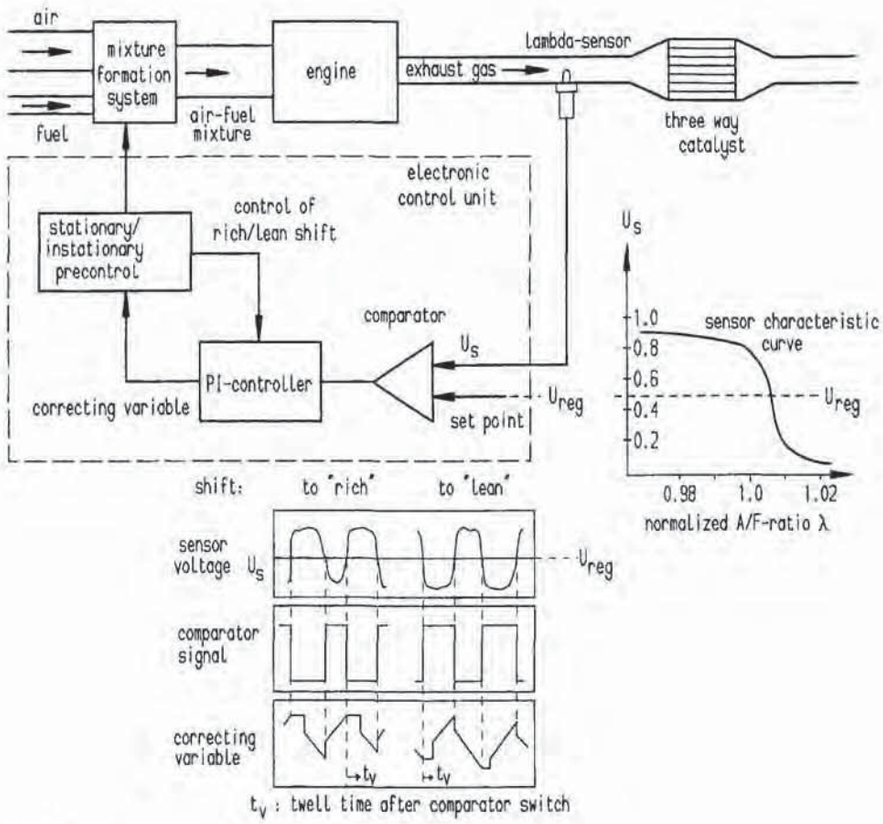


FIGURE 6.3 Operating diagram for lambda control.

use in the engine's exhaust stream. As an alternative, there exist concepts that employ a second oxygen sensor behind the catalytic converter to detect aging in the converter and/or the lambda sensor.

6.2 PRINCIPLES OF EXHAUST GAS SENSORS FOR LAMBDA CONTROL

6.2.1 Lambda = 1 Sensor: Nernst Type (ZrO_2)

Sensing Mechanism. In principle, the lambda sensor operates as a solid-electrolyte galvanic oxygen-concentration cell (Fig. 6.4). A ceramic element consisting of zirconium dioxide and yttrium oxide is employed as a gas-impermeable solid electrolyte. This mixed oxide is an almost perfect conductor of oxygen ions over a wide temperature range (Sec. 6.3). The solid electrolyte is designed to separate the exhaust gas from the reference atmosphere. Both sides feature catalytically active platinum electrodes. At the inner electrode (air; $pO_2'' - 0.21$ bar), the electron reaction

$$O_2 + 4e^- \rightarrow 2\,O^{2-} \tag{6.3}$$

incorporates oxygen ions in the electrolyte. These migrate to the outer electrode (exhaust gas; pO_2' variable $< pO_2''$), where the counterreaction occurs at the three-phase boundary (elec-

PETITIONER'S EXHIBIT 1002
US PATENT NO. 6,557,540

trolyte-platinum-gas). A counteractive electrical field is created, and an electrical voltage U_s corresponding to the partial-pressure ratio is generated in accordance with the Nernst equation:

$$U_s = \frac{RT}{4F} \ln \frac{pO_2''}{pO_2'} \tag{6.4}$$

where R = general gas constant
F = Faraday's constant
T = absolute temperature
pO_2 = partial pressure of oxygen

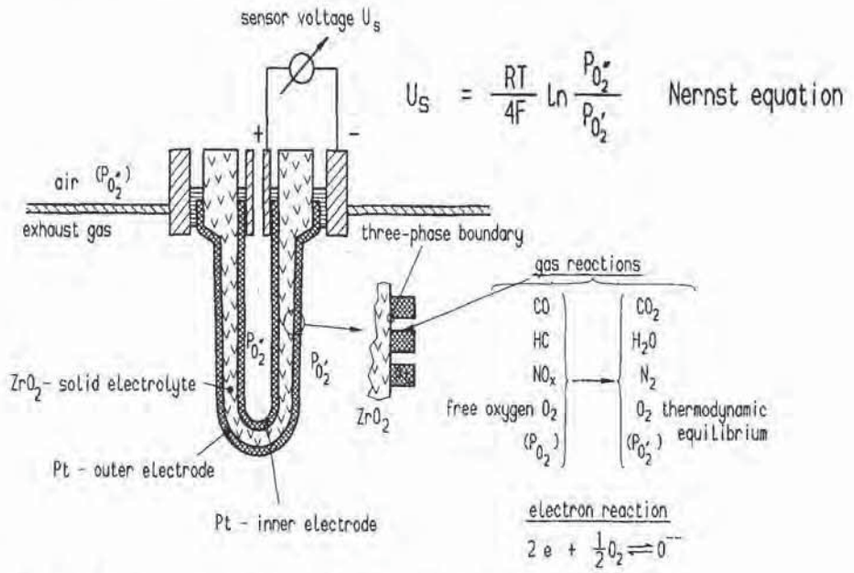


FIGURE 6.4 Diagram illustrating design and operation of a lambda = 1 sensor.

Catalytic Process. Measurements of oxygen content can only serve as the basis for unambiguous conclusions regarding the lambda of the exhaust gas when a state of thermodynamic gas equilibrium is established at the catalytically active electrodes on the oxygen sensor (residual oxygen). The absolute concentrations of the individual components in the engine's exhaust gases fluctuate across a wide range in accordance with the instantaneous operating conditions (warm-up, acceleration, steady-state operation, deceleration). The oxygen sensor must thus be capable of converting the gas mixture that it receives into a state of complete thermodynamic equilibrium. The resulting requirements are a high level of catalytic activity at the electrode and a protective layer capable of limiting the gas quantity. Should it prove impossible to achieve thermodynamic equilibrium at the electrode, the sensor's lambda signal will be erroneous.

Characteristic Curve. The concentration of residual oxygen fluctuates exponentially (by several orders of 10) in the vicinity of a stoichiometric air/fuel mixture (lambda = 1). In accordance with Eq. (6.4), this leads to massive variations in sensor voltage (lambda = 1 jump) with the characteristic lambda curve (Fig. 6.5).

Reference Atmosphere. Ambient air is the most commonly used O_2 reference. Alternatives include a metal-metal oxide mixture or a pumped reference medium. With this method, an O_2 reference pumping current is superimposed on the voltage measurement to generate an approximately constant O_2 partial pressure at the encapsulated reference electrode.

PETITIONER'S EXHIBIT 1002
US PATENT NO. 6,557,540

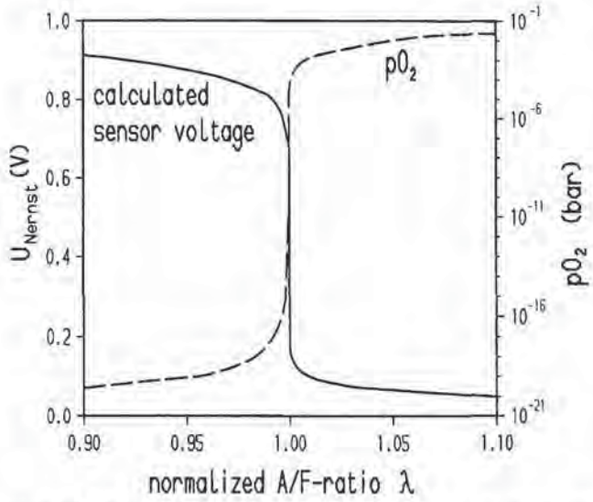


FIGURE 6.5 Equilibrium partial pressure of oxygen pO_2 and resulting curve for Nernst voltage at ≈ 700 °C relative to the normalized air-fuel ratio lambda.

6.2.2 Lambda = 1 Sensor: Semiconductor Type

Sensing Mechanism. Oxidic semiconductors such as TiO_2 and $SrTiO_3$ rapidly achieve equilibrium with the oxygen partial pressure in the surrounding gas phase at relatively low temperatures. Changes in the partial pressure of the adjacent oxygen produce variations in the oxygen vacancy concentration of the material (TiO_{2-x} respectively $SrTiO_{3-x}$), thereby modifying its volume conductivity.

$$R_T = A\, pO_2^n \exp\left(\frac{E}{kT}\right) \tag{6.5}$$

where R_T = semiconductor resistance
A = constant
E = activation energy
k = Boltzmann constant
T = absolute temperature
$n \approx 1/4$.

This effect, which is exploited to determine lambda, is also superposed by the conductivity's temperature dependence. Electrical resistance and sensor response times are both inversely proportional to temperature, as equilibrium is achieved more rapidly through diffusion in the oxygen vacancies.

Design. The ability to dispense with an O_2 reference allows an extremely simple design featuring an integrated heater. The porous semiconductor thick-film layer is generally positioned and sintered onto a planar Al_2O_3 substrate between two electrodes. Thin-film layers are also being developed as an alternative.

Characteristic Curve. At lambda = 1, the sensor layer displays an extreme change in conductivity due to the large pO_2 variation (see Sec. 6.2.1 and Fig. 6.5). When new, TiO_2 sensors provide essentially the same response as ZrO_2-based lambda = 1 probes. Variations in the rates of increase for lean and rich resistance and for response time occur over its lifetime, with the emission-control system undergoing a significant shift toward lean.

PETITIONER'S EXHIBIT 1002
US PATENT NO. 6,557,540

Principles of Operation. A voltage is applied to the TiO_2 resistor R_T and a serial reference resistor. The voltage drop at the serial resistor depends on R_T, respectively on lambda. In a three-pole version, the applied voltage is taken from the heater voltage; for the four-pole version (insulated ground) a separate supply is employed. Temperature compensation may be required, depending upon the specific application.

6.2.3 Lean A/F Sensor: Nernst Type

Sensing Mechanism. It is always possible to employ a potentiometric lambda = 1 sensor (Sec. 6.2.1) as a lean A/F sensor by using the flat part of the Nernst voltage curve (Sec. 6.4 and Fig. 6.5) to derive the values at lambda > 1. The diminutive characteristic sensor voltages in this lambda range (U_S < 65 mV at lambda > 1.05) mean that stringent requirements for consistency must be met. Minute voltage deviations of just a few mV are sufficient to produce substantial errors in lambda.

Design. For this reason, special sensors must be employed in applications in which quantitative determination of lambda > 1.05 is required. To this end, special electrode manufacturing techniques are used to enhance catalytic activity, while a power heater (18 W) is used in conjunction with a protection tube featuring a lower gas-flow rate to provide a more constant ceramic temperature.

Principles of Operation. A high-output input amplifier is required for measurement of the low voltage levels associated with lean exhaust gases. In vehicle testing, lambda control has proven effective when used together with a classical mixture regulator. Even alternating operation (lambda = 1 and lean) with a sensor in the same vehicle is possible. Depending upon accuracy requirements, lean operation is possible in a range extending to lambda ≈ 1.5.

Nonautomotive Applications. Lambda-controlled operation can be employed to maintain narrow tolerances and to limit drift in oil- and gas-fired units; the benefits include low fuel consumption, enhanced safety, and lower emissions. The use of sensors in stationary power plants—for instance, in central heating plants—is particularly interesting as a potential means of dealing with fluctuations in the calorific content of the fuel.

6.2.4 Lean A/F Sensor: Limiting-Current Type

Sensing Mechanism. An external electrical voltage is applied to two electrodes on a heated ZrO_2 electrolyte to pump O_2 ions from the cathode to the anode (electrochemical O_2 pumping cell) (Fig. 6.6*a*). When a diffusion barrier impedes the flow of O_2 molecules from the exhaust gas to the cathode, the result is current saturation beyond a certain pumping voltage threshold (limiting current condition). Because the resulting limiting current I_l is roughly proportional to the exhaust gas' oxygen concentration c_{O2}

$$I_l = 4FD \frac{Q}{L} c_{O2} \tag{6.6}$$

where F = Faraday's constant
D = diffusion coefficient
Q = effective diffusion cross section
L = effective diffusion length

Design. Figure 6.6*b* provides a schematic illustration of this sensor type featuring planar technology and an integrated electric heater element.

PETITIONER'S EXHIBIT 1002
US PATENT NO. 6,557,540

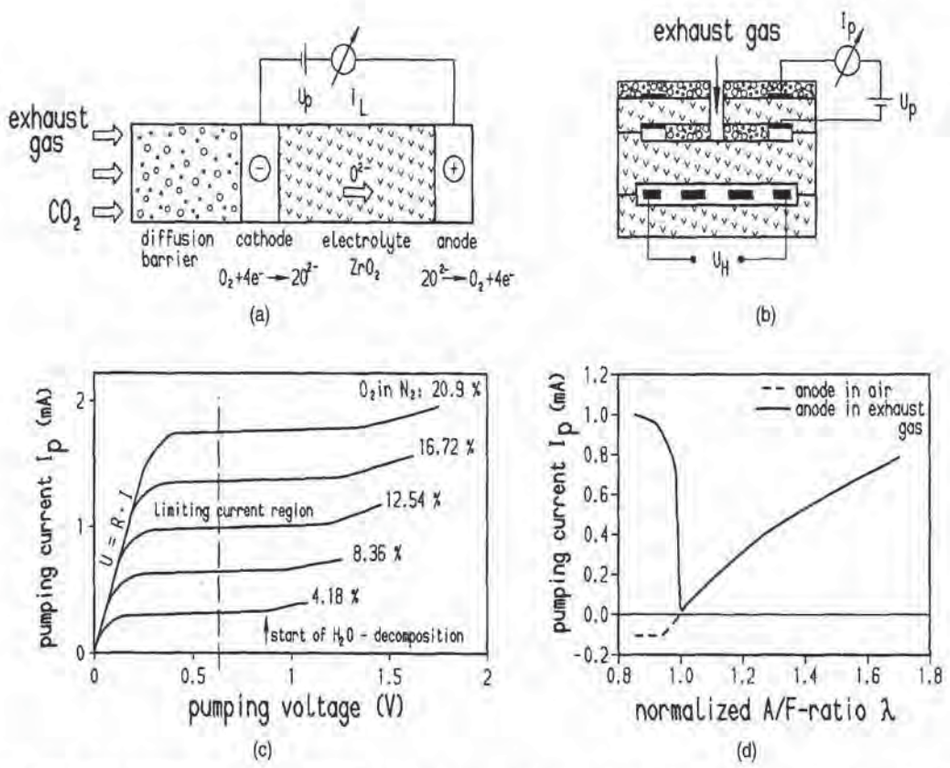


FIGURE 6.6 Limiting current sensor: (*a*) principle of operation; (*b*) schematic diagram; (*c*) current/voltage characteristics; (*d*) response curve as function of lambda.

Characteristic Curve. Figure 6.6c shows the current-voltage pattern for a limiting current sensor at various O_2 concentrations. If, at a constant pumping voltage, the pumping current is entered above lambda instead of c_{O2}, the resulting curve will correspond to Fig. 6.6*d*. In lean exhaust gas, the signal drops in response to reductions in lambda as indicated in Eq. (6.7), but below lambda = 1 there is a radical surge. This response pattern is at variance with the basic theory, and can be explained as the result of decomposition effects at the cathode. As a result, this sensor is only suitable for use in lean gases. Depending upon the design of the diffusion barrier (pore radius to free path length for the gas molecules, according to the proportion of gas phases to Knudsen diffusion), various relationships are observed between pumping current (measurement signal) and exhaust pressure and sensor temperature.

Principles of Operation. Depending on the accuracy requirements, a stable operating temperature in the range 600 to 800 °C is needed. Pumping voltages must always be selected to satisfy the conditions for limiting current. In addition, this limiting current has to be calibrated due to the manufacture scattering of the diffusion gap.

6.2.5 Wide-Range A/F Sensor: Single-Cell

Design and Operation. When the anode of a limiting current sensor of the type described in Sec. 6.2.4 is exposed to reference air instead of to the exhaust gas, the total voltage U_S at the probe will be the sum of the effective pumping voltage U_P and a superimposed Nernst voltage U_N.

$$U_S = U_P + U_N \tag{6.7}$$

PETITIONER'S EXHIBIT 1002
US PATENT NO. 6,557,540

In operation, holding U_S to, as an example, 500 mV will produce a positive pumping voltage in lean exhaust gases ($U_N < 500$ mV); the diffusion limits the rate at which O_2 is pumped from the cathode to the anode. At lambda = 1 ($U_N \approx 500$ mV), the pumping voltage and, with it, the pumping current drop toward zero. In rich exhaust gas ($U_N > 500$ mV), the effective pumping voltage U_P becomes negative, causing oxygen to be pumped from the reference air electrode to the exhaust gas electrode ($I_P < 0$), where it reacts with the rich gas components CO, H_2, and HC.

Characteristic Curve. The pumping current displays a uniform upward trend between mildly rich and extremely lean lambda values (Fig. 6.6*d*).

Applications. This type of sensor is in series production as a thimble-type design for lean-mix concepts. In this application, operation as a limiting current sensor is restricted to lean conditions; during operation at lambda = 1, the pumping voltage is switched off and the Nernst voltage serves as the control signal.

6.2.6 Wide-Range A/F Sensor: Dual-Cell

Design. Skillful combination of a limiting-current sensor with a Nernst concentration cell on a single substrate will produce a dual-cell wide-range A/F sensor. The pumping and concentration cells are made of ZrO_2. Each cell is coated with two porous platinum electrodes, and they

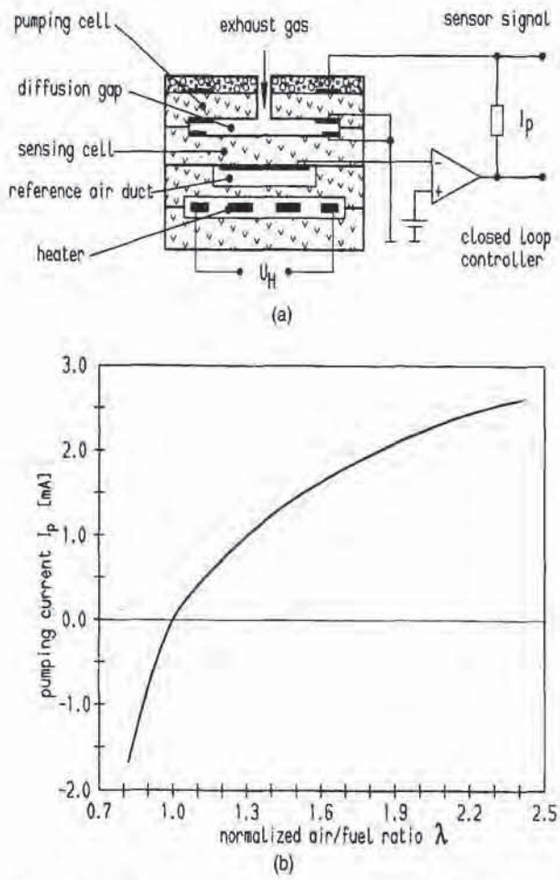


FIGURE 6.7 Dual-cell wide-range A-F sensor: (*a*) schematic diagram; (*b*) response curve as function of lambda ($T_{gas} \approx 400$ °C, $P_H \approx 12$ W).

PETITIONER'S EXHIBIT 1002
US PATENT NO. 6,557,540

are arranged with a measurement gap of approximately 10 to 50 μm in height between them. A gas-intake opening in the solid electrolyte connects this measurement gap to the exhaust gas while the gap is serving as a diffusion barrier to control limiting current (Fig. 6.7).

Operation Mode. An electronic circuit regulates the current applied to the pumping cell to maintain a constant gas composition (for instance, lambda = 1) in the measurement gap. This corresponds to a Nernst-cell voltage of $U_N \approx 450$ mV. If the exhaust gas is lean, the pumping cell drives the oxygen outward from the measurement gap. If the exhaust gas is rich, the flow direction is reversed and oxygen from the surrounding exhaust gas (e.g., from decomposition of CO_2 and H_2O) is pumped into the measurement gap.

Characteristic Curve. The pumping current is proportional to the oxygen concentration (or oxygen requirement). With the attendant electronic control circuitry, an unambiguous, linear signal increase over a wide lambda range of 0.7 < lambda < infinite (air) can be obtained if the current is calibrated due to the manufacture scattering (Fig. 6.7). The integrated heating element provides an operating temperature in excess of 600 °C.

6.3 TECHNOLOGY OF CERAMIC EXHAUST GAS SENSORS

6.3.1 ZrO_2-based Sensors

The zirconium dioxide used to manufacture oxygen sensors is not pure; instead, the solid electrolyte consists of a mixed oxide, ZrO_2/Y_2O_3. The Y_2O_3 concentration used for actual applications lies in the 4 to 5 mol% range. This level is commensurate with optimum sensor operation in the important properties of ion conductivity, thermal stability, and mechanical strength.

Ion Conductivity. The substitution of trivalent yttrium ions for quadrivalent zirconium ions leads to the formation of oxygen vacancies through which the oxygen ions can move. Initially, the increases in ion conductivity are roughly proportional to the rise in Y_2O_3 content, as they are accompanied by a simultaneous rise in the number of oxygen vacancies. This pattern is observed with yttrium as well as with other bi- and trivalent alkaline earth metals, at least until a certain level of defect concentration is reached. Beyond this limit, the mutual influence of the vacancies reaches such levels that any further increases in defect concentration are accompanied by reductions in ion conductivity. The maximum is obtained at approximately 9 to 10 mol% Y_2O_3.

Phase Composition and Mechanical Stability. At room temperature, zirconium dioxide is monocline. It becomes tetragonal (metastable) above 1200 °C, and assumes a cubic form beyond 2370 °C. Yttrium doping can be employed to partially or completely stabilize the tetragonal and cubic modification, even at room temperature (PSZ—partially stabilized zirconium; FSZ—fully stabilized zirconium, above approximately 10 mol%, with certain manufacturing processes 7 to 8 mol% Y_2O_3). ZrO_2, with an essentially monocline structure, does not display sufficient resistance to temperature fluctuations for application in automotive exhaust systems—the changes in the geometry of the individual crystallites which accompany the phase transition lead to fatigue symptoms in the ceramic material. At the same time, the cubic phase does not possess the physical strength required to resist the physical shocks and thermal stresses. However, good mechanical characteristics can be obtained by using partially stabilized ceramic materials, with maximum strength being achieved within the range of 2 to 4 mol% Y_2O_3.

Manufacture of Partially Stabilized ZrO_2 Ceramics. The most common procedure consists of mixing and grinding the ZrO_2 and Y_2O_3 together (mixed oxide). The differences in the

PETITIONER'S EXHIBIT 1002
US PATENT NO. 6,557,540

length of the diffusion paths—the two oxides are located adjacently as separate powder particles—do not generally produce a completely homogeneous distribution of yttrium in the ZrO_2. Thus, both fully stabilized cubic crystallites and tetragonal crystallites can be formed during the sintering process. During the phase transition to monocline ZrO_2 that takes place during cooling, the latter provoke internal tension, causing the ceramic material to harden. Certain combinations of yttrium concentration and manufacturing techniques can be employed to obtain exclusively tetragonal crystallites, which remain stable even after cooling (TSZ—tetragonal stabilized zirconia). Due to the absence of a phase transition within the temperature range associated with the intended application, stabilized tetragonal zirconium dioxide displays a virtually constant coefficient of thermal expansion. Both of the partially stabilized ZrO_2 ceramics described here are used in the manufacture of oxygen sensors.

6.3.2 Thimble-Type Sensors

Shaping. The ceramic base (Fig. 6.4) is shaped in the usual manner with dry pressing of granulated ZrO_2 and subsequent grinding of the compact material.

Electrodes. The application of the gas-permeable platinum electrodes is one of the most critical processes in the manufacture of oxygen sensors. A basic distinction is made between two different procedures:

Thin-Film Process. In this process, a thin microporous platinum layer (electrode thickness < 1 μm) is applied to the previously sintered base using one of three methods: thermal evaporation, sputtering, or chemical deposition with subsequent thermal treatment.

Thick-Film Process. In this process, a (for example) platinum-cermet layer (mixture of noble metal and ceramic phase) is printed onto the unsintered base (electrode thickness 5 to 10 μm).

As far as actual operation is concerned, the salient difference between the two processes resides in the fact that the three-phase boundary required for the conversion of oxygen (common border of platinum, zirconia, and gas phase) remains restricted to the surface of the base when thin-film electrodes are used. In contrast, the use of thick-film cermet electrodes with a ceramic phase of ZrO_2 results in a substantially larger border area along with enhanced high-temperature adhesion.

Protective Layer. As the outer electrode is exposed to the exhaust gases, a suitable protective layer, combining the requisite porosity with optimal adhesive properties, is essential to ensure the long-term stability of the oxygen sensor. In the conventional plasma or flame-spraying process, a porous layer 50 to 300 μm in thickness (e.g., magnesium spinel) is applied to the sintered and electrodes-equipped base. A cofiring technique with ZrO_2-based protective layers or a combination of both processes is being employed in the production of a new generation of oxygen sensors with enhanced long-term stability.

Well-defined porosity levels must be maintained to ensure satisfactory operation. With cofired protective layers, the required porosity level can be obtained by using organic pore-forming substances, which are burned out during sintering, or by adding a second, sinter-inactive ceramic phase, such as Al_2O_3. Porous protective layers also provide a diffusion barrier for the exhaust-gas molecules before they reach the electrodes. These layers thus exercise a determining influence on the sensor's control characteristics because the components of the exhaust gas which exhibit various diffusion coefficients are not in a state of thermodynamic equilibrium (see Sec. 6.4). This effect can be partially neutralized through defined pigmentation in the protective layers, which not only display catalytic characteristics, but can also inhibit contamination.

6.3.3 Planar Oxygen Sensors

The planar oxygen sensor derives its designation from the fact that, as opposed to the thimble-type sensor, its design arranges all operating layers in plain, consecutive surfaces. The

PETITIONER'S EXHIBIT 1002
US PATENT NO. 6,557,540

technology applied in their manufacture is quite similar to the multilayer technology employed to produce ceramic multilayer capacitors and high-density electronic circuit boards (e.g., MCM—multichip modules).

Manufacture of Ceramic Green Sheet. First, an organic binder phase is added to the ZrO_2 powder in a tape-casting process to produce ceramic substrate layers.

Printing on the Ceramic Green Sheet. A screen-printing process (thick-film process) is employed to attach the individual function groups, e.g., galvanic cell, pumping cell, reference-air duct and heater (see also Sec. 6.2) to the green tape in the desired layer sequence. Several printed layers are generally required for each side of the tape; these layers can also consist of various inorganic materials.

Lamination. A number of screen-printed substrates can be stacked and laminated (bonded in a process combining temperature and pressure) to form composite structures representing virtually any desired level of complexity. A simplified version of a lambda = 1 sensor in planar technology is illustrated in Fig. 6.8.

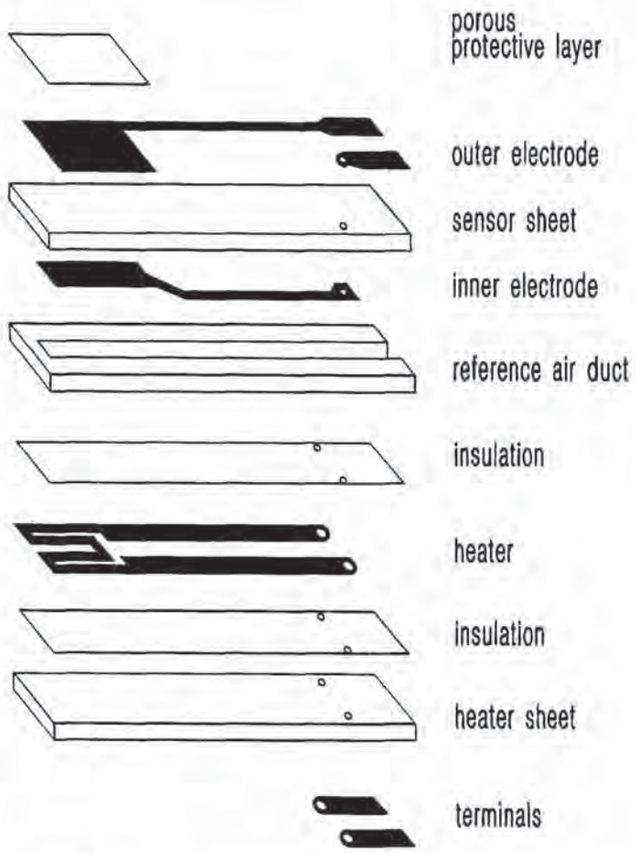


FIGURE 6.8 Layer structure of planar lambda = 1 sensor.

Advantages of Planar Technology. The application of surface-design technology also provides an additional advantage by making it possible to combine a number of individual elements on a single substrate for subsequent separation (multiple application) and sintering to form monolithic sensors with integrated heating elements. The coefficients of thermal expan-

PETITIONER'S EXHIBIT 1002
US PATENT NO. 6,557,540

sion of the ZrO_2, cermet, and insulation layers must be precisely matched to ensure that the resulting ceramic elements display adequate thermal and mechanical stability.

Sensor elements manufactured with this new technology offer a number of advantages: the integration of heater and sensor provides a single unit with a lower total thermal mass, allowing substantial reductions in the continuous heating requirement (30 to 40 percent of that required with a thimble-type sensor), shorter delay between activation and readiness for active control, and smaller sensor dimensions. These characteristics make the unit ideal for meeting the demands of the modern motor vehicle (reductions in energy requirements, weight and space savings, and more stringent emission requirements). In addition, planar technology is an essential factor in obtaining complicated operating abilities such as those found in the dual-cell wide-range A/F sensor (see Sec. 6.2.6).

6.3.4 Al_2O_3-based Sensors

Sensors for oxygen and other exhaust gases which employ variations in the conductivity of the sensor material (TiO_2, SnO_2, etc.) to detect changes in the gas concentration are usually designed as planar sensors. The preferred substrate material is Al_2O_3. As the combinations of functions (e.g., heater, electrodes, etc.) are essentially those required with planar ZrO_2 sensors, the manufacturing techniques are also quite similar. Al_2O_3 provides advantages in the form of lower material costs and a simplified internal structure, made possible by the fact that Al_2O_3 maintains its good insulation properties at high temperatures. A disadvantage, particularly in terms of long-term stability, is the difficulty with sintering and sensor-material adhesion, as cofiring technology cannot be employed for this procedure.

6.3.5 Construction

Figure 6.9 shows completely assembled a heated thimble sensor and a planar lambda sensor. Although similar in external appearance—the planar sensor is somewhat shorter and narrower—the two units differ substantially in their respective internal structures. The differences are largely a result of the fact that heater and sensor in the heated thimble-type sensor are two separate components requiring assembly and electrical contact. Various ceramic support components are incorporated to enhance structural integrity and to ensure an impermeable seal between the reference air and the exhaust gases while also providing a degree of impact protection for the sensor unit. On the exhaust-gas side, the sensor elements receive both physical and thermal protection from a protection tube. Due to its basic design configuration, the planar sensor element does not share the rotational symmetry of its thimble-type counterpart. Thus, it must be installed in a specific position; the protection tube features a partial double wall to facilitate orientation. The offset inlet openings provide a uniform flow of exhaust gases past the measurement electrode, regardless of its position relative to the exhaust-gas stream. Thermal insulation from the exhaust gases is also improved.

Although unheated thimble-type sensors are still on the market, they are becoming less important due to the increasing demands for precision of emission control systems.

6.4 FACTORS AFFECTING THE CONTROL CHARACTERISTICS OF LAMBDA = 1 SENSORS

6.4.1 Factors Affecting the Static Curve

Due to the porous protective layer around the electrode, the steep voltage change in the sensor's characteristic curve does not occur at precisely lambda = 1; instead, it is displaced a small

PETITIONER'S EXHIBIT 1002
US PATENT NO. 6,557,540

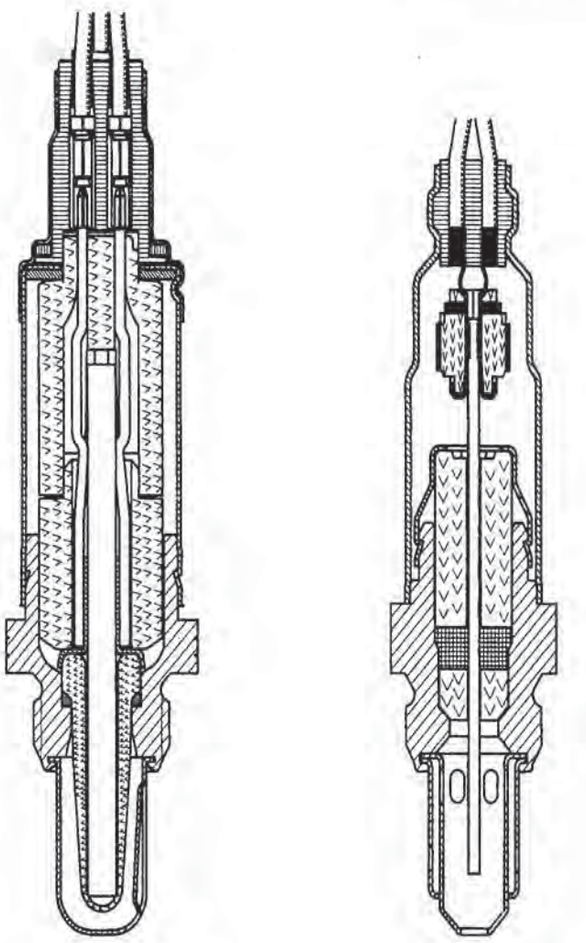


FIGURE 6.9 Construction of thimble-type and planar-type oxygen sensors.

amount into the lean range. The lower the porosity of the protective layer, the greater the diffusion of H_2 relative to O_2 toward the electrode. This phenomenon induces changes in the lambda value at the electrode relative to the lambda of the exhaust gas, the electrode detects richer exhaust gas and the lambda characteristic curve is displaced into the lean range.

Lean Shift. The lean shift is caused by exhaust-gas residue, such as oil ash and SiO_2, which partially plug the pores of the protective layer, and by reductions in sensor temperature.

Rich Shift. Fractures and flake-off of the protective layer lead to reductions in response times and shift the static characteristic curve toward rich. Electrode deactivation, especially due to lead contamination, will produce a flatter static response curve, as free, unconverted oxygen will also be detected. This effect also displaces the switchpoint threshold toward a lower lambda. A similar effect occurs when the reference atmosphere is contaminated (Chemical Shift Down, or CSD), for instance, with exhaust gases or water. Figure 6.10 shows typical characteristic curves for these conditions.

PETITIONER'S EXHIBIT 1002
US PATENT NO. 6,557,540

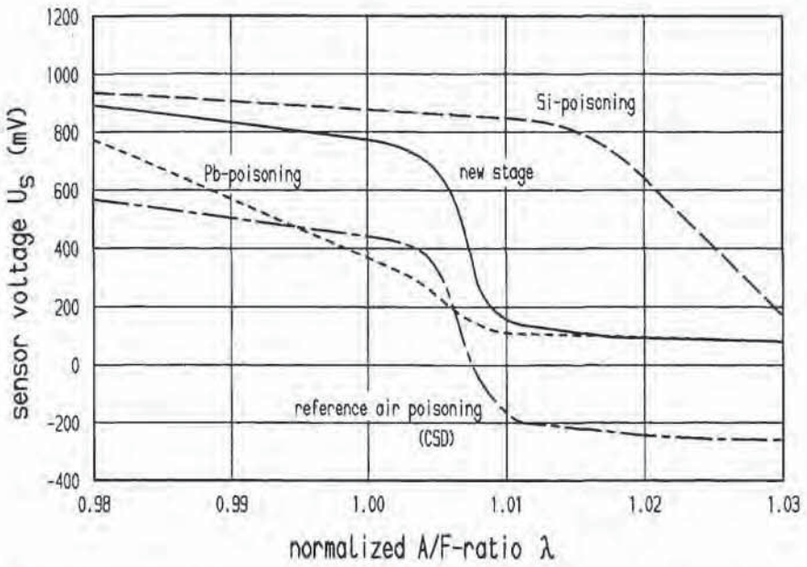


FIGURE 6.10 Effects of contamination on the static response curve of a lambda = 1 sensor as measured at laboratory test stand at $T_{gas} \approx 350$ °C.

6.4.2 Factors Affecting Sensor Dynamics and Control State

Factors. The control state (adjusted lambda) depends upon a number of factors. These include static sensor characteristics, sensor dynamics and asymmetry in sensor response times (switching times), t_{rs} (rich to switchpoint) during the surge from rich to lean, and t_{ls} (lean to switchpoint) during the jump from lean to rich. The sensor switching times t_{rs} and t_{ls} are strongly influenced by the configuration of the protection tube, the protective layer, and the sensor's temperature. Without the protection tube, switching times of less than 10 ms have been measured for ZrO_2 sensors with $T_{ceramic} \approx 900$ °C. However, such rapid response times are neither necessary nor desirable with many of the systems presently in use.

Response Times. An increase in response time that is not accompanied by a variation in the differential between t_{rs} and t_{ls} results in worse emissions with a constant control state due to the fact that the control amplitude increases while the conversion rate of the catalytic converter is reduced (see sec. 6.1.4 and Fig. 6.2).

Asymmetry. An asymmetrical increase in the response times t_{rs} and t_{ls} will also affect the control state due to the lambda shift.

Lean Shift. A pronounced increase in t_{rs} leads to a displacement toward lean. This can occur for any of several reasons. The dwell time in the rich exhaust gas is determined by control frequency and amplitude, and affects t_{rs} through the adsorption of CO and HC. Should the protective layer be obstructed (for instance, by oil ash), or should the sensor temperature drop, t_{rs} will generally rise more than t_{ls}.

Rich Shift. In contrast, a more pronounced rise in t_{ls} will lead to a displacement toward the rich range. The conversion rate of the electrode and the protective layer exercise a major influence on t_{ls}. Lead deposits diminish catalytic activity, causing t_{ls} to rise without exercising any substantive effect on t_{rs}.

Temperature. As a general rule, the susceptibility to sensor contamination is inversely proportional to electrode temperature. The factors determining the temperature of the ceramic material are the heater, the gas temperature, the gas flow rate (rpm, load), and the protection

PETITIONER'S EXHIBIT 1002
US PATENT NO. 6,557,540

tube. Depending upon the installation location, the ceramic temperature generally lies between 350 and 1000 °C for exhaust temperatures ranging between 150 and 900 °C. The flow velocity of the gas varies between 2 m/s at idle, 40 m/s at moderate rpm and load, and up to 80 m/s under full load. The influence exercised by gas temperature and the protection tube can be seen in Fig. 6.11. The ceramic temperature has a major effect on the controlled lambda. A protection tube providing a lower gas flow (see Fig. 6.11: 1 hole/4 flaps) and a higher heater

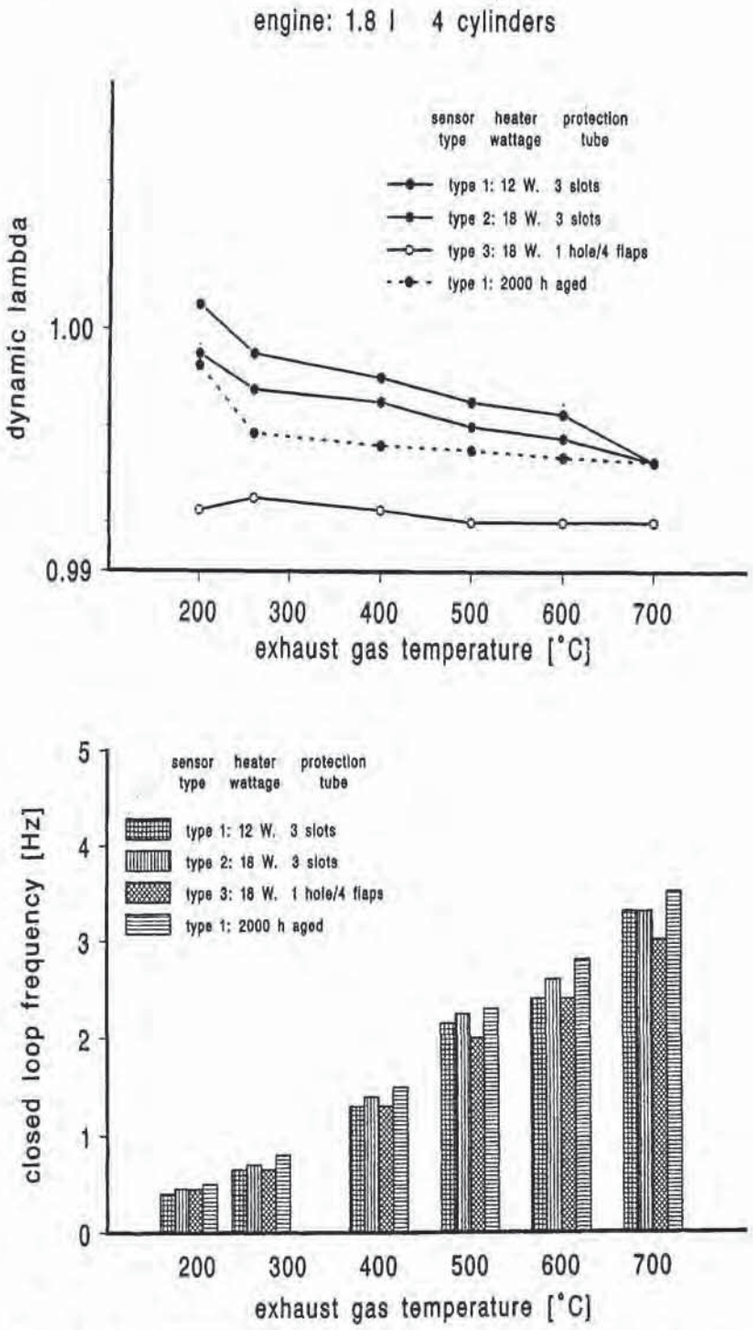


FIGURE 6.11 Effects of exhaust-gas temperature (rpm) on dynamic lambda and control frequency.

PETITIONER'S EXHIBIT 1002
US PATENT NO. 6,557,540

power (18 W) will lead to higher ceramic temperatures with enhanced temperature consistency relative to exhaust temperature. This measure is employed to obtain a more stable controlled lambda. The lambda value displays a moderate rich shift compared to that obtained with a more open tube (see Fig. 6.11: 3 slots) and 12 W heater power.

System Lag. System lag is dependent on the sensor's installation position (0.2 to 2 m downstream from the exhaust manifold, with approx. 1 meter downstream from the exhaust valve being typical) and the gas velocity as determined by load, rpm, and the exhaust pipe diameter. It can be up to 500 ms at idle, and drops down to delays as low as 20 ms at full load. The sensor (protection tube, heater power) is of secondary significance (Fig. 6.11). The influence of sensor response times (t_{ts}, t_{ls}) on the control state increases as a function of their share of the total system lag.

tv Shift. The cumulative effect of all extraneous influences is a slight lean control state of the lambda = 1 sensor. Electronic compensation for the lean shift is available in the form of an asymmetrical control-oscillation pattern (see Sec. 6.1.4). This is provided either by means of a switching delay after the sensor surge (tv shift, Fig. 6.3), through variations in the controller's surge amplitude, and/or via asymmetrical ramp slope. Those parameters for the electronic lambda displacement which vary according to load and rpm can be stored as a program map in the electronic control unit (ECU). This method can be employed for lambda corrections up to $|\Delta\lambda| \leq 0.015$.

6.5 APPLICATIONS

6.5.1 Operating Conditions

Environmental Factors. Table 6.3 provides a summary of the types and magnitudes of the major stress factors affecting the sensor. Beyond the actual function of the sensor itself, optimal selection and precise mixture of all applied materials (ceramics, metals, synthetics) are essential factors in obtaining the thermal, mechanical, and chemical characteristics needed to achieve the obligatory extended service life of over 100,000 miles.

Sensor Installation Location. Because it is of determining significance for both external influences and control function, correct sensor location is a critical factor in calibrating the performance of the total lambda-control system. The sensor must be far enough from the exhaust valves to ensure that it monitors representative exhaust gases for all cylinders, but near enough to hold system lag to acceptable levels. Both factors affect emissions.

Thermal Stress. Thermal stresses at the sensor stem from the high-potential exhaust-gas temperatures as well as from the temperature gradients that occur. Exhaust temperature is essentially a function of engine speed, and can reach a maximum of 1000 °C at the sensor on high-performance engines. The most extreme temperature gradients at the sensor occur during hard driving directly in the wake of a warm start at which the exhaust system and the sensor have already cooled off. These conditions can produce exhaust-gas temperature gradients of up to 500 K/s.

Thermal Shock. In the warm-up phase following a cold start, condensation on the pipe walls can cause the ceramic material to crack once the electric heater warms it beyond the critical temperature of approximately 300 °C. Accumulations of condensation can be largely avoided by locating the sensor as close as possible to the engine to provide rapid heating of the upstream exhaust pipe. Depending upon the specific vehicle, a time delay for switching on the sensor heater may be required.

PETITIONER'S EXHIBIT 1002
US PATENT NO. 6,557,540

TABLE 6.3 Overview of Stress Factors for Exhaust Gas Sensors

Mechanical stress	Stress caused by environmental conditions	Thermal stress	Stress caused by exposition to exhaust gas
Vibrational stress (<1300 m/s²) by engine vibration (<5 kHz) by pulsation of the exhaust gas (< ±300 mbar) by ambient wind (cable, <10 Hz)	Splash water, gush of water (in case containing NaCl, $CaCl_2$, $MgCl_2$)	Exhaust gas temperature (150 °C ... 1000 °C)	Exhaust gas composition ch between lambda = 0.85 (fuel load enrichment) and lambda infinite (overrun fuel)
Stone impact (<1.5 Nm)	Dust (organic, inorganic origin)	Exhaust gas temperature gradients at cold start (<500 K/s) at overrun fuel cutoff (<200 K/s)	Catalyst poisoning from fuel additives: permissible lead content: <0.013 g/l sulfur content: <0.1 % Br-, Cl-compounds
Installation/removal (torque about 50 Nm when assembled)	Oil, dirt undercarriage protection	Temperature increase after engine stalling (<300 °C at cable outlet)	Oil ash (Ca-, P-, S-, Zn-compounds up to 1 kg within ~60000)
Wire pull test (>70 N)	Fluctuation of the electrical supply system (9 ... 15 V)	Radiant heat (may require corresponding protective measures)	Miscellaneous corrosion products (e.g., Fe-oxides)
Handling (shock load up to 1000 g)	EMC (<200 V/m)		Condensation water
	Variation of climatic conditions (–40 °C ... +50 °C, 10 ... 100% rel. humidity)		

Mechanical Stresses. The main sources of mechanical stress on the sensor are vibration, exhaust-gas pulsation, stone impact, and cable tension (Table 6.3).

Sealing. The cable outlet of the sensor must be sealed to prevent water splash from penetrating to its interior and distorting the reference air (see Sec. 6.4.1 and Fig. 6.10). At the same time, the sealing element must be flexible enough to absorb the accelerative forces associated with vibration as well as any tensile forces transmitted through the cable.

6.5.2 Emission Certification

It would be impossible for a vehicle equipped only with an unregulated catalytic converter and lacking an oxygen sensor to achieve compliance with the American emission standards. When a regulated catalytic converter is used together with an oxygen sensor, emissions remain well below the limits. Even after vehicle mileage corresponding to more than 100,000 miles, the sensor limits emission increases to a minimum (Fig. 6.12). The introduction of a new system must be accompanied by precise calibration of the engine-control system to match the production tolerances and aging characteristics which affect the sensor's control response. The considerable effects that temperature and aging exercise on the catalytic converter must also be considered.

Durability Tests

Life Cycle. To determine aging behavior, the sensors undergo a standard durability test in the exhaust-gas stream of a test engine. The test cycle is designed to simulate combined urban and rural operation, and has been adopted by many automobile manufacturers as a standard program. The mean average speed is approximately 100 km/h for a midrange car. All newly developed products must withstand 2000 h (more than 100,000 miles) operation in this program without failure.

Hot Durability Testing. In a substantially more demanding test, essentially consisting of simulated full-load operation, the sensors must survive at least 1000 h (roughly 100,000 miles). The main stress factors for the sensors in these tests are thermal exposure (exhaust-gas temperatures reaching 950 °C, housing temperatures up to 650 °C), exhaust gas loads, and vibration.

PETITIONER'S EXHIBIT 1002
US PATENT NO. 6,557,540

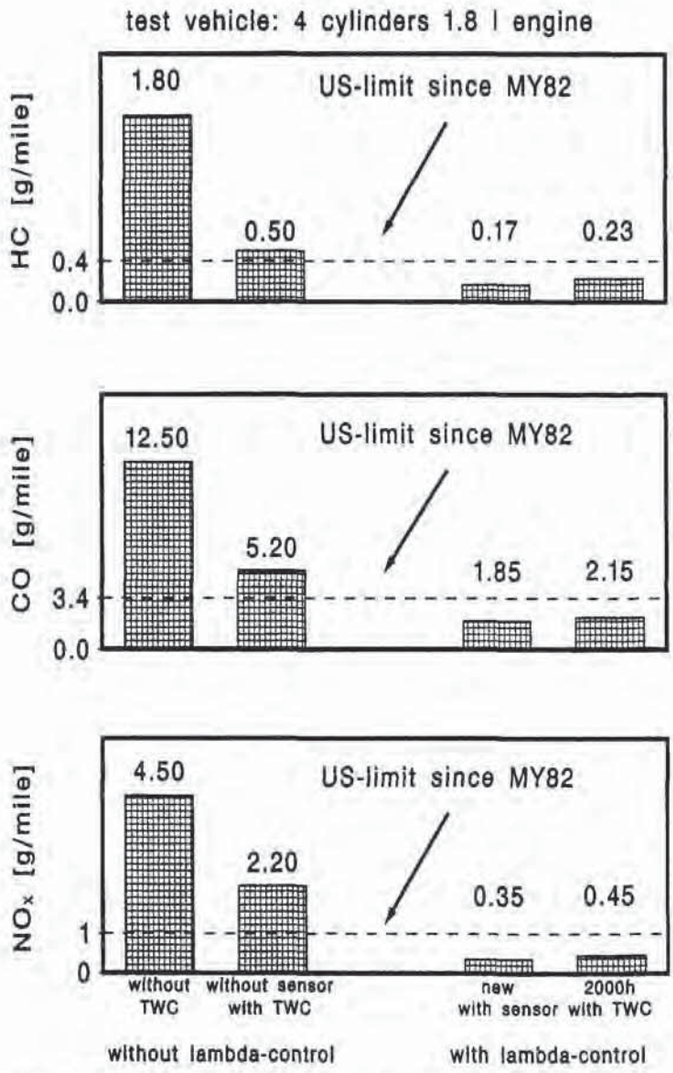


FIGURE 6.12 Comparison of emissions levels without catalytic converter, with unregulated converter, with controlled converter (new and old sensors, converter approx. 10,000 km).

Durability Testing of Contamination Resistance. Short durability tests featuring higher levels of Pb, Si, and oil are employed to determine the sensor's resistance to contamination damage.

6.6 SENSOR PRINCIPLES FOR OTHER EXHAUST GAS COMPONENTS

Sensors capable of monitoring the levels of the regulated toxic exhaust substances—CO, NO_x, and HC—would be desirable as elements of the On-Board Diagnosis systems (OBD I and OBD II) specified by the California Air Resources Board. Due to the extreme operating con-

PETITIONER'S EXHIBIT 1002
US PATENT NO. 6,557,540

ditions, only a few of the many tested configurations have a chance to be used in engine-exhaust gas.

6.6.1 Mixed-Potential Sensors

Sensing Mechanism. If reduced catalytic activity prevents gas equilibrium from being achieved at the electrode of a galvanic ZrO_2 cell, competing reactions can occur. These, in turn, prevent a state of reduction/oxidation equilibrium in the oxygen, and lead to the formation of a mixed potential. This potential is determined by electrode activity, temperature, and gas composition. It is difficult to design manufacturing techniques that can consistently produce electrodes capable of maintaining specific, defined rates of catalytic activity over extended periods of time. Every change in electrode activity (for instance, due to aging) leads to a variation in mixed potential. Pt electrodes give rise to a mixed potential at very low temperatures, with extended response delays relative to lambda sensors. Other electrode materials with lower rates of catalytic activity continue to provide a mixed potential at higher temperatures, making it possible to achieve response times < 1 s.

Selectivity. Careful selection of electrode materials, operating temperature, and selective precatalyzation layers offers opportunities for improving selectivity.

Operation Mode. Because the effect is temperature-sensitive, a constant sensor temperature must be regulated in the range of 300 to 600 °C, depending upon the individual application.

6.6.2 Semiconductor Gas Sensors

Sensing Mechanism

Ceramic and Thick-Film Layers. On the surface of nonstoichiometric metal oxides such as SnO_2, TiO_2, In_2O_3, and Fe_2O_3 (*n*-type semiconductors), oxygen is absorbed and dissociated in air at high temperatures and is bonded to the crystal lattice. This leads to the formation of a thin depletion layer at the crystallite surface with a resultant arch in the potential curve. This phenomenon produces reductions in surface conductivity and higher intercrystalline resistance at the boundaries between two crystallites; this is the major factor determining the total resistance of the polycrystalline metal oxide. Oxidation gases such as CO, H_2, and C_xH_y, which react with surface oxygen, increase the density of charge carriers in the boundary layer and reduce the potential barrier. Reduction gases, such as NO_x and SO_x raise the potential barrier and, with it, the surface/intercrystalline resistance.

Thin-Film Layers. Compared to porous polycrystalline materials, thin-film layers display only limited numbers of crystalline boundaries at the layer surface for reaction with the exhaust gases. The depletion-layer barrier makes up a substantial proportion of the layer thickness on thin-film devices, meaning that changes in charge-carrier density within the barrier layer due to adsorbed gases will also result in substantial variations in the total resistance.

Selectivity. Selected doping materials and temperatures can be employed to achieve selectivity for CO, HC, or NO_x. The resistance of metal-oxide semiconductors is always a function of the partial pressure of the O_2.

Specific Influences of Exhaust Gas. Engine exhaust gas with minimal, highly variable O_2 partial pressures is characterized by a high level of O_2 cross-axis sensitivity. Within the lambda = 1 to lambda < 1 operating range, an irreversible long-term change in sensor resistance leading to disintegration of the metal oxide is also possible. High operating temperatures are conducive to the diffusion of oxygen vacancies and doping materials. When amplified by sintering effects, these lead to resistance drift and attenuated sensor response.

PETITIONER'S EXHIBIT 1002
US PATENT NO. 6,557,540

Standard operating temperatures for metal-oxide gas sensors range from 100 to 500 °C, with up to 600 °C being seen in some restricted applications. With SnO_2, a high level of selectivity for, for example, CO can be achieved at temperatures as low as the 100 to 200 °C range. However, the response times can be measured in minutes. At higher temperatures, in the 300 to 550 °C range, response times of less than 1 s can be obtained, but with reduced selectivity.

6.6.3 Catalytic Gas Sensors

Sensing Mechanism. The catalytic gas sensor is essentially a temperature sensor featuring a catalytically active surface. An exothermic reaction (basically an oxidation reaction in air) at the catalytically active surface causes the temperature of the sensor to rise. The increase in temperature is proportional to the concentration of an oxidation gas in an excess-oxygen atmosphere. A temperature sensor of the same basic design—but without the catalytic response—is employed to enhance sensitivity and to provide temperature compensation by means of differential-signal evaluation. Materials employed for the temperature sensor include coiled Pt wire, Pt thin-film and thick-film layers, transistors, and NTC and PTC thermistors.

Operating Conditions. Catalytic gas sensors are relatively insensitive and can be employed in a range >1000 ppm. Excess oxygen is required to monitor concentrations. Due to the sensitivity to flow rate, these units are generally operated in flowheads with diffusion limiters. Measurement and reference sensors must be exposed to the same flow conditions, with no mutual thermal influences. Symmetrical configurations in pellet form are thus preferred over planar shapes. Operating temperatures for commercial sensors are in the 500 to 600 °C range, but extension to higher temperatures is possible. The requirement for long-term stability in the catalytic converter is the limiting factor governing the operating temperature. Catalytic gas sensors are not selective, instead providing a summing signal for all combustion gases. Thus catalytic sensors for application in exhaust gases are restricted to monitoring the state of the catalytic converter.

BIBLIOGRAPHY

Arndt, J., "Ceramics and Oxides," in W. Göpel, J. Hesse, and J. N. Zemel (eds.), *Sensors—Fundamentals and General Aspects,* vol. 1, S.252 ff, VCH Verlagsgesellschaft, Weinheim, 1989.

Barnes, G. J., R. L. Klimisch, and B. B. Krieger, "Equilibrium Considerations in Catalytic Emission Control," SAE Paper 730200, *SAE National Automobile Engineering Meeting,* Detroit, Jan. 1973.

Bosch, *Automotive Electric/Electronic Systems,* VDI, Düsseldorf, May 1987.

Bosch, *Automotive Handbook,* VDI-Verlag, Düsseldorf, 1986.

Duecker, H., K.-H. Friese, and W.-D. Haecker, "Ceramic Aspects of the Bosch Lambda-Sensor," SAE Paper 750223, *SAE National Automobile Engineering Meeting,* Detroit, 1975.

Gruber, H. U., and H. M. Wiedenmann, "Three Years Field Experience with the Lambda-Sensor in Automotive Control Systems," SAE Paper 800017, *SAE National Automobile Engineering Meeting,* Detroit, Feb. 1980.

Moseley, P. T., and B. C. Tofield (eds.), *Solid State Gas Sensors,* Adam Hilger, Bristol and Philadelphia, 1987.

Saji, K., "Characteristics of Limiting Current-Type Oxygen Sensor," *J. Electrochem. Soc.: Electrochem. Science and Technology,* vol. 134, no. 10, 1987, pp. 534–542.

Saji, K., H. Kondo, T. Takeuchi, and I. Igarashi, "EMF Characteristics of Zirconia Oxygen Sensor in Nonequilibrium Gas Mixtures Containing Combustible Gas and Oxygen," *Proc. 1st Sensor Symposium,* Tsukuba, Japan, June 1981, pp. 103–107.

Soejima, S., and S. Mase, "Multi-Layered Zirconia Oxygen Sensor for Lean Burn Engine Application," SAE Paper 850378, *SAE National Automobile Engineering Meeting,* Detroit, 1985.

PETITIONER'S EXHIBIT 1002
US PATENT NO. 6,557,540

Takami, A., "Development of Titania Heated Exhaust-Gas Oxygen Sensor," *Ceramic Bulletin*, vol. 67, no. 12, 1988, pp. 1956–1960.

Wiedenmann, H. M., "Characteristics of Oxygen Sensors for Lean Exhaust Gas," *VDI Berichte* 578, S.129–151, VDI-Verlag, Düsseldorf, 1985.

ABOUT THE AUTHORS

HANS-MARTIN WIEDENMANN studied physics and meterology in Tübingen and Munich, where he received his Ph.D. in Physics in 1969. He joined Bosch in 1970 and is now senior manager for the development of lambda oxygen sensors.

GERHARD HÖTZEL studied chemistry in Konstanz and received his Ph.D. in 1986 at the University of Stuttgart. At Bosch, he is responsible for physical bases and measurement techniques for lambda oxygen sensors.

HARALD NEUMANN studied solid-state electronics in Aachen where he received a Ph.D. in 1988. Since that time, at Bosch he has been responsible for the technology of planar-type ceramic sensors.

JOHANN RIEGEL studied electrical engineering in Karlsruhe and received a Ph.D. in 1989. At Bosch he is responsible for the investigation of planar-type ceramic sensors.

HELMUT WEYL studied mechanical engineering in Darmstadt and was graduated from there in 1966. He has been with Bosch since 1968 and is now responsible for proving lambda oxygen sensors.

PETITIONER'S EXHIBIT 1002
US PATENT NO. 6,557,540

PETITIONER'S EXHIBIT 1002
US PATENT NO. 6,557,540

CHAPTER 7
SPEED AND ACCELERATION SENSORS

William C. Dunn
Motorola Inc.
Semiconductor Products Sector

7.1 INTRODUCTION

In the automotive arena, speed and acceleration sensors are used in a wide variety of applications, from improving engine performance through safety to helping to provide creature comforts.

Speed sensing can be divided into rotational and linear applications. Rotational speed sensing has two major application areas: engine speed monitoring to enhance engine control, and performance and antilock breaking and traction control systems for improved road handling and safety. Linear sensing can be used for ground-speed monitoring for vehicle control, obstacle detection, and crash avoidance. Acceleration sensors are used in air bag deployment, ride control, antilock brake, traction, and inertial navigation systems.

In most cases, there are a number of different sensor types available for a specific monitoring function. However, the choice of sensor for a specific application can be difficult to make. The selection may be determined by the familiarity of the system's designer with the sensor. On the other hand, the output from one sensor can be used for several applications, and the individual requirements of each application may eventually determine the sensor to be used.

Electronics and electronic sensors are making rapid inroads into the automotive market. In order to analyze the large amounts of sensor data needed for low emissions and efficient engine control, it is necessary to process the information using microcontrollers (MCUs), which can operate at high speeds and in real time. Sensors that can convert information directly into a digital format for MCU compatibility have a distinct advantage over an analog output format. Digital signals are also supply-line voltage-insensitive, virtually unaffected by noise, and have better resolution than can be obtained with analog signals. If the addition of an analog-to-digital converter (on or off the MCU) is required for compatibility, the system cost is increased. The accuracy of the control system is only as good as the integrity of the sensor data supplied to the MCU. Hence, the importance of the performance of the sensor.

This chapter concentrates on speed and acceleration, and therefore does not go into all the other different types of applications for which many of these sensors can be used in the automobile.

PETITIONER'S EXHIBIT 1002
US PATENT NO. 6,557,540

7.2 SPEED-SENSING DEVICES

In automotive applications, the environment must be taken into consideration. The sensing must be accurate, the devices must be rugged and reliable, and they must function in the presence of oil, grease, dirt, and inclement weather conditions. These requirements have severely limited the use of a number of otherwise practical alternatives, such as optical sensors and contact sensing.

In the area of rotational speed monitoring, the most practical devices use magnetic field sensing. These sensors are Hall effect devices, variable reluctance (VR), and magnetoresistive or magnetic resistance element (MRE) devices. Both the Hall effect and VR devices have been widely used and have a proven track record. The MRE device has only recently come into its own with improved technology and provides a viable alternative to the Hall effect device. The MRE device has a higher sensitivity and a wider operating temperature range than the Hall effect device.

For the measurement of ground speed and object detection, optical, radar, laser, infrared, and ultrasonics have been explored. Linear sensing devices typically use the Doppler effect for speed sensing and pulse modulation for distance measuring. These devices are used for object detection in blind spots when reversing or changing lanes, and in such applications as collision avoidance systems.

7.2.1 Variable Reluctance Devices

Variable reluctance devices are in effect small ac generators with an output voltage proportional to speed, but they are limited in applications where zero speed sensing is required. The operating frequency range of the VR device is from about 10 Hz to 50 kHz. It is insensitive to mechanical stress and has a wide temperature operating range from −40 to 190 °C. The supply voltage and offset drift will depend upon the control electronics. The VR device, originally designed around existing automotive electromechanical systems, was adapted for electronic control. The ferrous metal in the VR system is designed for maximum output voltage at low rpm (revolutions per minute), to get as close as possible to zero speed sensing without generating excessive voltages at maximum rpm (up to 150 V). This device gives a linear output voltage with frequency. Most systems use MCUs for data processing, so the VR device needs an analog-to-digital (A/D) converter to generate a digital signal for compatibility with the MCU. Although the VR device itself is inexpensive, the extra costs for data conversion may eventually lead to its demise in many automotive applications.

7.2.2 Hall Effect Devices

The Hall effect exists when a current flowing in a carrier experiencing a magnetic field perpendicular to the direction of current flow results in the current being deflected perpendicular to the field and to the direction of the current. The Hall effect is shown in Fig. 7.1. A current I_c flowing through the device between terminals 1 and 2 will produce a potential VH between terminals 3 and 4, when a magnetic field **B** is applied perpendicular to the device. The potential VH is determined by the strength of the magnetic field and the current flowing. Hall effect devices can be manufactured with indium, gallium arsenide, or silicon. A comparison of their properties is given in Table 7.1.

As can be seen, silicon is the most sensitive material. It is compatible with ICs and has a wide operating temperature range. The Hall effect device is well known both in industry and in the automotive arena for rotational and position-sensing applications. However, recent developments in Hall sensing devices, such as differential sensing and integration, have given improved sensor characteristics, which may result in greater potential in automotive applications.

PETITIONER'S EXHIBIT 1002
US PATENT NO. 6,557,540

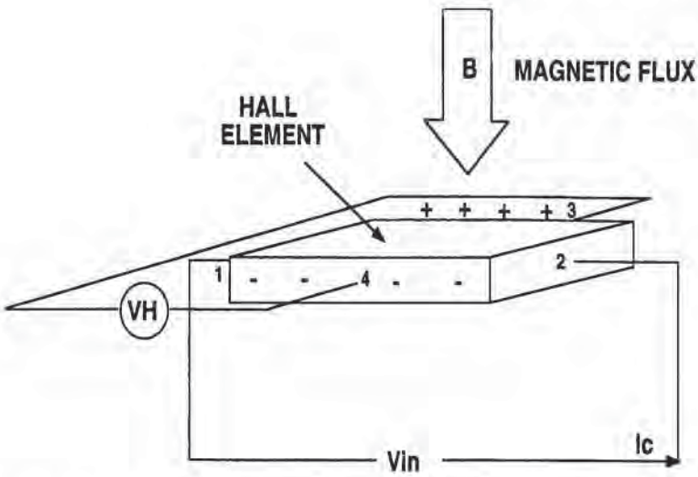


FIGURE 7.1 Hall effect.

The Hall effect device is very versatile, flexible in use, easy to package, and can be used for zero speed sensing (it can give an output when there is no rotation). Hall devices give a frequency output that is proportional to speed, making them compatible with MCUs. The Hall device is normally configured as a bridge to minimize temperature effects and to increase the sensitivity of the sensor.

A typical Hall effect sensor configuration with waveforms is shown in Fig. 7.2. The teeth of the ferrous wheel concentrate the magnetic flux when the teeth come into close proximity to the Hall sensor and magnet. The output from the sensor is a sinusoidal waveform, whose frequency is the rpm of the ferrous wheel multiplied by the number of teeth on the wheel. The resolution of the system depends on the number of teeth in the wheel (typically 20).

7.2.3 Magnetoresistive Devices

The magnetoresistive effect is the property of a current-carrying ferromagnetic material to change its resistivity in the presence of an external magnetic field. For example, a ferromagnetic (permalloy) element (an alloy containing 20 percent iron and 80 percent nickel) will change its resistivity by 2 to 3 percent when it experiences a 90° rotation in a magnetic field.[1] The resistivity value rises to a maximum when the direction of current and magnetic field are coincident, and is a minimum when the fields are perpendicular to each other. This relationship is shown in Fig. 7.3. This attribute is known as the Anisotropic Magneto Resistive Effect. The resistance R of an element is related to the angle q between the current and the magnetic field directions by the expression:

$$R = R_{\parallel} \cos^2 q + R_{l} \sin^2 q \tag{7.1}$$

TABLE 7.1 Comparison of Properties of Hall Effect Materials

Material	Operating temp. °C	Supply voltage	Sensitivity @ 1 kA/m	Frequency range
Indium	–40 to 100	1V	7 mV	0 to 1 MHz
GaAs	–40 to 150	5 V	1.2 mV	0 to 1 MHz
Si (with conditioning)	–40 to 150	12 V	94 mV	0 to 100 kHz

PETITIONER'S EXHIBIT 1002
US PATENT NO. 6,557,540

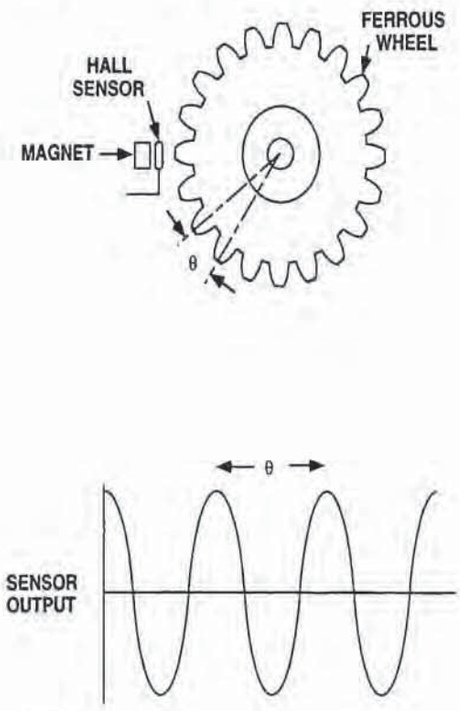


FIGURE 7.2 Hall sensor and output waveforms.

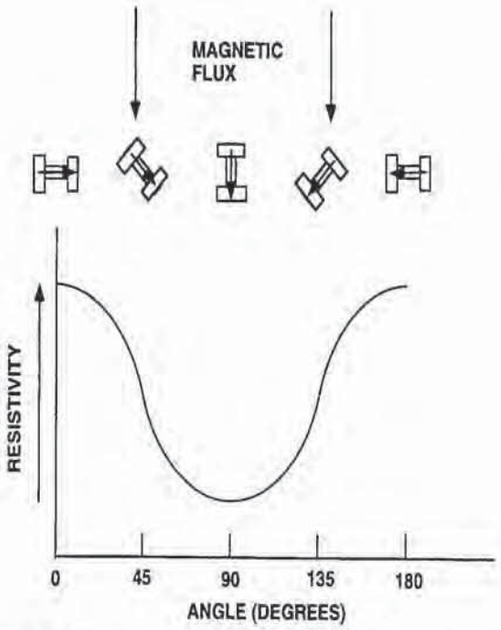


FIGURE 7.3 Relationship between magnetic field and resistivity change in MRE devices.

where $R_{\parallel}$ is the resistance when the current and the magnetic field directions are parallel and $R_{\perp}$ is the resistance when the current and the magnetic field directions are perpendicular.

MRE devices give an output when stationary, which make them suitable for zero speed sensing. MRE devices also give an output frequency that is proportional to speed, making for ease of interfacing with an MCU. For good sensitivity and to minimize temperature effects, a bridge configuration is normally used. In an MRE sensor, aluminum strips can be put across the permalloy element to linearize the device. This configuration is shown in Fig. 7.4 together with a typical MRE characteristic. The low-resistance aluminum stripes cause the current to flow at 45° in the permalloy element, which biases the element into a linear operating region.

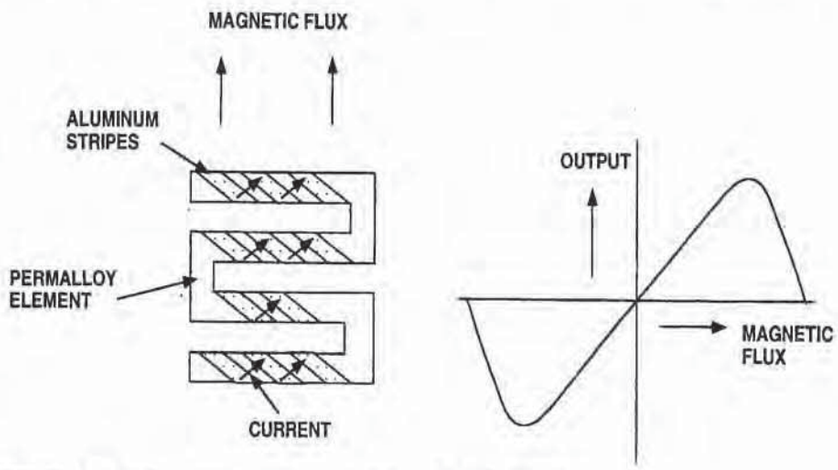


FIGURE 7.4 Use of permalloy strip for linearization in MRE devices.

PETITIONER'S EXHIBIT 1002
US PATENT NO. 6,557,540

Integrated MRE devices can typically operate from –40 to 150 °C, over a supply voltage range of 8 to 16 V, and at frequencies from 0 to 1 MHz. In comparing the MRE sensor to a Hall effect device, the MRE has a higher sensitivity, is less prone to mechanical stress, has a wider operating frequency range, has the potential of being more cost effective, gives better linearity, and is more reproducible. However, it is more sensitive to external magnetic fields. Table 7.2 shows a comparison of rotational sensing devices.

TABLE 7.2 Comparison of Sensing Devices

Sensor type	Operating temperature (°C)	Sensitivity 1 kA/m (mV)	Frequency range	Mechanical stress
Hall effect	–40 to 150	90	0 to 100 kHz	High
MRE	–40 to 150	140	0 to 1 MHz	Low
VR	–40 to 190		1 to 50 kHz	None
Magnetic transistor	–40 to 150	250	0 to 500 kHz	Low

It should be noted that Hall effect and MRE devices have many applications in the automobile outside of rotational speed sensing, such as position sensing, fuel-level sensing, and active suspension. The magnetic transistor is showing potential in rotational speed sensing and position-sensing applications, and may eventually be another viable contender to the Hall effect device in the automotive market.

7.2.4 Ultrasonic Devices

Ultrasonic devices can be used to measure distance, ground speed, and as a proximity detector. To give direction and beam shape, the signals are transmitted and received via specially configured horns and orifices. The transmitter and receiver horns are similar in shape, but are normally separate to accommodate different characteristics. The ultrasonic devices are made from PZT crystal-oriented piezoelectric material ($PbZrO_3$—$PbTiO_3$).

For the measurement of distance or object detection, a pulse of ultrasonic energy is transmitted and the time is measured for the reflected pulse to return to the receiver. The frequency of the transmitted ultrasonic waves are typically about 40 kHz and travel with a velocity of 340 m/s at 15 °C. This velocity changes with temperature and pressure. However, these parameters can be measured and corrections made if high accuracy is required. The repetition frequency and power requirements depend on the distance to be measured. To measure speed, the distance variation with time can be measured and the velocity calculated. A more common method is to use the Doppler effect, which is a change in the transmitted frequency as detected by the receiver due to motion of the target (or, in this case, the motion of the transmitter and receiver).

7.2.5 Optical and Radio Frequency Devices

Optical devices are still being used for rotational speed sensing. They are normally light-emitting diodes (LEDs) with optical sensors. Figure 7.5 shows a typical optical sensor system. An optical sensor detects light from an LED through a series of slits cut into the rotating disc, so that the output from the sensor is a pulse train whose frequency is equal to the rpm of the disc multiplied by the number of slits. The higher the number of slits in the disc, the smaller the angle of rotation that can be measured. The optical sensor can be a single photodiode or a photodiode array as shown. This array gives a more accurate determination of the position of the slit, resulting in higher resolution of the position of the disc.

PETITIONER'S EXHIBIT 1002
US PATENT NO. 6,557,540

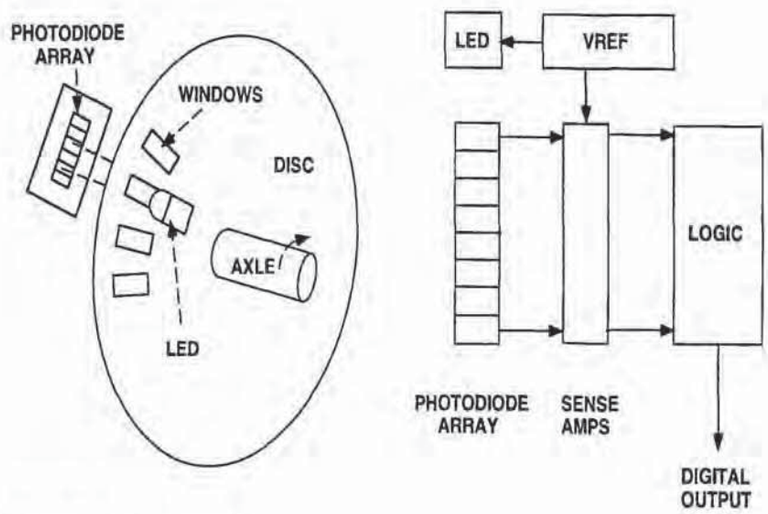


FIGURE 7.5 Optical sensor.

Optical and radio frequency (RF) devices are used for object detection, linear approach speed, and distance measurements in crash avoidance systems where distances greater than about 10 m are involved. These devices use the same principles as the ultrasonic devices. Optical devices normally use lasers or infrared devices for the transmitting source and optical sensors for the receivers. RF devices use gallium arsenide or Gunn devices to obtain the power and high frequency (about 100 GHz) required in the transmitter. The high operating frequency is set to a large extent by the need for a small antenna. These applications are under development and are discussed in Sec. 7.7.2.

7.3 AUTOMOTIVE APPLICATIONS FOR SPEED SENSING

There are several applications for rotational speed sensing. First it is necessary to monitor engine speed. This information is used for transmission control, engine control, cruise control, and possibly for a tachometer. Electronics and electronic sensing in the automobile were brought about by the need for higher-efficiency engines, better fuel economy, increased power and performance, and lower emissions. Second, wheel speed sensing is required for use in transmissions, cruise control, speedometers, antilock brake systems (ABS), traction control (ASR), variable ratio power steering assist, four-wheel steering, and possibly in inertial navigation and air bag deployment applications.

Linear speed sensing can be used to measure the ground speed. This measurement also has the possibly of use in ABS, ASR, and inertial navigation. Similar types of sensors can be used in crash avoidance, proximity, and obstacle detection applications.

7.3.1 Rotational Applications

The high timing accuracy that can be obtained with fuel injection systems and replacement of points by sensors have made cost-effective engine control and low maintenance a reality. Adjustment of the stoichiometric ratio of air to fuel, accurate ignition timing, and oxygen sensors in the exhaust system, have vastly improved engine performance and greatly reduced emissions over widely varying operating conditions. The two important factors in engine con-

PETITIONER'S EXHIBIT 1002
US PATENT NO. 6,557,540

trol are the engine speed in rpm and the crank angle. These signals are used by the engine control MCU for determination of fuel injection and ignition timing. The engine rpm measurement range is from 50 to (say) 8000 rpm. A resolution of about 10 rpm is required for an accuracy of about 0.2 percent. For injection and ignition control in a six-cylinder engine, the interval between combustion at maximum rpm is 2.5 ms, so that this time sets the injection period. In practice, a crank angle accuracy of between 1 and 2 degrees per revolution is required. Newer systems with sequential fuel injection, may also require information on TDC (top dead center) for each cylinder to determine the timing. With the low frequencies involved in this application, either Hall effect or MRE devices can be used for monitoring both the engine rpm and crank angle.

Vehicle speed measurements are in the range 0 to 180 km/h (120 mph) and digital displays must have an accuracy of 1 km/h. Some systems have a mechanical pickoff from the drive shaft, which can then use optical sensors for the measurement of road speed. However, newer systems have a pickoff located directly on the drive shaft, which makes optical devices less practical. It is preferred to eliminate the remote sensing via mechanical coupling to save the cost of the associated mechanical components, seals, maintenance, and so on. One method of pickoff is a ring magnet with between 4 and 20 magnetic poles (depending on the required resolution). Figure 7.6 shows such a system using an MRE sensing device. The magnetic flux changes are sensed by an MRE bridge sensor when the magnet disc is rotating. The bridge is supplied from a voltage reference circuit, and its output is amplified and shaped to give a frequency output that is proportional to shaft rotation speed. A ferrous toothed wheel pickoff with magnet and flux concentrator can also be used (see Fig. 7.2). Vehicle speed sensing can be performed with Hall effect, MRE, or VR devices. The number of pulses P per second from the detector are counted to measure speed S, from the following relationship:

$$P = N \times S \times K \tag{7.2}$$

where N = the number of magnetic poles on ring magnet or wheel teeth
K = a constant determined by axle ratio and wheel size

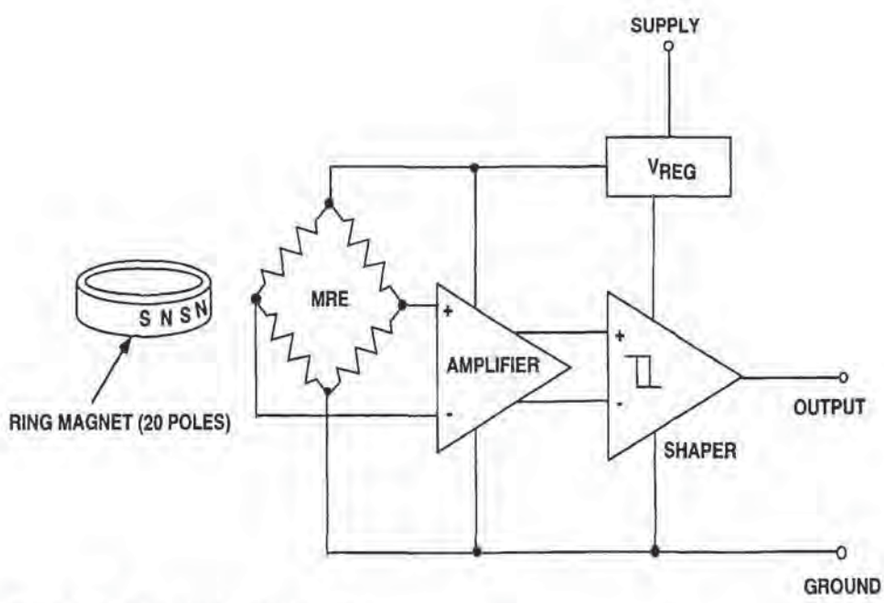


FIGURE 7.6 MRE speed-sensing module.

PETITIONER'S EXHIBIT 1002
US PATENT NO. 6,557,540

The resolution in vehicle speed is then:

$$\frac{P}{S} = N \times K \tag{7.3}$$

The typical system requirements are an operating temperature of –40 to 120 °C, rotational speed detection of 5 to 3000 rpm (1000 p/s), and a duty cycle ratio of 50 ± 10%.

In applications such as ABS, ASR, and four-wheel steering, additional speed sensors are attached to all four wheels so that the slip differential between the wheels can be measured. VR devices have been used and are very cost effective in this application. But the cost of other devices is dropping and as they become cost effective, they are being designed into new systems. In electronic transmission applications, information from the road and engine speed sensors, as well as torque data and throttle position are required for the MCU to select the optimum gear ratio. Electronic control can ensure smooth transition between gear ratios. Transmissions using electronic control are also smaller than conventional automatic transmissions, thus enabling more gear ratios for better performance, higher torque, efficiency, and acceleration.

Cruise control systems require information from the road and engine speed sensors to control the throttle position, and possibly the optimum selection of transmission ratios. Variable ratio assisted power steering also requires information from the wheel speed sensors for adjustment of the steering ratios for ease of turning at low speeds and good road control at high speeds. If automatic tire pressure adjustment becomes a reality, this system may also require information from the wheel speed sensors.

Another application for rotational speed sensing is to control the speed of the radiator cooling fan. The speed of the fan is determined by the coolant temperature. Hall effect devices (MRE can also be used) have been used to monitor the position of the armature and speed of the cooling fan motor. The motor controller uses this information to modulate the power to the motor through a three-phase bridge driving circuit for the control of the fan motor speed.

7.3.2 Linear Applications

Under linear applications are the detection of obstacles close to the vehicle, crash avoidance, distance of the chassis relative to the ground for ride control, measurement of ground speed for ABS, ASR, and inertial navigation. Ultrasonic devices are normally used for short distance measurements (<10 m) and RF devices for long distance measurements (see Sec. 7.6.2). For the measurement of objects from 0.5 to 2 m using ultrasonics, a pulse repetition rate of about 15 Hz is used. The reflected pulses take from 3 to 12 ms to return. The return time T is given by

$$L = C \times \frac{T}{2} \text{ (m)} \tag{7.4}$$

where L = distance to target
C = the transmission speed [given by $C = 331 + 0.6\,t$ (m/sec)]
T = temperature (at 15 °C), the speed of ultrasonic waves is 340 m/s.

In the case of chassis-to-ground measurements for ride control and ground speed measurements, the distance to be measured is from 15 to 50 cm and a higher pulse repetition rate can be used (up to 50 Hz). In this case, the reflected pulse takes from 0.9 to 3 ms to return. For ride control applications, an accelerometer has an advantage over distance measurement, in that it is unaffected by varying distance measurements over rough terrain.

7.4 ACCELERATION SENSING DEVICES

Acceleration sensors vary widely in their construction and operation. In applications such as crash sensors for air bag deployment, mechanical devices (simple mechanical switches) have

PETITIONER'S EXHIBIT 1002
US PATENT NO. 6,557,540

been developed and are in use. Mechanical switches are normally located at the point of impact in the crash zone. With the development of micromachined devices, solid state analog accelerometers have been designed for air bag applications. The analog accelerometers are centrally placed on the automotive frame. These devices can be very cost effective when compared to mechanical switches and are rapidly replacing the electromechanical devices. Silicon micromachined sensors provide a higher degree of functionality, can be programmed, have high reliability, have excellent device-to-device uniformity, and can be integrated with memory circuits to create a more accurate sensor. Additional features such as self-test and diagnostics are also available.

7.4.1 Mechanical Sensing Devices

Mechanical switches are simple make-break devices. Figure 7.7 shows the cross section of a Breed type of switch or sensor. The device contains a spring, a metal ball, and electric contacts in a tube. On impact, the inertia in the ball causes it to move against the retaining force of the spring and closes the electric contacts at the end of travel. An alternative to this device is the one shown in Fig. 7.8. It consists of a cylindrical mass wound in a flat spring. The seismic mass

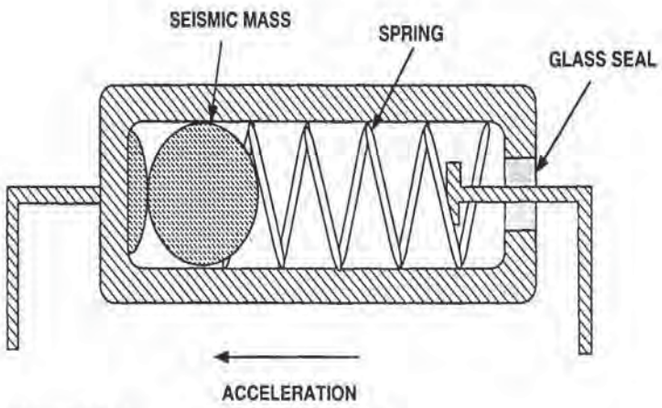


FIGURE 7.7 Cross section of mechanical sensor.

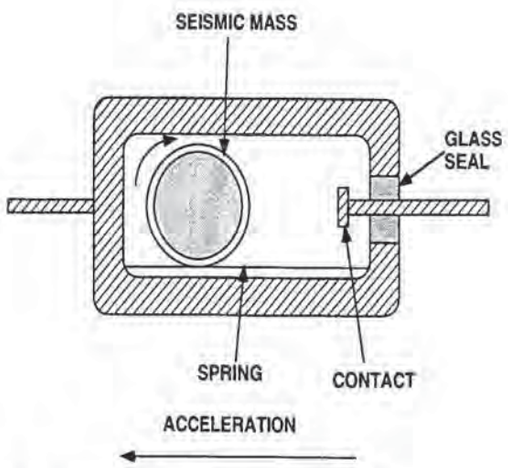


FIGURE 7.8 Cross section of mechanical switch.

PETITIONER'S EXHIBIT 1002
US PATENT NO. 6,557,540

rolls on impact against the spring tension, and again makes electrical contact at the end of travel. The machining tolerances on these devices are high and give wide variations in the acceleration trigger point.

7.4.2 Piezoelectric Sensing Devices

Piezoelectric devices consist of a layer of piezoelectric material (such as quartz) sandwiched between a mounting plate and a seismic mass. Electric connections are made to both sides of the piezoelectric material. The cross section of such a device is shown in Fig. 7.9. Piezoelectric material has the unique property that when a force or pressure is applied to opposite faces of the material, an electrical charge is produced. This charge can be amplified to give an output voltage that is proportional to the applied force. Piezoelectric devices can be effective in some applications, but are not suitable for sensing zero- or low-frequency acceleration, that is <5 Hz due to offset and temperature problems (pyroelectric effect). Piezoelectric sensors have a high Q, low damping, and a very high output impedance. Self-test features are also difficult to implement. The main advantages of piezoelectric devices are their wide operating temperature range (up to 300 °C), and high operating frequency (100 kHz).

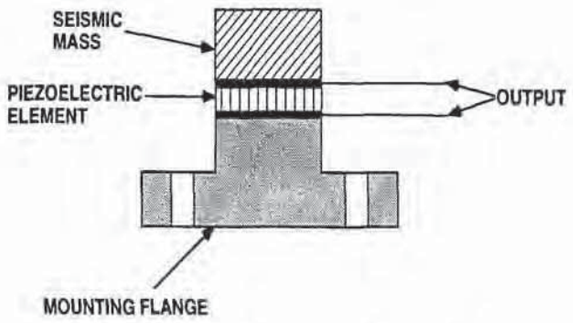


FIGURE 7.9 Cross section of a piezoelectric accelerometer.

Figure 7.10 shows a typical signal-conditioning circuit[2] and the trimming network used with piezoelectric sensors. The output from the sensor is fed to a charge amplifier, which converts the charge generated by the sensor into a voltage proportional to the charge. The circuit

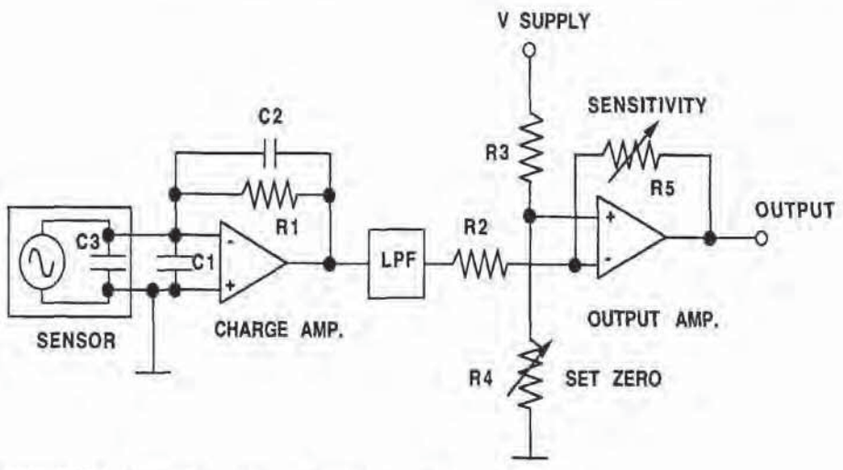


FIGURE 7.10 Piezoelectric signal-conditioning circuit.

PETITIONER'S EXHIBIT 1002
US PATENT NO. 6,557,540

is a modified virtual ground voltage amplifier. Feedback via capacitor C2 and resistor R1 is used to maintain the input at a virtual ground potential. This type of circuit minimizes the effect of stray or ground capacitance C1. The output voltage from the amplifier is fed via a low-pass filter (LPF) to an output amplifier, where it is trimmed for offset by R4 and sensitivity by R5. In system development, the sensitivity is set by the piezoelectric material used. Higher-sensitivity materials however, exhibit higher sensitivity to temperature variations.

7.4.3 Piezoresistive Sensing Devices

The property of some materials to change their resistivity when exposed to stress is called the piezoresistive effect. In silicon, the sensing resistors can be either P or N type doped regions, which can be very sensitive to strain. The resistors are also sensitive to temperature, so that the strain gauge is normally designed as a bridge configuration to minimize temperature effects and to obtain higher sensitivities (see also Chap. 2). In order to maintain good linearity, the operating temperature of piezoresistive devices is limited to about 100 °C. The nonlinearity is caused by excessive junction leakage current at high temperatures. Higher operating temperatures have been obtained using oxide-isolated strain gages (up to 175 °C). An uncompensated strain gauge has a typical error of 3 percent over the operating temperature range –20 to 80 °C. This error can be reduced with a compensating resistor, and still further reduced to about 0.5 percent by the use of thermistors, over an improved operating temperature range of –40 to 110 °C.

Piezoresistive sensing can be used with bulk micromachined accelerometers. Such a device is shown in Fig. 7.11. The strain-sensing elements are diffused into the suspension arms. These elements can then detect strain in the arms caused by acceleration forces on the seismic mass.

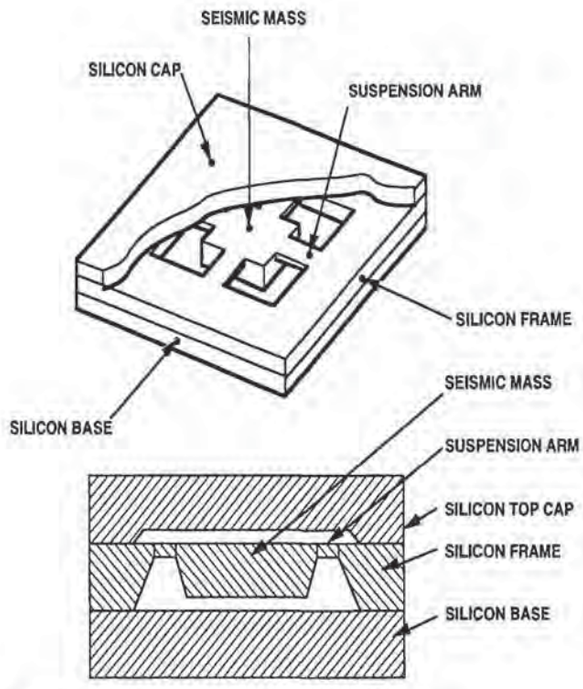


FIGURE 7.11 Bulk micromachined accelerometer.

PETITIONER'S EXHIBIT 1002
US PATENT NO. 6,557,540

7.4.4 Capacitive Sensing Devices

When used with micromachined structures as shown in Figs. 7.11 and 7.12, differential capacitive sensing has a number of attractive features when compared to other methods of sensing: easily implemented self-test, temperature insensitivity, and smaller size. In addition, comparing capacitive sensing to piezoelectric sensing reveals that capacitive sensing has the advantages of dc and low-frequency operation and well-controlled damping. When compared to piezoresistive sensing; differential capacitive sensing has the advantage of a wider operating temperature range and requires less complex trimming. Capacitive sensing has one other major advantage over other sensing methods in that it can be used in closed-loop servo systems. In these systems, voltages can be applied to the capacitive plates to produce electrostatic forces, which will balance the forces on the seismic mass due to acceleration. The main advantage of closed-loop operation is to make the sensor to a large extent independent of process variations. Signal-conditioning circuits can be designed to detect changes in capacitance of <0.1 fF, so that plate capacitances in the range of 200 to 400 fF can be used. The small spacing between capacitor plates in micromachining technology (2 μ) enables practical acceleration sensors as small as 500 μ × 500 μ. When designing capacitive sensors, care must be taken to ensure that the sensing voltages are properly balanced to minimize offsets due to electrostatic forces. These forces can also be produced by internal noise sources. The attributes of capacitive sensing are a linear response, operation over wide temperature ranges (–40 to 150 °C), and a frequency response from dc to about 2 kHz.

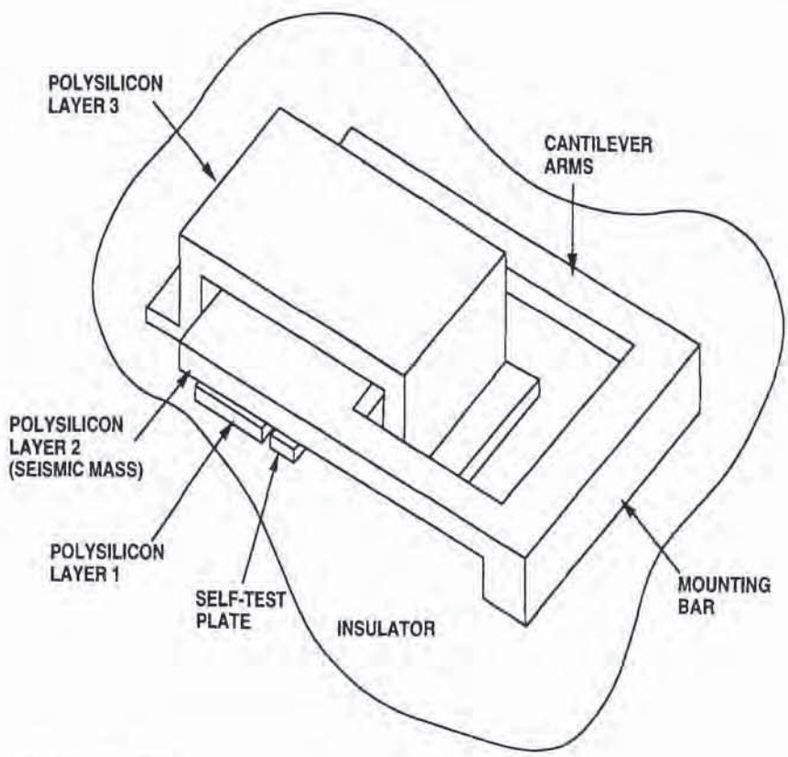


FIGURE 7.12 Surface micromachined accelerometer.

Micromachined Structures. There are a variety of types of micromachined structures that can be used in accelerometers. These structures fall into two technologies: bulk micromachined structures and surface micromachined structures. Bulk micromachined devices are structures

PETITIONER'S EXHIBIT 1002
US PATENT NO. 6,557,540

etched out of silicon wafers. Figure 7.11 shows the cross section of a bulk micromachined device consisting of three layers of silicon bonded together. The center layer is shaped to form a seismic mass suspended by four arms[3] (a cantilever structure has also been designed with two suspension arms[4]). When acted upon by acceleration forces, the seismic mass moves between the top and bottom plates. In this case, the movement can be sensed using piezoresistive elements diffused into the suspension arms, or differential capacitive sensing can be used between the seismic mass and the upper and lower silicon plates. The top and bottom plates can also be made of glass with metalized areas to form the top and bottom capacitors. Such devices have been designed to operate from the high g range (>1000 g), down to sensors with resolution in the μg range. Closed-loop control techniques are normally used in these lower g ranges.

The surface micromachined device shown in Fig. 7.12 is built using layers of polysilicon and sacrificial glass, which are alternately deposited and shaped. In this case, three layers of polysilicon and two layers of sacrificial glass were used. After deposition of the third polysilicon layer, the sacrificial glass is etched away leaving the freestanding structure as shown. A number of etch holes are normally placed in the second and third layer of polysilicon to speed up the etch process. These etch holes are also used to control the squeeze film damping and bandwidth of the device. The seismic mass of the second-layer polysilicon in these devices is of the order of 5×10^{-10} kg. A second plate under the middle polysilicon can be used for self-test. This function is achieved by applying a voltage to the self-test plate, which in turn will produce an electrostatic force on the center polysilicon plate causing it to deflect. This deflection will simulate an external acceleration force. An alternative to the polysilicon and glass structure is nickel with sacrificial copper.[5]

Differential capacitive sensing is used with all of these structures. Both bulk and surface micromachined devices have a very rugged construction. These devices use squeeze film damping to control bandwidth and to ensure critical damping of the resonant frequency (about 2 kHz for bulk and 10 kHz for surface micromachined devices). Film damping also ensures high resistance to shock in the sensing direction. In the directions perpendicular to the sensitive axes, the devices are rugged by construction with low cross-axis sensitivity (<3 percent). An accelerometer designed to sense a few g will typically have a shock tolerance of well over 5000 g. As already noted, surface micromachined devices that have been developed for air bag deployment have analog outputs. These devices normally operate from a 5-V supply, have a bandwidth of about 1 kHz and a sensitivity of 40 mV per g, giving a full-scale output with ±50 g input. Both open- and closed-loop techniques have been used for sensing. In comparing bulk and surface micromachined devices, the bulk structure is larger, using crystal-oriented etching with end stops, which require extra diffusions; whereas, the surface micromachined device uses isotropic etching (masking) with different materials acting as end stops. Surface structures have the potential for easier integration and use a simpler less costly process, but do require annealing.

Open-Loop Sensing. Open-loop signal-conditioning circuits amplify and convert the capacitance changes into a voltage. Such a CMOS circuit using switched capacitor techniques is shown in Fig. 7.13. The circuit contains a virtual ground amplifier to minimize the effect of stray capacitance. The positive input of the amplifier is referenced to a voltage of $V_{REF}/2$, when switch $S2$ is closed the amplifier has unity gain, and the voltage on the middle plate of the sensor is set to $V_{REF}/2$. After $S2$ is opened, $S1$ is switched so that any differences between sensor capacitors C_1 and C_2 produces a charge at the negative input of the amplifier. This charge produces a voltage (V_{out}) at the output of the integrating amplifier. The output voltage of the amplifier is given by

$$V_{out} = V_{REF} \frac{C_1 - C_2}{C_3} \tag{7.5}$$

where C_1 and C_2 are the sensor capacitances
C_3 is the integrator capacitance

PETITIONER'S EXHIBIT 1002
US PATENT NO. 6,557,540

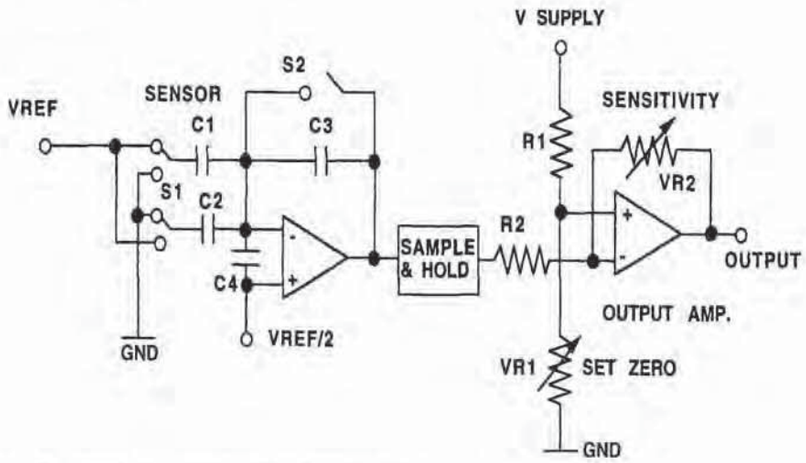


FIGURE 7.13 Capacitive sensing integrator circuit.

If the reference voltage is made proportional to the supply voltage, a ratiometric output is obtained. That is, the system gain is proportional to the supply voltage. This is a requirement in some systems to facilitate the design of the A/D converter.

A block diagram of the system is shown in Fig. 7.14. The system contains an internal oscillator, voltage reference, amplifier, sample and hold, switched capacitor filter, trim network, and output buffer. The output voltage in such a circuit is proportional to the capacitance change. This change is proportional to 1/displacement, or 1/acceleration, giving rise to some nonlinearities. However, the displacement is small compared to the spacing between the plates, so that the output voltage approximates to acceleration, giving less than 3 percent nonlinearity. The filter is used for noise reduction and to set the bandwidth for specific applications. Trimming is used to set the zero operating point and sensitivity of the system.

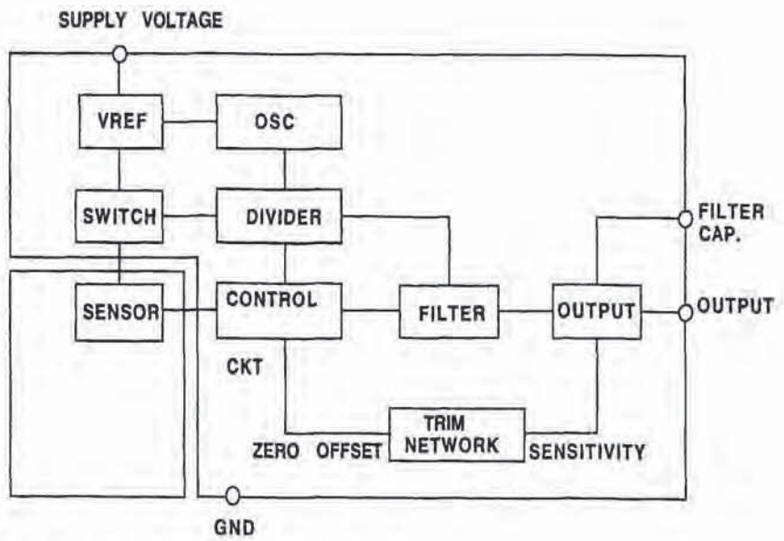


FIGURE 7.14 Signal-conditioning block diagram.

PETITIONER'S EXHIBIT 1002
US PATENT NO. 6,557,540

An alternate circuit with improved linearity is shown in Fig. 7.15. In this case, the output voltage is fed back to the input of the integrator, forming a bridge circuit. The feedback also sets the amplitude of the driving voltage across the sensing capacitors, so that it is proportional to their displacement. This also balances the electrostatic forces on the middle plate.

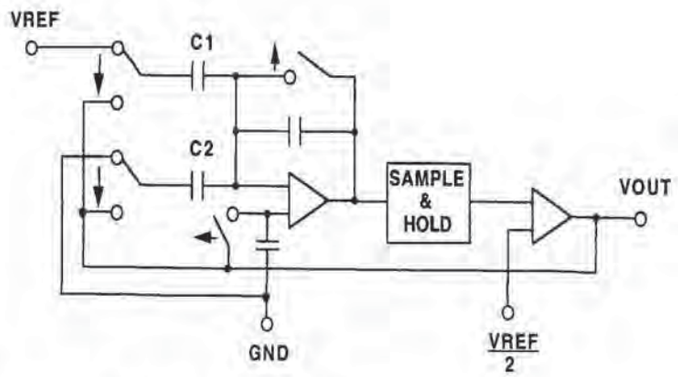


FIGURE 7.15 Linearized circuit schematic.

In this case

$$V_{out} = \frac{(C_1 - C_2)}{(C_1 + C_2)} \frac{V_{REF}}{2} \tag{7.6}$$

where $C_1 \propto 1/d_1$
$C_2 \propto 1/d_2$
$d_1 + d_2 = K$ (constant)

so that

$$V_{out} = V_{in} \frac{(d_1 - d_2)}{K} \tag{7.7}$$

showing that, in this case, V_{out} is proportional to displacement and acceleration giving improved linearity (<1 percent nonlinearity).

Closed-Loop Sensing. An alternative to the open-loop sensing circuit is the closed-loop sensing circuit, which can be configured to give an analog or digital output. Figure 7.16*a* shows the balanced electrostatic forces exerted on a seismic mass by upper and lower capacitor plates, which are at voltages of $+V$ and $-V$. If the seismic mass experiences a force due to acceleration, and a voltage δV is applied to the middle plate to generate enough electrostatic force to counterbalance the acceleration force, then the forces are as shown in Fig. 7.16*b*.

That is

$$m \times a = \frac{C(V + \delta V)^2}{2d} - \frac{C(V - \delta V)^2}{2d} \tag{7.8}$$

from which

$$m \times a = 2\,C \times V \times \frac{\delta V}{d} \tag{7.9}$$

PETITIONER'S EXHIBIT 1002
US PATENT NO. 6,557,540

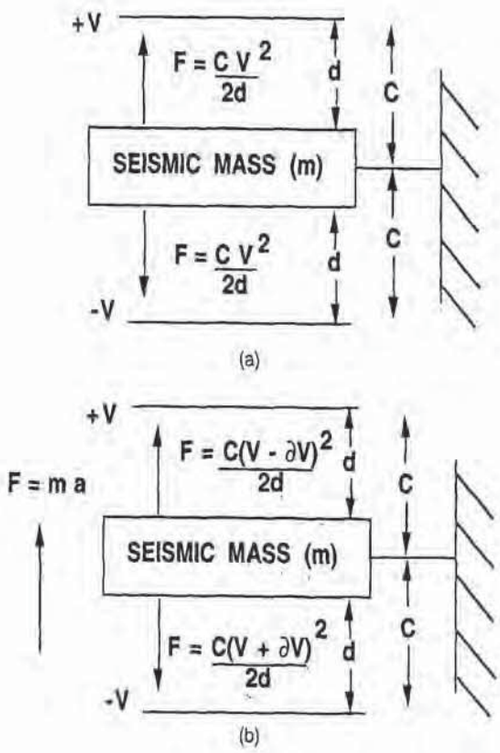


FIGURE 7.16 Electrostatic force diagram.

This shows that an acceleration force can be balanced by a linear voltage applied to the center plate. This voltage can be amplified to give a linear output voltage proportional to acceleration.[6]

In a micromachined structure, the electrostatic force produced by a δV of about 1 V can counterbalance the force produced by an acceleration of 50 g on the seismic mass. Figure 7.17 shows a block diagram of the analog closed-loop system. The top and bottom plates are dc-biased by the resistor divider network consisting of R1, R2, and R3. The ac antiphase signals used for sensing the position of the center plate are fed to the top and bottom sensor plates via the capacitors (C1, C2) from the control logic. The analog output voltage from the filter is feedback to the positive input of the integrator. When the integrator is clocked into the unity gain phase, the feedback voltage is applied to the center plate of the sensor. The electrostatic forces produced on the center plate by the differential voltage between the top and bottom plates, and the feedback voltage on the center plate, will force the center plate back to its normalized position as given in Eq. (7.9). Other methods that have been used for closed-loop operation are pulse width modulation (PWM), and delta sigma modulation (DSM).

The block diagram and waveforms of a PWM system are shown in Fig. 7.18. In this case, the center plate is held at a fixed voltage (0). The output of the integrator is amplified and converted into a PWM signal (VP), this signal and the inverted signal (VPN) are fed to the top and bottom plates of the sensor. The leading edges of the VP and VPN signals are used to sense the position of the middle plate. The electrostatic force generated by the voltage × time differential between the middle plate and the top and bottom plates, will act on the middle plate to counterbalance the forces on the plate due to acceleration. With zero acceleration, the PWM signal has a 50 percent duty cycle, so that the resulting electrostatic forces on the seismic mass are zero. The transfer function of the PWM system is given by

$$\text{Duty cycle} = \frac{\text{Acc} \times g \times d}{C \times V_{\text{REF}}^2} \tag{7.10}$$

PETITIONER'S EXHIBIT 1002
US PATENT NO. 6,557,540

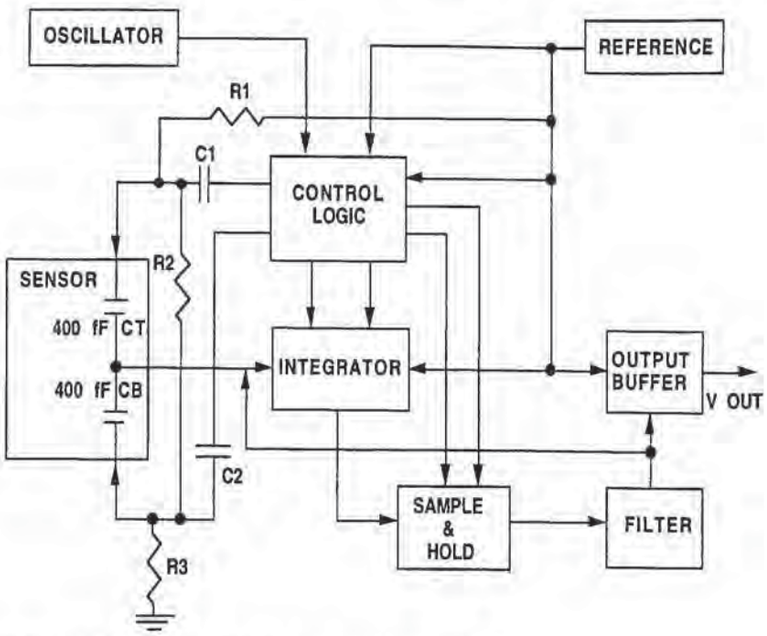


FIGURE 7.17 Block diagram of analog closed-loop system.

where g = gravitational constant
d = plate spacing
C = plate capacitance

The output can either be the PWM digital signal, or an analog output (obtained by feeding the PWM signal through a low pass filter).

Figure 7.19 shows the block diagram and waveforms of a DSM system. In this case, the middle plate is held at VF (volts). As can be seen, transient edges of the plate-drive waveforms are used for sensing the position of the center plate. The output from the integrator is fed to a comparator, whose output is then clocked into a latch where it sets up a "1" or a "0" (high or low) depending on the output from the integrator. The output from the latch is used to apply a voltage V_{REF} to the appropriate top or bottom capacitor plate, so that the electrostatic forces generated by the voltage V_{REF} – VF will maintain the center plate in its no-load position. The one-bit serial data stream from the latch can be fed directly to the MCU, or fed via a decimator circuit (which will convert the data into an 8-bit word) to the MCU. Alternatively, an LPF can be used to convert the data into an analog output. Bipolar or CMOS circuits can be used for signal conditioning. However, CMOS signal conditioning has the following advantages: a very high input impedance, good switching characteristics, low power requirements, small size, compatibility with MCU processes with the prospect of future integration, switched capacitor filters are available for noise reduction and bandwidth control, and EPROM technology is available for trimming (see Fig. 7.14). BiMOS circuits have also been used for signal conditioning.[6] In the BiMOS circuits, thin-film resistors are used to enable laser trimming of the zero offset and voltage reference; external capacitors and resistors are used for filtering and gain control.

Single vs. Multichip Control Circuits. The processing of sensors is not completely compatible with IC fabrication. Consequently, for the integration of sensors and ICs, a number of additional steps are required, which can have a detrimental effect on yields. The question then arises as to which is the most cost effective: a sensor die plus a control die with the additional cost of assembly, or a monolithic approach.

PETITIONER'S EXHIBIT 1002
US PATENT NO. 6,557,540

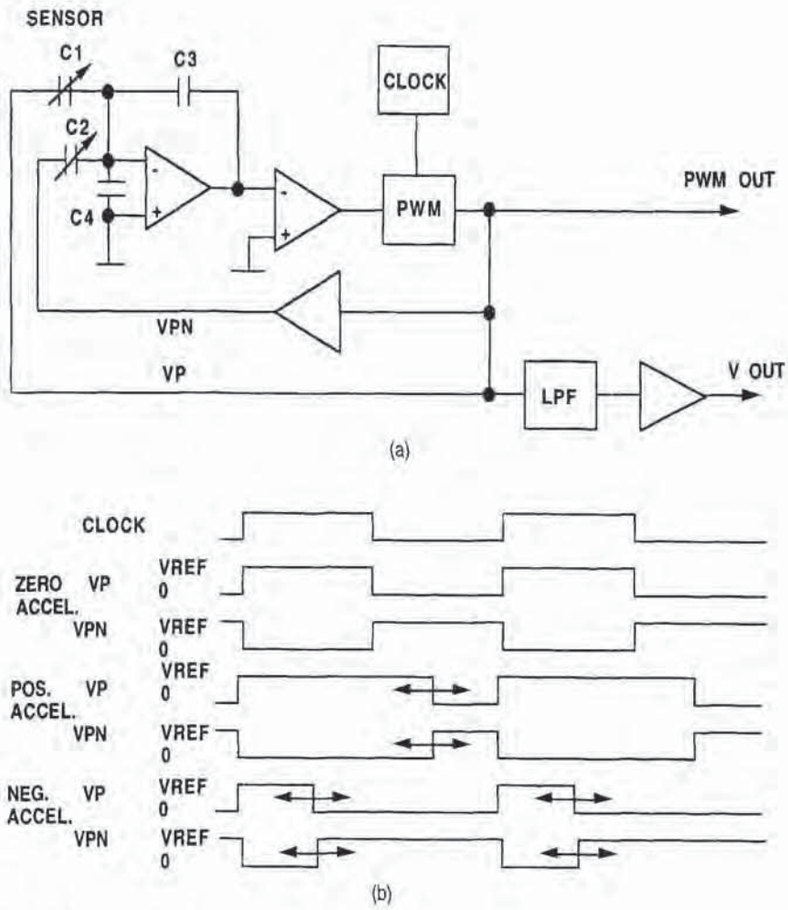


FIGURE 7.18 PWM block diagram.

In the case of micromachined devices, there are a number of advantages to using the dual-chip approach, such as flexibility, in that one type of sensor can be interfaced with a number of different types of control die, or several types of sensors can be interfaced with one type of control die. This provides a variety of input and output options. The control die and sensor can be developed simultaneously, minimizing development time. Problem solving is made easier, and the processing for both die can be optimized for performance. With the two-die approach, the sensor can also be capped and sealed during processing in a clean room atmosphere, thus eliminating contaminants and particles for good longevity. In the monolithic approach, this is not the case. In the monolithic approach, changes required to improve one section can affect the other section, which may then require additional changes in that section. The main disadvantage of the dual-chip approach is the introduction of parasitic capacitances. However, these can be addressed by existing control circuit design techniques.

7.5 AUTOMOTIVE APPLICATIONS FOR ACCELEROMETERS

Accelerometers have a wide variety of uses in the automobile. The initial application is as a crash sensor for air bag deployment. This application is normally associated with head-on collisions, but can also be applied to rear-end impact collisions to prevent rebound impact between the passengers and the windshield. An extension of this application is the use of

PETITIONER'S EXHIBIT 1002
US PATENT NO. 6,557,540